JPTM
Journal of Pathology and Translational Medicine

Journal of Pathology and Translational Medicine

JPTM

Journal of Pathology and Translational Medicine

March 2015
Vol. 49 / No. 2
jpatholtm.org
pISSN: 2383-7837
eISSN: 2383-7845

Utility of Transmission Electron Microscopy in Small Round Cell Tumors

Role of Osteal Macrophages in Bone Metabolism

Vol. 49, No. 2, pp 93-179, March 2015

Journal of Pathology and Translational Medicine

Volume 49 • Number 2 • March 2015 (bimonthly)
Published since 1967
Printed on 11 March 2015 Published on 15 March 2015

J Pathol Transl Med
pISSN: 2383-7837
eISSN: 2383-7845

Aims & Scope

The Journal of Pathology and Translational Medicine is an open venue for the rapid publication of major achievements in various fields of pathology, cytopathology, and biomedical and translational research. The Journal aims to share new insights into the molecular and cellular mechanisms of human diseases and to report major advances in both experimental and clinical medicine, with a particular emphasis on translational research. The investigations of human cells and tissues using high-dimensional biology techniques such as genomics and proteomics will be given a high priority. Articles on stem cell biology are also welcome. The categories of manuscript include original articles, review and perspective articles, case studies, brief case reports, and letters to the editor.

Subscription Information

To subscribe to this journal, please contact the Korean Society of Pathologists/the Korean Society for Cytopathology. Full text PDF files are also available at the official website (http://jpatholtm.org). *Journal of Pathology and Translational Medicine* is indexed by PubMed, PubMed Central, Scopus, KoreaMed, KoMCI, WRPIM and CrossRef. Circulation number per issue is 700.

Contact the Korean Society of Pathologists/the Korean Society for Cytopathology

Publishers: Changsuk Kang, M.D., So Young Jin, M.D.
Editors-in-Chief: Soon Won Hong, M.D., Chong Jai Kim, M.D.
Published by the Korean Society of Pathologists/the Korean Society for Cytopathology

Editorial Office
Room 1209 Gwanghwamun Officia, 92 Saemunan-ro, Jongno-gu,
Seoul 110-999, Korea/#406 Lilla Swami Bldg, 68 Dongsan-ro,
Seocho-gu, Seoul 137-899, Korea
Tel: +82-2-795-3094/+82-2-593-6943
Fax: +82-2-790-6635/+82-2-593-6944
E-mail: office@jpatholtm.org

Printed by Academya Publishing Co.
Room 2003 Daeryung Techno Town, 401 Simin-daero, Dongan-gu, Anyang 431-060, Korea
Tel: +82-31-389-8811 Fax: +82-31-389-8817 E-mail: academya@korea.com

Manuscript Editing by InfoLumi Co.
210-202, 421 Pangyo-ro, Bundang-gu, Seongnam 463-926, Korea
Tel: +82-70-8839-8800 E-mail: infolumi.chang@gmail.com

Front cover image: Transmission Electron Microscopy in Small Round Cell Tumors. p 95.

This journal was supported by the Korean Federation of Science and Technology Societies Grant funded by the Korean Government.

Journal of Pathology and Translational Medicine

J Pathol Transl Med
pISSN: 2383-7837
eISSN: 2383-7845

Volume 49, Number 2, March 2015

CONTENTS

REVIEWS

ORIGINAL ARTICLES

CASE REPORTS

CONTENTS CONTINUED

Instructions for Authors for *Journal of Pathology and Translational Medicine* are available at http://jpatholtm.org/authors/authors.php

Journal of Pathology and Translational Medicine 2015; 49: 93-101
http://dx.doi.org/10.4132/jptm.2015.01.30

■ REVIEW ■

Utility of Transmission Electron Microscopy in Small Round Cell Tumors

Na Rae Kim · Seung Yeon Ha
Hyun Yee Cho

Department of Pathology, Gachon University Gil Medical Center, Incheon, Korea

Received: August 31, 2014
Revised: January 28, 2015
Accepted: January 30, 2015

Corresponding Author
Hyun Yee Cho, M.D.
Department of Pathology, Gachon University Gil Medical Center, 21 Namdong-daero 774beon-gil, Namdong-gu, Incheon 405-760, Korea
Tel: +82-32-460-3865
Fax: +82-32-460-2394
E-mail: hicho@gilhospital.com

Small round cell tumors (SRCTs) are a heterogeneous group of neoplasms composed of small, primitive, and undifferentiated cells sharing similar histology under light microscopy. SRCTs include Ewing sarcoma/peripheral neuroectodermal tumor family tumors, neuroblastoma, desmoplastic SRCT, rhabdomyosarcoma, poorly differentiated round cell synovial sarcoma, mesenchymal chondrosarcoma, small cell osteosarcoma, small cell malignant peripheral nerve sheath tumor, and small cell schwannoma. Non-Hodgkin's malignant lymphoma, myeloid sarcoma, malignant melanoma, and gastrointestinal stromal tumor may also present as SRCT. The current shift towards immunohistochemistry and cytogenetic molecular techniques for SRCT may be inappropriate because of antigenic overlapping or inconclusive molecular results due to the lack of differentiation of primitive cells and unavailable genetic service or limited moleculocytogenetic experience. Although usage has declined, electron microscopy (EM) remains very useful and shows salient features for the diagnosis of SRCTs. Although EM is not always required, it provides reliability and validity in the diagnosis of SRCT. Here, the ultrastructural characteristics of SRCTs are reviewed and we suggest that EM would be utilized as one of the reliable modalities for the diagnosis of undifferentiated and poorly differentiated SRCTs.

Key Words: Small round cell tumor; Microscopy, electron; Pathology

Small round cell tumor (SRCT) is a collective term, not a single disease entity, that refers to a tumor composed of small, round and relatively undifferentiated primitive cells with scant cytoplasm under light microscopy after excluding neoplasms of the central nervous system (CNS).[1] The term 'small' indicates slightly larger than or double the size of the red blood cells in air-dried smears.[2] Most of them are solid malignant tumors with histologic resemblance reflecting their dysembryonic, undifferentiated, and primitive features. Tumor cells of this category are poorly differentiated or undifferentiated with high nuclear/cytoplasmic (N/C) ratio and little cytoplasm, subsequently presenting an overall bluish picture on hematoxylin and eosin stain; thus, it is also referred to as small blue round cell tumor.[3] SRCT is actually a heterogeneous group of neoplasms dominating in childhood and adolescence, and histologic diagnoses of SRCTs are diverse, as shown in Table 1.[1,4-16] Therefore, the diagnosis of SRCT is challenging, necessitating the use of multimodal ancillary techniques.[17-19] Traditional work flow for a diagnosis of SRCT was light microscopic examination with special stains at first and ultrastructural examination as a second step when the light microscopic findings are equivocal.[4] Poorly differentiated or undifferentiated tumors require further immunohistochemistry and cytogenetic molecular studies.[19] Currently, however, as a matter of convenience, immunohistochemistry has become the routine diagnostic modality due to the relative ease of use and interpretation, while electron microscopy (EM) is frequently skipped due to its declined usage in diagnostic fields.[1,20] Sometimes, cytogenetic or molecular studies are employed at firsthand because these methods are now widely considered as a confirmative modality in the diagnosis of SRCT. Not unexpectedly, a combination of more than two modalities results in a higher rate of specific diagnosis than either alone.[4] Immunohistochemistry frequently shows equivocally positive or negative reactions, particularly in poorly differentiated tumors, and overlapping of antigenicities between several SRCTs requires large panels of antibodies for the diagnosis.[1,17,21]

Over the last two decades, advances in molecular diagnostic techniques for SRCT or soft tissue tumors have been remarkable and such diagnostic techniques have been rapidly integrated. For example, the FLI1 protein, the gene product of *FLI1*, t(11;22), is detected in up to 85% of Ewing sarcoma/peripheral neuroectodermal tumors (ES/PNET), and *WT1* on 11p13 is unique and central to the pathogenesis of desmoplastic small round cell tumor (DSRCT).[21-23] It is yet uncertain whether SRCTs showing aberrant translocation should be included as a specific entity or be left as undifferentiated or high-grade sarcomas.[13,24,25] Al-

pISSN 2383-7837
eISSN 2383-7845

Table 1. Disease entities appearing as small round cell tumors along with ultrastructural differential characteristic findings

Findings	Basal lamina	Cytoplasmic organelles
Tumors of unknown histogenesis		
ES/PNET	Rare basal lamina	Primitive polygonal cells containing sparse organelles, abundant glycogen, occasional neural differentiation; rare epithelial differentiation such as tonofilaments
Neuroblastoma	Rare basal lamina	Round cells having cell processes containing neural differentiation such as microtubules, neurofilaments, neurosecretory granules, glycogen, synaptic vesicles
Desmoplastic small round cell tumor	Discontinuous basal lamina	Paranuclear whorls of intermediate filaments, rare dense core granules, scant organelles, occasional microtubules, glycogen particles
Malignant rhabdoid tumor	No basal lamina	Paranuclear bundles of cytoplasmic intermediate filaments (about 10 nm in thickness), glycogen particles
Soft tissue tumor		
Monophasic synovial sarcoma	Focal basal lamina	Spindle to oval cells mimicking fibroblasts (less RERs than fibroblasts) having intermediate filaments, microvilli, pinocytotic vesicles
Small cell schwannoma or small cell malignant peripheral nerve sheath tumor	Continuous reduplicated basal lamina	Long-spacing collagen, i.e., Luse bodies
Alveolar rhabdomyosarcoma, solid variant	Basal lamina	Myosin-ribosome complexes, dense plaques
Small cell osteosarcoma	No basal lamina	Fibroblast-like cells containing abundant RERs, glycogen, flocculent premineralized stage osteoid matrix, needle-like dense hydroxyapatite crystals on collagen fibrils, i.e., osteoid
Mesenchymal chondrosarcoma	No basal lamina	Glycogen in cytoplasm, rare scalloped villous cell surfaces
Hematologic malignancies		
Leukemia/myeloid sarcoma	No basal lamina	Ovoid-shaped myeloid cells containing myeloid granules of various stage or Auer bodies
Malignant lymphoma	No basal lamina	Polygonal shaped cells with abundant ribosomes or variable amount of RERs
Others		
Small cell or rhabdoid melanoma	Focal basal lamina	Round cells having Golgi complex, atypical melanosomes of various stage

ES/PNET, Ewing sarcoma/peripheral neuroectodermal tumors; RER, rough endoplasmic reticulums.

though these cytogenetic or molecular studies are the most suitable for confirming a specific diagnosis and the usage of the "old" ultrastructural examination in the diagnostic field is still limited to some disease entities, the cytogenetic or molecular studies have several limitations;[26] requirement for very meticulous technique, discrepancy with histomorphology, low sensitivity, and unpredicted variant rearrangements.

As stated above, current usage of EM has declined as following limitation; first, EM lacks distinction between benignity and malignancy. Second, EM lacks heterogeneous findings due to varying differentiation and overlapping ultrastructural structures in different types of cells as well as sampling error.[4,27] Even with EM studies, some tumors still exhibit unknown lineage of differentiation, especially when the tumor cells are primitive and undifferentiated.[28] Although new models of digitalized EM have redeemed the time-consuming process and cost-ineffectiveness, EM has become unfamiliar to pathologists.[12,29-31]

Here, we discuss the advantages and disadvantages of ultrastructural studies for the diagnosis of SRCTs with suggested applications of EM.

ULTRASTRUCTURAL FINDINGS OF SMALL ROUND CELL TUMORS

In this review, we explain SRCTs with following subdivisions; first, SRCTs are mainly comprised of tumors with unknown histogenesis. In this group, ES/PNET, neuroblastoma, DSRCT, and malignant rhabdoid tumor (MRT) are included. Second, certain types of soft tissue neoplasms can rarely appear as SRCTs. The third group is hematologic malignancies, including non-Hodgkin's lymphoma and leukemia.[7,16] Others include epithelioid gastrointestinal stromal tumor (GIST), small cell or rhabdoid type melanomas.[8,15,32] Among these groups, certain type of SRCTs can be diagnosed under light microscopy and immunohistochemistry by their unique histologic features such as GIST or small cell liposarcoma, which are not discussed here.

SRCT of unknown histogenesis

ES/PNET, neuroblastoma, DSRCT, and MRT are categorized as tumors of unknown histogenesis.[8,31] ES and PNET that present primarily in bone and soft tissues have been reported and previously studied as separate entities. However, there has been

 http://dx.doi.org/10.4132/jptm.2015.01.30

a recognition of a shared cytogenetic abnormality between the two and they are now regarded as different manifestations of the same entity at the genetic level (i.e., ES/PNET family tumors including Askin tumor).[12]

ES/PNET family tumors show diverse heterogeneous histologic features, including large cell atypical types or adamantinoma-like variant ES/PNET, which have shared moleculogenetic abnormalities. ES/PNET family tumors show varying degrees of neuroectodermal differentiation. The ultrastructural findings of ES/PNET show undifferentiated mesenchymal cells arising from a mesenchymal stem cell and differentiating to neural cells.[12,33] Ultrastructural findings of this neural differentiation include intermediate filaments, microtubules, or neurosecretory granules and processes.[12] Small amounts of glycogen can be seen in other types of tumors, but in ES, glycogen deposits usually form lakes or pools (Fig. 1A). The tumors show undifferentiated primitive cells with no discernible characteristics except for abundant glycogen pools. Rich glycogen within the cytoplasm is a notable and distinctive finding for ES/PNET, but is not specific;[33] MRT may show plentiful glycogen particles and no other specialized structures, mimicking ES/PNET (Fig. 1B).[11] MRT of soft tissue show large paranuclear whorls of intermediate filaments, with entrapped organelles and lipid droplets.[34] These paranuclear cytoplasmic whorls of intermediate filaments are shared by DSRCT of the abdominal wall.[5,21,22,35]

DSRCT is a rare malignant pediatric tumor that usually affects the abdominal cavity.[22] When DSRCT is presented in visceral organs, its diagnosis poses significant difficulty. In such

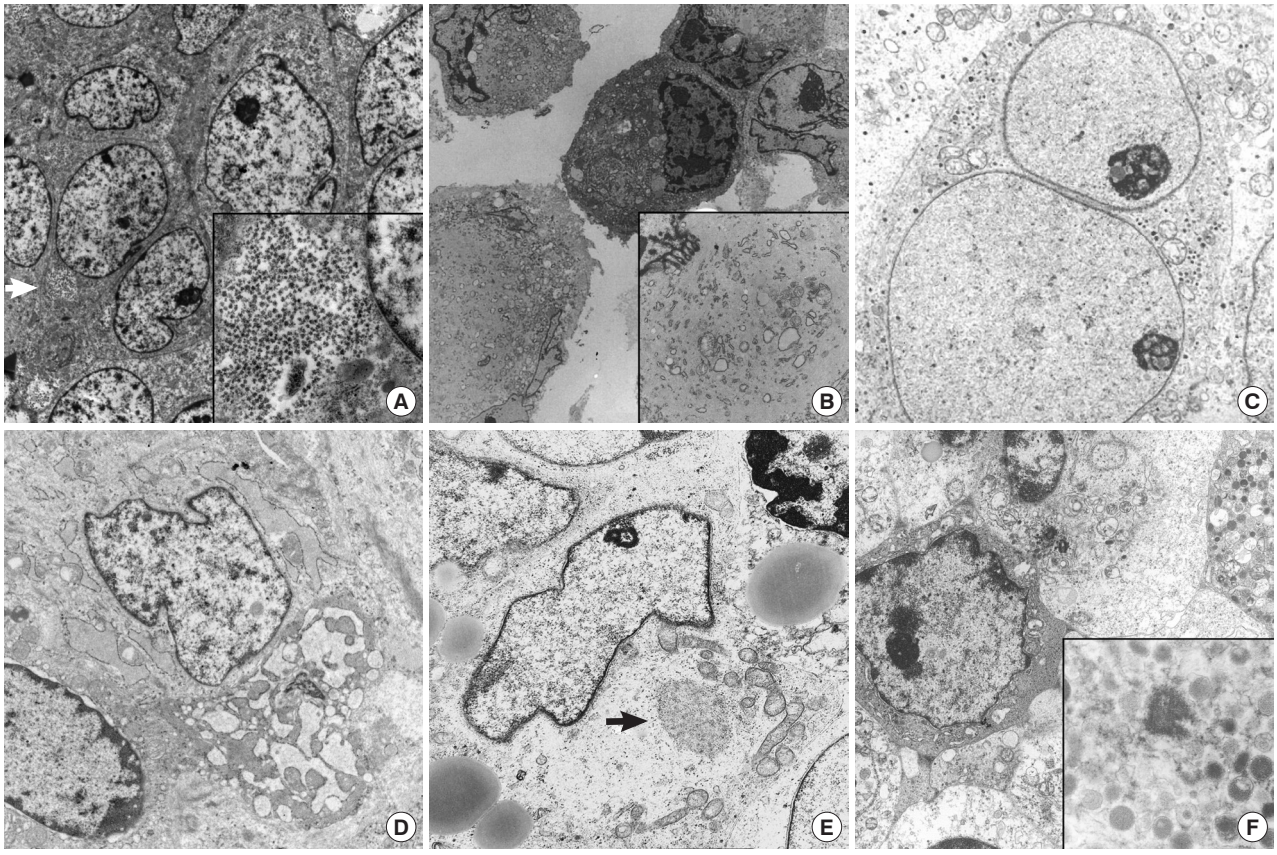

Fig. 1. (A) Ewing sarcoma shows polygonal shaped cells having large round cells and a small amount of cytoplasm with mainly glycogen pools (arrow) (×7,500). Inset indicates abundant cytoplasmic glycogen particles (×10,000). (B) Tumor cells of malignant rhabdoid tumor show paranuclear whorls packed with intermediate filaments intermingled with cytoplasmic organelles (×2,000). Inset shows paranuclear whorls filled with dense intermediate filaments, dilated rough endoplasmic reticulum (RER) cisternae and degenerated mitochondria (×8,000). (C) Neuroblastoma. Round shaped tumor cells have neurosecretory dense core granules in the cytoplasm (×8,000). (D) Small cell osteosarcoma shows ovoid shaped tumor cells containing a moderate amount of mitochondria and ribosomes with dilated RERs (×8,500). (E) Alveolar rhabdomyosarcoma, solid variant. Closely apposed round to ovoid shaped cells have irregular shaped nuclei and a moderate amount of cytoplasm containing lipid vacuoles, mitochondria, and Golgi apparatuses (×3,500). Arrow indicates myosin-ribosome complexes (×12,000). (F) Myeloid sarcoma demonstrates cytoplasmic myeloid granules, measuring 200 nm on average (×1,500). Inset shows membrane bound myeloid granules (×6,000).

circumstances, DSRCT showing multidirectional differentiation may add diagnostic confusion.[5,23,35] Neural differentiation characteristics such as neurosecretory granules, microtubules, dendritic interdigitating processes, or epithelial differentiation such as cell junctions or intracytoplasmic lumen can also be identified in DSRCT. Confirmation of neurosecretory granules, formerly known as dense core granules, requires careful examination because they may be easily confused with primary lysosomes, which are larger than the former. DSRCT have mitochondria, lipid aggregates, and a few groups of paranuclear intermediate filaments.[21] The multidirectional differentiation is concordant with t(11;22)(p13;q12), resulting in a chimeric EWS/WT1 transcript.[23] Presence of paranuclear whorls of intermediate filaments corresponds to the dot-like immunostaining with desmin or vimentin, together with the absence of specialized ultrastructural structures.[21] Among pediatric SRCTs, a tumor showing only neural differentiation is a neuroblastoma, the most frequently encountered extracranial pediatric solid tumor.[36,37] It originates from neural crest cells of the sympathetic nervous system and EM is very helpful in its diagnosis. These neoplasms have neurosecretory granules (50–200 nm in diameter) with membrane-bound dense core granules, cytoplasmic processes containing parallel arranged microtubules of 20 nm in diameter, and primitive cell junctions (Fig. 1C). Cell junctions are not demonstrated in neuroblastoma.

SRCT categorized as a soft tissue neoplasm

Soft tissue tumors are classified according to morphology and histogenesis. As up to 30% of soft tissue tumors show chromosomal alterations, integration of molecular study in the diagnosis of soft tissue tumors has been recommended. However, accumulating data on these molecular alterations sometimes further complicates the molecular diagnoses of some soft tissue tumors. Certain types of soft tissue tumors can present as SRCTs including monophasic synovial sarcoma,[8] small cell osteosarcoma,[18] mesenchymal chondrosarcoma,[38,39] small cell variant of melanoma,[15,40] solid variant of alveolar rhabdomyosarcoma,[41] round cell liposarcoma,[42] small cell schwannoma, and small cell malignant peripheral nerve sheath tumor (MPNST).[9,36] ES/PNET family tumors are too undifferentiated to have characterized ultrastructural findings, and ultrastructural morphology is hardly distinguished from the undifferentiated cells of small osteosarcoma and mesenchymal chondrosarcoma of soft tissue.[43-46] In primitive cells differentiating to chondrocytes in mesenchymal chondrosarcoma, some thin cytoplasmic projections to the extracellular spaces are the only distinguishing finding.[13,46-48] The chondrocyte-like tumor cells usually found in conventional myxoid chondrosarcoma are not found in most undifferentiated forms of chondrosarcomas.[48] The chondrocytes of well differentiated forms are ovoid to fusiform shaped ones with an eccentric nucleus and cytoplasm having abundant mitochondria, conspicuous endoplasmic reticulum with dilated cisternae of rough endoplasmic reticulums (RERs), cytoplasmic glycogen, lipid droplets, and numerous thin cytoplasmic projections such as microvilli into the extracellular area, which is filled with glycosaminoglycan granules, and collagen fibrils.[49] The higher the grade of chondrosarcoma, the lower the number of organelles, along with less prominent cytoplasmic projections into the extracellular spaces, bizarre nuclei, and more prominent nucleoli.[50,51] More immature cells correspond to small undifferentiated cells mimicking fibroblasts. Cells of mesenchymal chondrosarcoma have rounded nuclei, scanty cytoplasm, and few organelles and glycogen, like ES/PNET.[13] The intercellular matrix is very scanty and does not contain collagen fibrils. The search for more differentiated foci and correlation with the light microscopic findings is rewarding in such cases. These well-formed microvilli are found in low to intermediate grade chondrosarcoma, and are well observed even in clear cell chondrosarcomas, which lack other organelles, but have abundant glycogen particles.[51] Small cell osteosarcoma should be differentiated from other more common SRCTs. Chondroblasts showing features similar to those of chondroblastoma or chondrosarcoma can be seen in osteosarcoma.[18] There are rare osteoblastic or multinucleated giant cells with a large amount of RERs without ruffled borders. The tumor cells of a rare variant of osteosarcoma are a primitive form of osteoblasts, and the critical point of its ultrastructural diagnosis is to search for extracellular osteoid, extracellular matrix containing collagen fibers with deposition of hydroxyapatite crystals, showing correlation with light microscopy. The tumor cells have round shaped nuclei with occasional infolding and a more moderate amount of cytoplasm than those of ES/PNET. They also have a considerable number of organelles, most of which are RERs and ribosomes (Fig. 1D). Although tumor cells in a small cell osteosarcoma resemble those of ES, osteoid will provide an ultrastructural distinguishing point as it does in the light microscopic diagnosis.[17,52]

In pediatric age, a solid variant of alveolar rhabdomyosarcoma rarely presents as SRCT.[41] Like other tumors, the EM features of a solid variant of alveolar rhabdomyosarcoma depend on the degree of differentiation of rhabdomyoblasts.[53] Contrary to much more differentiated rhabdomyosarcoma, the primitive small cells are monomorphous round to elongated in shape and

 http://dx.doi.org/10.4132/jptm.2015.01.30

are surrounded by external lamina with a moderate amount of cytoplasm filled with glycogen and other organelles and have no easily detectable muscular features such as thick myosin-ribosome complexes or dense plaques. A careful search for thick myosin filament-ribosome complexes defined as 15-nm filaments intimately associated with numerous free ribosomes, the earliest evidence of rhabdomyoblast, can confirm the diagnosis of a rare solid variant of rhabdomyosarcoma (Fig. 1E).[41] Ultrastructural evidence of skeletal differentiation such as specific myofilament arrays, focal density, Z-band material, and pinocytotic vesicles may not be detectable in solid variants of alveolar rhabdomyosarcoma.[53] Caution is needed because such neoplastic rhabdomyoblastic differentiation may be found in other SRCTs, such as malignant melanomas or schwannian Triton tumors.

MPNST can present with small cell components, and it may cause confusion in small biopsy samples.[54] For example, benign peripheral nerve sheath tumor such as schwannoma, may show small cell components.[55] The presence of small cell changes of peripheral nerve sheath tumors is mainly regarded as malignant transformation; however, it sometimes implies differentiation toward immature neural cells.[9] Distinguishing poorly differentiated small cell MPNST from ES/PNET is not easy, at least on histologic and immunohistochemical grounds alone because MPNST has neither a reliable immunohistochemical marker nor specific moleculogenetic changes. Therefore, EM is often useful in detecting elongated interdigitating cytoplasmic processes, pinocytotic vesicles, and fragments of basal lamina.[56] In particular, the presence of basal lamina around tumor cells under EM confirms bidirectional differentiation into melanocytes and nerve sheath tumor. In such cases, basal lamina can be found in epithelial, myoepithelial, endothelial, Schwann or perineurial cells, or muscle cells, but cannot be seen in neurons, glial, hematolymphoid cells, and myofibroblastic cells.[57] Therefore, misinterpretation of the basal lamina of these surrounding reactive cells for the lamina of tumor cells should be avoided.

Small cell variant of poorly differentiated monophasic synovial sarcoma, one of the poorly differentiated monophasic synovial sarcoma, should be distinguished from other SRCTs.[8,58] Monophasic synovial sarcoma showing epithelial membrane antigen–negative and cytokeratin-negative poorly differentiated one, requires either molecular cytogenetic study to evaluate the specific translocation t(X;18)(p11;q11) or EM examination.[59] Ultrastructurally, differentiation of synovial sarcoma ranges from unclassifiable spindle cells to fully differentiated epithelioid cells.[60] The spindle to fusiform-shaped tumor cells of synovial sarcoma has a high N/C ratio and non-descript cytoplasm devoid of schwannian differentiation, fibroblastic and leiomyosarcomatous differentiation, continuous basal lamina, long spacing collagen, and long intervening processes. Tapering bipolar processes joined by occasional rudimentary cell junctions or desmosomes, or infrequent tonofibrils must be distinguished from MPNST.[60]

SRCT of hematologic malignancies

The tumor cells of some SRCTs, particularly the solid variant of alveolar rhabdomyosarcomas, resemble lymphoblastic leukemic cells or non-Hodgkin's lymphoma.[61,62] Conversely, dense infiltrates of relatively small undifferentiated tumor cells of uncertain origin, which mimic undifferentiated sarcoma, may be the first presentation of hematologic and lymphoid malignancies.[63] In particular, myeloid sarcomas with no evidence of circulating blasts may manifest as undifferentiated tumors with small round cell morphology, which frequently show aberrant immunophenotypes for myeloperoxidase, terminal deoxynucleotidyl transferase, CD68 (KP1), lysozyme, CD117, or CD34.[64] Ultrastructural demonstration of myeloid granules of various morphology and stage are crucial in such cases.[65-68] Elongated Auer bodies as well as round or rod-like primary or azurophilic granules are useful ultrastructural findings. Primitive myeloid blasts have little cytoplasm but show greatly enlarged nucleoli with coarse granular nucleoplasm and thin peripheral heterochromatin (Fig. 1F).[16] Myeloid tumors show morphological forms ranging from myeloblasts through promyelocytes to monocytes.[68] This is not the case for lymphoid malignancy[19,65,66] and subtyping of lymphoma has been attempted. EM cannot determine the line of differentiation in lymphoid malignancy, but it plays a role in excluding lymphoid malignancy. Abundant ribosomes and polysomes with an absence of cell junctions or basal lamina are the most common features of lymphoid malignancy.

Other tumors presented with SRCTs

As previously mentioned in the SRCT of unknown histogenesis, MRTs showing rhabdoid morphology under light microscopy have been reported in every location of the body including the brain, liver, soft tissues, lung, skin, heart, and kidney, in which the tumor was originally described.[11,69-72] Recent immunohistochemistry reveals that the tumor cells have nuclear immunoreactivity for integrase interactor 1 (INI-1), which is critical for the diagnosis of this highly aggressive tumor, and show paranuclear bundles of intermediate filaments under ultrastructural examination.[70] Cell junctions are not observed in MRT. These paranuclear whorls of intermediate filaments are seen in

other tumors of rhabdoid appearance; a rhabdoid variant of malignant melanoma also shows prominent nuclei and cytoplasmic accumulation of whorls of intermediate filaments, which compress the nuclei and a few organelles entrapped in the cytoplasm and melanosomes. As stated above, DSRCT also shares these ultrastructural findings. The so called rhabdoid appearance under light microscopy mimicking renal MRT (i.e., large cells with eccentrically located nuclei and abundant, eosinophilic cytoplasm) refers to tumors showing diffuse organoid sheets of round or polygonal shaped cells with paranuclear whorls of intermediate filaments. Tumors showing rhabdoid appearance are found in various tumors including pleomorphic fibrosarcoma with rhabdoid appearance, rhabdoid tumors of the CNS such as atypical teratoid/rhabdoid tumor, the CNS counterpart of MRT, rhabdoid meningioma, astroblastoma with rhabdoid appearance or rhabdoid choroid plexus carcinoma.[70,71] Extrarenal rhabdoid tumors are a heterogeneous group of neoplasms and it is also described as poorly differentiated neoplasms with rhabdoid features for these undifferentiated tumors.[72] Ultrastructural features shared with other tumors with rhabdoid features may not provide a diagnostic clue other than loss of INI-1 nuclear staining, which is critical for the diagnosis of this highly aggressive tumor.

Under light microscopy, small cell (Merkel-like) melanomas appearing in adolescents and children are composed of small undifferentiated cells of melanocytic-lineage.[15] Ultrastructural examination is required to determine if the cells are pre-melanosomes or melanosomes of various stages and differentiating them from the reactive cells is important.[73] Pathologists should search meticulously for melanosome granules of various stages.

CONCLUSION

In summary, the current shift in SRCT diagnosis is towards immunohistochemistry and cytogenetic molecular techniques, but sometimes these techniques are inadequate. Even with careful traditional analyses, the correct diagnosis remains elusive. Immunohistochemistry has limitations in sensitivity and specificity, while moleculocytogenetic study has proven to be useful in characterization of SRCTs; however, it has also become evident that some genetic abnormalities are not tumor specific, and even demonstrate results not correlating with the histologic morphology. As stated above, light microscopy should remain as the main diagnostic tool. As EM has several overlapping features (Table 1), it may not be able to identify a line of differentiation if the tumor cells are cytologically undifferentiated. However, EM should be included in the standard diagnostic processes for SRCTs, as it can provide both validity and reliability in its specificity.

Here, we emphasize that pathologists need to understand the appropriate applications and pitfalls as well as the benefits of EM, which permits optimal diagnosis of SRCTs.

Conflicts of Interest

No potential conflict of interest relevant to this article was reported.

Acknowledgments

Authors wish to express special thanks to Emeritus Professor Je Geun Chi, Professor Sung-Hyeh Park in Seoul National University and Professor Yeon-Lim Suh in Sungkyunkwan University for providing electron microscopic pictures.

REFERENCES

1. Bahrami A, Truong LD, Ro JY. Undifferentiated tumor: true identity by immunohistochemistry. Arch Pathol Lab Med 2008; 132: 326-48.
2. Rajwanshi A, Srinivas R, Upasana G. Malignant small round cell tumors. J Cytol 2009; 26: 1-10.
3. Ponce-Castañeda MV, García-Chéquer AJ, Eguía Aguilar P, *et al.* Detection of common chromosomal translocations in small round blue cell pediatric tumors. Arch Med Res 2014; 45: 143-51.
4. Peydró-Olaya A, Llombart-Bosch A, Carda-Batalla C, Lopez-Guerrero JA. Electron microscopy and other ancillary techniques in the diagnosis of small round cell tumors. Semin Diagn Pathol 2003; 20: 25-45.
5. de Alava E, Ladanyi M, Rosai J, Gerald WL. Detection of chimeric transcripts in desmoplastic small round cell tumor and related developmental tumors by reverse transcriptase polymerase chain reaction: a specific diagnostic assay. Am J Pathol 1995; 147: 1584-91.
6. Rossouw DJ, Cinti S, Dickersin GR. Liposarcoma: an ultrastructural study of 15 cases. Am J Clin Pathol 1986; 85: 649-67.
7. Alameda F, Corominas JM, Barranco C, *et al.* Primitive round cell liposarcoma of the omentum: diagnostic value of ultrastructural study. Ultrastruct Pathol 2003; 27: 433-7.
8. d'Amore ES, Ninfo V. Soft tissue small round cell tumors: morphological parameters. Semin Diagn Pathol 1996; 13: 184-203.
9. Roncaroli F, Consales A, Betts C, Dorji T, Calbucci F, Eusebi V. Schwannoma with small cell component. Virchows Arch 2003; 443: 586-8.
10. Masjosthusmann K, Bielack SS, Köhler G, *et al.* Concomitant Ewing sarcoma and acute lymphoblastic leukemia in a 5-year-old girl. Pe-

diatr Blood Cancer 2005; 45: 846-9.
11. Wagner LM, Garrett JK, Ballard ET, *et al.* Malignant rhabdoid tumor mimicking hepatoblastoma: a case report and literature review. Pediatr Dev Pathol 2007; 10: 409-15.
12. Franchi A, Pasquinelli G, Cenacchi G, *et al.* Immunohistochemical and ultrastructural investigation of neural differentiation in Ewing sarcoma/PNET of bone and soft tissues. Ultrastruct Pathol 2001; 25: 219-25.
13. Kurotaki H, Tateoka H, Takeuchi M, Yagihashi S, Kamata Y, Nagai K. Primary mesenchymal chondrosarcoma of the lung: a case report with immunohistochemical and ultrastructural studies. Acta Pathol Jpn 1992; 42: 364-71.
14. Steiner GC, Forest M, Vacher-Lavenu MC. Ultrastructure of low-grade intraosseous osteosarcoma of bone: a comparative study with fibrous dysplasia and parosteal osteosarcoma. Ultrastruct Pathol 2006; 30: 293-9.
15. Barnhill RL. Childhood melanoma. Semin Diagn Pathol 1998; 15: 189-94.
16. Terzakis JA, Taskin M. Bone marrow leukemias and lymphoproliferative disorders: scanning electron microscope diagnosis. Ultrastruct Pathol 2002; 26: 143-52.
17. Salhany KE, Feldman M, Kahn MJ, *et al.* Hepatosplenic gammadelta T-cell lymphoma: ultrastructural, immunophenotypic, and functional evidence for cytotoxic T lymphocyte differentiation. Hum Pathol 1997; 28: 674-85.
18. Park SH, Kim I. Small cell osteogenic sarcoma of the ribs: cytological, immunohistochemical, and ultrastructural study with literature review. Ultrastruct Pathol 1999; 23: 133-40.
19. Mierau GW, Weeks DA, Hicks MJ. Role of electron microscopy and other special techniques in the diagnosis of childhood round cell tumors. Hum Pathol 1998; 29: 1347-55.
20. D'Cruze L, Dutta R, Rao S, R A, Varadarajan S, Kuruvilla S. The role of immunohistochemistry in the analysis of the spectrum of small round cell tumours at a tertiary care centre. J Clin Diagn Res 2013; 7: 1377-82.
21. Ordóñez NG. Desmoplastic small round cell tumor: II: an ultrastructural and immunohistochemical study with emphasis on new immunohistochemical markers. Am J Surg Pathol 1998; 22: 1314-27.
22. Ordonez NG. Desmoplastic small round cell tumor: I: a histopathologic study of 39 cases with emphasis on unusual histological patterns. Am J Surg Pathol 1998; 22: 1303-13.
23. Sawyer JR, Tryka AF, Lewis JM. A novel reciprocal chromosome translocation t(11;22)(p13;q12) in an intraabdominal desmoplastic small round-cell tumor. Am J Surg Pathol 1992; 16: 411-6.
24. Demicco EG. Sarcoma diagnosis in the age of molecular pathology. Adv Anat Pathol 2013; 20: 264-74.
25. Neuville A, Chibon F, Coindre JM. Grading of soft tissue sarcomas: from histological to molecular assessment. Pathology 2014; 46: 113-20.
26. Chibon F, Lagarde P, Salas S, *et al.* Validated prediction of clinical outcome in sarcomas and multiple types of cancer on the basis of a gene expression signature related to genome complexity. Nat Med 2010; 16: 781-7.
27. Min KW. Usefulness of electron microscopy in the diagnosis of "small" round cell tumors of the sinonasal region. Ultrastruct Pathol 1995; 19: 347-63.
28. Ghadially FN. Ultrastructural pathology of the cell and matrix. 4th ed. Newton: Butterworth-Heinemann, 1997.
29. Shindo D, Ikematsu Y, Lim SH, Yonenaga I. Digital electron microscopy on advanced materials. Mater Charact 2000; 44: 375-84.
30. Tucker JA. The continuing value of electron microscopy in surgical pathology. Ultrastruct Pathol 2000; 24: 383-9.
31. Turbat-Herrera EA, Herrera GA. Electron microscopy renders the diagnostic capabilities of cytopathology more precise: an approach to everyday practice. Ultrastruct Pathol 2005; 29: 475-82.
32. Laforga JB. Malignant epithelioid gastrointestinal stromal tumors: report of a case with cytologic and immunohistochemical studies. Acta Cytol 2005; 49: 435-40.
33. Sorensen PH, Lessnick SL, Lopez-Terrada D, Liu XF, Triche TJ, Denny CT. A second Ewing's sarcoma translocation, t(21;22), fuses the EWS gene to another ETS-family transcription factor, ERG. Nat Genet 1994; 6: 146-51.
34. Chen Y, Jung SM, Chao TC. Malignant rhabdoid tumor of the small intestine in an adult: a case report with immunohistochemical and ultrastructural findings. Dig Dis Sci 1998; 43: 975-9.
35. Leuschner I, Radig K, Harms D. Desmoplastic small round cell tumor. Semin Diagn Pathol 1996; 13: 204-12.
36. Castleberry RP, Pritchard J, Ambros P, *et al.* The International Neuroblastoma Risk Groups (INRG): a preliminary report. Eur J Cancer 1997; 33: 2113-6.
37. Devall JM, Frush KM, Steiner L. Small blue round cell tumor: an unusual case presentation in the foot. J Am Podiatr Med Assoc 2011; 101: 363-9.
38. Santacruz MR, Proctor L, Thomas DB, Gehrig PA. Extraskeletal myxoid chondrosarcoma: a report of a gynecologic case. Gynecol Oncol 2005; 98: 498-501.
39. Shakked RJ, Geller DS, Gorlick R, Dorfman HD. Mesenchymal chondrosarcoma: clinicopathologic study of 20 cases. Arch Pathol Lab Med 2012; 136: 61-75.
40. Chong SM, Nilsson BS, Quah TC, Wee A. Malignant melanoma: an uncommon cause of small round cell malignancy in childhood. Acta Cytol 1997; 41: 609-10.

41. Bianchi L, Orlandi A, Iraci S, Spagnoli LG, Nini G. Solid alveolar rhabdomyosarcoma of the hand in adolescence: a clinical, histologic, immunologic, and ultrastructural study. Pediatr Dermatol 1995; 12: 343-7.
42. Kilpatrick SE, Doyon J, Choong PF, Sim FH, Nascimento AG. The clinicopathologic spectrum of myxoid and round cell liposarcoma. A study of 95 cases. Cancer 1996; 77: 1450-8.
43. Tsokos M, Alaggio RD, Dehner LP, Dickman PS. Ewing sarcoma/peripheral primitive neuroectodermal tumor and related tumors. Pediatr Dev Pathol 2012; 15(1 Suppl): 108-26.
44. Abe S. Ultrastructural and immunohistochemical study of Ewing's sarcoma and related tumors: morphological neural markers suggesting neural histogenesis in 32 small round-cell sarcomas. J Orthop Sci 1997; 2: 75-83.
45. Fisher C. The comparative roles of electron microscopy and immunohistochemistry in the diagnosis of soft tissue tumours. Histopathology 2006; 48: 32-41.
46. Joo M, Kang YK, Kim HS, Lee HK, Park YK. Mesenchymal chondrosarcoma of the hyoid bone: a case report. J Korean Med Sci 1998; 13: 696-700.
47. Llombart-Bosch A, Contesso G, Peydro-Olaya A. Histology, immunohistochemistry, and electron microscopy of small round cell tumors of bone. Semin Diagn Pathol 1996; 13: 153-70.
48. Martinez-Tello FJ, Navas-Palacios JJ. Ultrastructural study of conventional chondrosarcomas and myxoid- and mesenchymal-chondrosarcomas. Virchows Arch A Pathol Anat Histol 1982; 396: 197-211.
49. Roy S, Meachim G. Chondrocyte ultrastructure in adult human articular cartilage. Ann Rheum Dis 1968; 27: 544-58.
50. Kuroda N, Sogoh T, Ohara M, *et al.* Clear cell chondrosarcoma: an ultrastructural study. Med Mol Morphol 2009; 42: 185-8.
51. Corradi D, Bacchini P, Campanini N, Bertoni F. Aggressive clear cell chondrosarcomas: do distinctive characteristics exist?: a report of 4 cases. Arch Pathol Lab Med 2006; 130: 1673-9.
52. Mawad JK, Mackay B, Raymond AK, Ayala AG. Electron microscopy in the diagnosis of small round cell tumors of bone. Ultrastruct Pathol 1994; 18: 263-8.
53. Erlandson RA. The ultrastructural distinction between rhabdomyosarcoma and other undifferentiated "sarcomas". Ultrastruct Pathol 1987; 11: 83-101.
54. Abe S, Imamura T, Park P, *et al.* Small round-cell type of malignant peripheral nerve sheath tumor. Mod Pathol 1998; 11: 747-53.
55. Kurtkaya-Yapicier O, Scheithauer B, Woodruff JM. The pathobiologic spectrum of Schwannomas. Histol Histopathol 2003; 18: 925-34.
56. Kim NR, Chung DH, Park CY, Ha SY. Malignant peripheral nerve sheath tumor of the uterine cervix expressing both S-100 protein and HMB-45. J Obstet Gynaecol Res 2009; 35: 1136-41.
57. Eyden B. The myofibroblast: a study of normal, reactive and neoplastic tissues, with an emphasis on ultrastructure. part 2 - tumours and tumour-like lesions. J Submicrosc Cytol Pathol 2005; 37: 231-96.
58. Silverman JF, Landreneau RJ, Sturgis CD, *et al.* Small-cell variant of synovial sarcoma: fine-needle aspiration with ancillary features and potential diagnostic pitfalls. Diagn Cytopathol 2000; 23: 118-23.
59. Rong R, Doxtader EE, Tull J, de la Roza G, Zhang S. Metastatic poorly differentiated monophasic synovial sarcoma to lung with unknown primary: a molecular genetic analysis. Int J Clin Exp Pathol 2009; 3: 217-21.
60. Dickersin GR. Synovial sarcoma: a review and update, with emphasis on the ultrastructural characterization of the nonglandular component. Ultrastruct Pathol 1991; 15: 379-402.
61. Sandberg AA, Stone JF, Czarnecki L, Cohen JD. Hematologic masquerade of rhabdomyosarcoma. Am J Hematol 2001; 68: 51-7.
62. Ganesan P, Thulkar S, Rajan A, Bakhshi S. Solid variant of alveolar rhabdomyosarcoma mimicking non-Hodgkin lymphoma: case report and review of literature. J Pediatr Hematol Oncol 2008; 30: 772-4.
63. Kim NR, Lee WK, Lee JI, Cho HY. Multiple jejunal myeloid sarcomas presenting with intestinal obstruction in a non-leukemic patient: a case report with ultrastructural observations. Korean J Pathol 2012; 46: 590-4.
64. Dohner H, Estey EH, Amadori S, *et al.* Diagnosis and management of acute myeloid leukemia in adults: recommendations from an international expert panel, on behalf of the European LeukemiaNet. Blood 2010; 115: 453-74.
65. Dickersin GR. Electron microscopy of leukemias and lymphomas. Clin Lab Med 1987; 7: 199-247.
66. Goedhals J, Beukes CA, Cooper S. The ultrastructural features of plasmablastic lymphoma. Ultrastruct Pathol 2006; 30: 427-33.
67. Anderson DR. Ultrastructure of normal and leukemic leukocytes in human peripheral blood. J Ultrastruct Res 1966; 9: 1-42.
68. Takemori N, Hirai K, Onodera R, Saito N. Ultrastructural study of periodic lamellar granules in human neutrophils. Cell Tissue Res 1995; 281: 69-76.
69. Petitt M, Doeden K, Harris A, Bocklage T. Cutaneous extrarenal rhabdoid tumor with myogenic differentiation. J Cutan Pathol 2005; 32: 690-5.
70. Haberler C, Laggner U, Slavc I, *et al.* Immunohistochemical analysis of INI1 protein in malignant pediatric CNS tumors: Lack of INI1 in atypical teratoid/rhabdoid tumors and in a fraction of primitive neuroectodermal tumors without rhabdoid phenotype. Am J Surg Pathol 2006; 30: 1462-8.
71. Peng HQ, Stanek AE, Teichberg S, Shepard B, Kahn E. Malignant

 http://dx.doi.org/10.4132/jptm.2015.01.30

rhabdoid tumor of the kidney in an adult: a case report and review of the literature. Arch Pathol Lab Med 2003; 127: e371-3.
72. Parham DM, Weeks DA, Beckwith JB. The clinicopathologic spectrum of putative extrarenal rhabdoid tumors: an analysis of 42 cases studied with immunohistochemistry or electron microscopy. Am J Surg Pathol 1994; 18: 1010-29.
73. Magro CM, Crowson AN, Mihm MC. Unusual variants of malignant melanoma. Mod Pathol 2006; 19 Suppl 2: S41-70.

Journal of Pathology and Translational Medicine 2015; 49: 102-104
http://dx.doi.org/10.4132/jptm.2015.02.02

REVIEW

Role of Osteal Macrophages in Bone Metabolism

Sun Wook Cho

Department of Internal Medicine, Seoul National University Hospital, Seoul, Korea

Received: January 31, 2015
Accepted: February 2, 2015

Corresponding Author
Sun Wook Cho, M.D., Ph.D.
Department of Internal Medicine, Seoul National University Hospital, 101 Daehak-ro, Jongno-gu, Seoul 110-744, Korea
Tel: +82-2-2072-2114
Fax: +82-2-762-2292
E-mail: swchomd@gmail.com

Macrophages have been shown to have pleiotropic functions in various pathophysiologies, especially in terms of anti-inflammatory and regenerative activity. Recently, the novel functions of bone marrow resident macrophages (called osteal macrophages) were intensively studied in bone development, remodeling and tissue repair processes. This review discusses the current evidence for a role of osteal macrophages in bone modeling, remodeling, and fracture healing processes.

Key Words: Osteal macrophage; Bone remodeling; Fracture healing

Macrophages are abundant immune cells in bone marrow. Classically, macrophages are rapidly recruited into infectious or injured sites where they play critical roles in innate immunity. Moreover, macrophages regulate tissue homeostasis in various pathophysiologic processes including innate and adaptive immunity, wound healing, hematopoiesis, and malignancy. For examples, macrophages not only initiate tissue inflammation, but also promote wound healing and tissue remodeling.[1] Macrophages are schematically classified into two subtypes: classically activated, pro-inflammatory M1-macrophages and alternatively activated, anti-inflammatory/regenerative M2-macrophages.[1]

Apart from osteoclasts, osteal macrophages in bone marrow were recently recounted as a pivotal player in bone metabolism. In murine tissues, F4/80 monoclonal antibody[2] has been widely used to distinguish mature macrophages from osteoclasts, since F4/80 is rapidly down-regulated in the early stage of osteoclastogenesis.[3] At the bone and marrow interface, especially in the bone multicellular units, osteal macrophages form a cellular canopy structure over the bone-forming osteoblast.[4] In particular, the bone remodeling site, which is affected by anabolic factors such as parathyroid hormone (PTH; PTH1-34), showed augmented osteal macrophages (Fig. 1).[5] These observations suggest that osteal macrophages might play a role in bone remodeling.

OSTEAL MACROPHAGES IN BONE FORMATION

Evidence suggests that macrophages participate in pleiotropic aspects of bone metabolism. Macrophages have been involved in vascular calcification in ectopic bone formation. Co-culture of macrophages with calcifying vascular cells[6] or human vascular smooth muscle cells[7] enhanced alkaline phosphatase activity and mineralization potential. Tumor necrosis factor[6,7] and oncostatin M[7] have been suggested as molecular mediators of macrophage-derived vascular calcification. In addition, depletion of macrophages reduced osteophyte formation in osteoarthritic models,[8-10] and macrophages have been implicated in the sites of pathologic bone loss in inflammatory bone disorders.[11,12] These observations suggest that macrophages play a critical role in bone formation and mineralization.

Depletion of macrophages in primary calvarial osteoblast cultures *in vitro* has been shown to delay osteogenic differentiation and mineralization.[4,13] In the macrophage fas-induced apoptosis (Mafia) transgenic mouse model, short-term depletion of macrophages with treatment of a synthetic ligand *in vivo* showed a quantitative reduction of bone formation sites in endocortical bones.[4,13] In a recent study, *in vivo* long-term depletion of macrophages in young (3–21 days) and adult (16–22 months) Mafia mice demonstrated an osteopenic phenotypes with suppressed

pISSN 2383-7837
eISSN 2383-7845

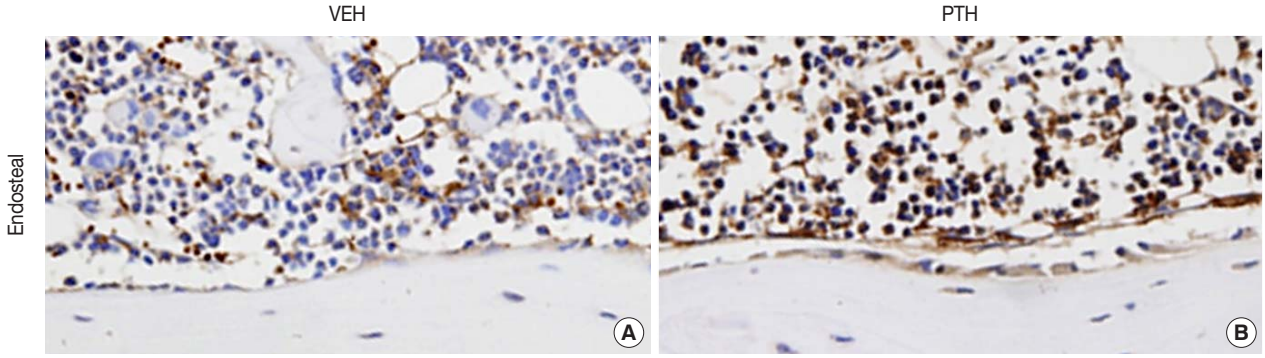

Fig. 1. Osteal macrophages at the bone formation sites of murine bones. F4/80-positive osteal macrophages create a canopy-like structure over the bone remodeling site. Compare to the vehicle (VEH) treatment (A), administration of parathyroid hormones (PTH) enhances bone formation, resulting in cuboidal-changes of osteoblasts and increased recruitment of osteal macrophages at bone remodeling sites (B).[5]

serum bone turnover markers.[5] The anabolic actions of PTH in bone were markedly reduced in this model.[5] This study reinforced the hypothesis that osteal macrophages play a pivotal role in bone anabolism. Another independent study with lysozyme M-deficient mice also showed that pre-natal macrophage depletion led to early skeletal growth retardation and progressive osteoporosis.[14] The latter two studies clearly showed that functional osteoclasts were not significantly affected in these macrophage-deficient models.[5,14] Taken together, these results suggest that osteal macrophages play an essential role in normal bone development and remodeling, especially through anabolic actions.

One of the critical concerns with osteal macrophages is how to distinguish bone marrow resident macrophages from osteoclasts, since they share the same precursors. Studies of Mafia mice[5] or lysozyme M-deficient mice[14] showed functionally active osteoclast activities, while macrophages were remarkably depleted, but still there were possible impacts of subtle changes in osteoclasts on overall bone metabolism. A recent study showed more clear evidence supporting the independent presence of functioning osteal macrophages apart from osteoclasts. CCL5-deficient mice showed decreased F4/80-positive macrophages at the endocortical bone surface, following reduced bone formation compared to the wild-type mice.[15] Osteoclastogenesis was enhanced in this model.[15] More studies with a bone marrow-specific macrophage depletion model are needed.

OSTEAL MACROPHAGES IN BONE REPAIR

Fracture healing is composed of inflammation and bone repair processes, including endochondral ossification. Previous studies have demonstrated that macrophages are present during multiple stages of fracture healing, and produce mesenchymal growth factors.[16] Macrophages are also associated with more stable callus formation and healthy union.[17]

Keeping pace with the studies of osteal macrophages in bone metabolism, several groups have extensively studied how osteal macrophages participate in fracture healing of bone. Both systemic and local depletions of macrophages delayed fracture healing and impaired woven bone formation, while treatment of colony stimulating factor 1 increased macrophage recruitment into the injury sites and supported woven bone formation.[18] This study showed that macrophages were essential for collagen type I-positive matrix formation and bone mineralization.[18] Similarly, an independent study also showed that depletion of macrophages during fracture repair, even after several days later to fracture, led to impaired bone union with incomplete callus formation accompanied with more fibrotic changes. They observed that macrophages were also involved in promoting the osteogenic differentiation of marrow mesenchymal progenitor cells.[14] Moreover, a recent study clarified that inflammatory M1-macrophages ($F4/80^+Mac\text{-}2^+$) played a crucial role in the initiation of early inflammation, and both inflammatory ($F4/80^+Mac\text{-}2^+$) and resident ($F4/80^+Mac\text{-}2^-$) macrophages derived anabolic signals for endochondral callus formations in murine fracture models.[19] Taken together, accumulating evidence suggests that macrophages and their specific molecular mediators contribute to fracture healing in a phase-specific polarization-dependent manner.

CONCLUSIONS AND FUTURE DIRECTIONS

To date, osteal macrophages have been considered a third cellular component, in addition to osteoblasts and osteoclasts. Mac-

rophages construct a cellular canopy structure over bone remodeling sites, coordinate osteoclast-to-osteoblast coupling, and drive anabolic cytokines for bone formation. Macrophages also create a regenerative microenvironment in the fracture healing processes. In addition, macrophages might play a role in bone and marrow interactions especially at the osteoblastic stem cell niche. Targeting osteal macrophages or their molecular mediators could be potent therapeutic challenges for developing anabolic therapies for bone disease. Further studies are needed to develop specific targets that could be distinguished from osteoclast or inflammatory macrophages.

Conflicts of Interest

No potential conflict of interest relevant to this article was reported.

REFERENCES

1. Murray PJ, Wynn TA. Protective and pathogenic functions of macrophage subsets. Nat Rev Immunol 2011; 11: 723-37.
2. Austyn JM, Gordon S. F4/80, a monoclonal antibody directed specifically against the mouse macrophage. Eur J Immunol 1981; 11: 805-15.
3. Lean JM, Matsuo K, Fox SW, *et al.* Osteoclast lineage commitment of bone marrow precursors through expression of membrane-bound TRANCE. Bone 2000; 27: 29-40.
4. Chang MK, Raggatt LJ, Alexander KA, *et al.* Osteal tissue macrophages are intercalated throughout human and mouse bone lining tissues and regulate osteoblast function *in vitro* and *in vivo*. J Immunol 2008; 181: 1232-44.
5. Cho SW, Soki FN, Koh AJ, *et al.* Osteal macrophages support physiologic skeletal remodeling and anabolic actions of parathyroid hormone in bone. Proc Natl Acad Sci U S A 2014; 111: 1545-50.
6. Tintut Y, Patel J, Territo M, Saini T, Parhami F, Demer LL. Monocyte/macrophage regulation of vascular calcification *in vitro*. Circulation 2002; 105: 650-5.
7. Shioi A, Katagi M, Okuno Y, *et al.* Induction of bone-type alkaline phosphatase in human vascular smooth muscle cells: roles of tumor necrosis factor-alpha and oncostatin M derived from macrophages. Circ Res 2002; 91: 9-16.
8. van Lent PL, Blom AB, van der Kraan P, *et al.* Crucial role of synovial lining macrophages in the promotion of transforming growth factor beta-mediated osteophyte formation. Arthritis Rheum 2004; 50: 103-11.
9. Blom AB, van Lent PL, Holthuysen AE, *et al.* Synovial lining macrophages mediate osteophyte formation during experimental osteoarthritis. Osteoarthritis Cartilage 2004; 12: 627-35.
10. Kamekura S, Hoshi K, Shimoaka T, *et al.* Osteoarthritis development in novel experimental mouse models induced by knee joint instability. Osteoarthritis Cartilage 2005; 13: 632-41.
11. Kaneko M, Tomita T, Nakase T, *et al.* Expression of proteinases and inflammatory cytokines in subchondral bone regions in the destructive joint of rheumatoid arthritis. Rheumatology (Oxford) 2001; 40: 247-55.
12. Haynes DR, Hay SJ, Rogers SD, Ohta S, Howie DW, Graves SE. Regulation of bone cells by particle-activated mononuclear phagocytes. J Bone Joint Surg Br 1997; 79: 988-94.
13. Pettit AR, Chang MK, Hume DA, Raggatt LJ. Osteal macrophages: a new twist on coupling during bone dynamics. Bone 2008; 43: 976-82.
14. Vi L, Baht GS, Whetstone H, *et al.* Macrophages promote osteoblastic differentiation in-vivo: implications in fracture repair and bone homeostasis. J Bone Miner Res 2014 Dec 8 [Epub]. http://dx.doi.org/10.1002/jbmr.2422.
15. Wintges K, Beil FT, Albers J, *et al.* Impaired bone formation and increased osteoclastogenesis in mice lacking chemokine (C-C motif) ligand 5 (Ccl5). J Bone Miner Res 2013; 28: 2070-80.
16. Bourque WT, Gross M, Hall BK. Expression of four growth factors during fracture repair. Int J Dev Biol 1993; 37: 573-9.
17. Hankemeier S, Grassel S, Plenz G, Spiegel HU, Bruckner P, Probst A. Alteration of fracture stability influences chondrogenesis, osteogenesis and immigration of macrophages. J Orthop Res 2001; 19: 531-8.
18. Alexander KA, Chang MK, Maylin ER, *et al.* Osteal macrophages promote *in vivo* intramembranous bone healing in a mouse tibial injury model. J Bone Miner Res 2011; 26: 1517-32.
19. Raggatt LJ, Wullschleger ME, Alexander KA, *et al.* Fracture healing via periosteal callus formation requires macrophages for both initiation and progression of early endochondral ossification. Am J Pathol 2014; 184: 3192-204.

 http://dx.doi.org/10.4132/jptm.2015.02.02

Journal of Pathology and Translational Medicine 2015; 49: 105-111
http://dx.doi.org/10.4132/jptm.2015.01.19

■ ORIGINAL ARTICLE ■

Overexpression of C-reactive Protein as a Poor Prognostic Marker of Resectable Hepatocellular Carcinomas

Jin Ho Shin · Chong Jai Kim
Eun Jeong Jeon · Chang Ohk Sung
Hwa Jeong Shin · Jene Choi
Eunsil Yu

Department of Pathology, Asan Medical Center, University of Ulsan College of Medicine, Seoul, Korea

Received: November 20, 2014
Revised: January 9, 2015
Accepted: January 19, 2015

Corresponding Authors
Chong Jai Kim, M.D.
Department of Pathology, Asan Medical Center, University of Ulsan College of Medicine, 88 Olympic-ro 43-gil, Songpa-gu, Seoul 138-736, Korea
Tel: +82-2-3010-4516
Fax: +82-2-472-7898
E-mail: ckim@amc.seoul.kr

Eunsil Yu, M.D.
Department of Pathology, Asan Medical Center, University of Ulsan College of Medicine, 88 Olympic-ro 43-gil, Songpa-gu, Seoul 138-736, Korea
Tel: +82-2-3010-4552
Fax: +82-2-472-7898
E-mail: esyu@amc.seoul.kr

Background: C-reactive protein (CRP) is an acute phase reactant synthesized in the liver. CRP immunoreactivity is a feature of inflammatory hepatocellular adenomas with a higher risk of malignant transformation. A high serum CRP level denotes poor prognosis in hepatocellular carcinoma (HCC) patients. This study was conducted to determine whether CRP is produced in HCC and to assess the clinicopathologic significance of CRP expression in cancer cells. **Methods:** CRP immunoreactivity was examined in treatment-naïve HCCs (n=224) using tissue microarrays and was correlated with clinicopathologic parameters. The expression of CRP mRNA and protein was also assessed in 12 HCC cases by quantitative real-time polymerase chain reaction and immunoblotting. Hep3B and SNU-449 HCC cell lines were used for the analysis of CRP mRNA regulation by interleukin 6 (IL-6). **Results:** CRP was expressed in 133 of 224 HCCs (59.4%) with a variable degree of immunoreactivity (grade 1 in 25.9%; grade 2 in 20.1%; grade 3 in 13.4%). There was an inverse relationship between grade 3 CRP immunoreactivity and cancer-specific survival (p=.0047), while no associations were found with other parameters, including recurrence-free survival. The CRP mRNA expression level was significantly higher in CRP immunopositive cases than in immunonegative cases (p<.05). CRP mRNA expression was increased in Hep3B cells, but was not detected in SNU-449 cells even after IL-6 treatment. **Conclusions:** We report the expression of CRP in HCC for the first time. CRP expression was associated with poor cancer-specific survival in patients with resectable HCC.

Key Words: Carcinoma, hepatocellular; C-reactive protein; Immunohistochemistry; Prognosis

Acute phase reactants are a group of hepatic proteins that are synthesized and released into the circulation in response to certain stresses such as infection and physical injury.[1] C-reactive protein (CRP) is a well-known, major acute phase reactant that was originally found in the sera of patients infected with *Streptococcus pneumoniae*.[2,3] CRP mRNA transcription is primarily induced by pro-inflammatory cytokines interleukin (IL)-6 and IL-1.[4-6] The blood concentration of CRP is increased in inflammatory conditions of both infectious and non-infectious etiologies such as urinary tract infection and hyperlipidemic acute pancreatitis.[7,8] A growing body of evidence indicates a solid pathobiological relationship between chronic inflammation and carcinogenesis.[9] Innate immune components such as Toll-like receptors and NOD-like receptors play a role in the regulation of inflammation and development of cancer.[10-12] Serum CRP level has been shown to be a prognostic marker in various human cancers.[13,14] Likewise, high serum CRP level is a poor prognostic factor in hepatocellular carcinoma (HCC) in relation to early recurrence.[15,16]

As hepatocytes are the primary origin of CRP synthesis, it is highly likely that neoplastic hepatocytes retain a functional capacity to synthesize CRP under the influence of pro-inflammatory stimuli. Not surprisingly, CRP expression has been rather extensively studied in hepatocellular adenomas,[17,18] and CRP immunoreactivity is a critical parameter for molecular phenotyping and defining of the inflammatory subtype of hepatocel-

pISSN 2383-7837
eISSN 2383-7845

lular adenoma, which has a higher risk of malignant transformation.[19-21] Of note, based on the results of immunohistochemistry using a panel of antibodies and fluorescence *in situ* hybridization for gains of chromosomes 1, 8, and MYC in HCC arising in adenoma, Kakar *et al.*[22] recently proposed that a certain subset of hepatocellular adenomas may represent a well-differentiated version of HCCs. However, CRP expression in HCCs has not yet been studied. We postulated that the evaluation of CRP expression in HCC may provide valuable information regarding the unique biology of HCCs. This study was conducted to determine whether CRP is produced by HCC cells and to assess its clinicopathologic significance.

MATERIALS AND METHODS

Patients and tissue samples

A total of 224 cases of treatment-naïve HCCs (n = 224) were retrieved from the files of the Department of Pathology, Asan Medical Center, Seoul, Korea. All cases were surgically resectable (R0). Early recurrence was defined as a recurrence of the tumor within 2 years after surgery. All patients provided written informed consent, and this study was approved by the Institutional Review Board of Asan Medical Center, Seoul, Korea.

Tissue microarray and immunohistochemistry

Tissue microarrays were prepared using representative formalin-fixed, paraffin-embedded blocks of HCC cases. Two 2-mm-thick tissue cores were obtained from the donor blocks and transferred onto the recipient blocks after reviewing hematoxylin and eosin–stained slides. Four-micrometer-thick tissue microarray sections were immunostained using a rabbit polyclonal anti-CRP antibody (1:1,000, AbCam, Cambridge, UK). The sections were transferred onto silanized slides, and heat-induced epitope retrieval was performed by treating the slides with Cell Conditioning 1 buffer for 32 minutes in a BenchMark XT automatic immunostainer (Ventana Medical Systems, Tucson, AZ, USA). The signals were detected using the OptiView DAB IHC Detection Kit (Ventana Medical Systems). The immunoreactivity was evaluated by a pathologist (C.J.K.) blinded to clinical information, using a 4-tier grading system: negative, grade 0; positive in less than 10% of tumor cells, grade 1; positive in less than 50% of tumor cells, grade 2; diffusely positive, grade 3.

Cell culture

Human HCC cell lines, Hep3B and SNU-449, were used for the analysis of CRP mRNA regulation by IL-6. Hep3B cells were cultured in Dulbecco's modified Eagle medium (Life Technologies, Carlsbad, CA, USA) supplemented with 10% fetal bovine serum (FBS) and 1% penicillin/streptomycin. SNU-449 cells were cultured in RPMI 1640 medium (GE Healthcare Life Sciences, Pittsburgh, PA, USA) supplemented with 10% FBS and 1% penicillin/streptomycin. For IL-6 treatment, 5×10^5 cells were seeded into 100-mm dishes and were treated with 50 ng/mL of IL-6 (Cell Sciences, Canton, MA, USA) on the following day for 6 hours.

Quantitative real-time polymerase chain reaction

Total RNA was isolated from liver tissues (n = 12) and cultured Hep3B and SNU-449 cells using Trizol and the miRNeasy Mini Kit (Qiagen, Hilden, Germany) according to the manufacturer's instructions. The extracted RNA (1 μg) was reverse-transcribed using the Reverse Transcription System (Promega, Madison, WI, USA). Quantitative real-time polymerase chain reaction (qRT-PCR) analyses of CRP mRNA expression were performed using a TaqMan Gene Expression Assay (Hs00357041_m1, Applied Biosystems, Carlsbad, CA, USA) and an ABI PRISM 7000 Sequence Detection System (Applied Biosystems). The human RPLPO (Large Ribosomal Protein) was used as an endogenous control for normalization.

Immunoblotting

Immunoblotting was done in 12 cases. Liver tissues were pulverized in liquid nitrogen, and total protein lysates were obtained using RIPA lysis buffer. Thirty micrograms of protein were electrophoresed in 12% sodium dodecyl sulfate–polyacrylamide gel and transferred onto polyvinylidene fluoride membranes (GE Healthcare Life Sciences). The membranes were blocked with 5% bovine serum albumin in Tris-buffered saline with 0.1% Tween 20 (TBS-T) and incubated at 4°C overnight with mouse monoclonal primary antibodies against CRP (1:1,000, AbCam, Cambridge, MA, USA) and vinculin (1:1,000; Sigma-Aldrich, St. Louis, MO, USA), respectively. The blots were subsequently incubated at room temperature with horseradish peroxidase–conjugated secondary antibody for 1 hour (Cell Signaling Technology, Danvers, MA, USA). The signals were detected using a SuperSignal West Dura Chemiluminescent Substrate (Thermo Scientific, Waltham, MA, USA).

Statistical analyses

The analyses of continuous variables and proportions were done using Pearson's chi-square test and Fisher exact test. The survival analysis was done using the Kaplan-Meier method. In-

http://dx.doi.org/10.4132/jptm.2015.01.19

dependent variables and groups were compared using the Mann-Whitney U test. SPSS ver. 18.0 software (SPSS Inc., Chicago, IL, USA) was used for all statistical analyses.

RESULTS

CRP expression in HCC

The demographics of the study population are summarized in Table 1. CRP immunoreactivity was observed as diffuse cytoplasmic immunostaining. Overall, 59.4% (133/224) of HCC cases were immunopositive for CRP, with grades 1, 2, and 3 immunoreactivity in 25.9% (58/224), 20.1% (45/224), and 13.4% (30/224) of the cases, respectively (Fig. 1). When we analyzed the relationship between multiple clinicopathologic parameters and CRP immunoreactivity, we found a significant difference in cancer-specific survival between CRP-negative or non-diffuse immunopositive cases (grades 0, 1, and 2) and grade 3 immunopositive cases (Fig. 2A). Grade 3 CRP immunopositive cases showed significantly shorter survival compared to CRP-negative or non-diffuse immunopositive cases (median of 50.7 months and range of 6-58 months vs. median of 58.5 months and range of 5–88 years; p = .0047). However, no significant correlation was found between the degree of CRP immunoreactivity and other clinicopathologic parameters including recurrence-free survival (Fig. 2B).

Table 1. Clinical parameters and their relationship with CRP immunoreactivity

Clinical parameter	CRP grade 0, 1, 2	CRP grade 3	p-value
Gender			.019
Male	150 (67.0)	20 (8.9)	
Female	44 (19.6)	10 (4.5)	
Age (yr)			.054
< 60	123 (54.9)	22 (9.8)	
≥ 60	71 (31.7)	8 (3.6)	
Tumor size (cm)			.110
< 5	138 (61.6)	19 (8.5)	
≥ 5	56 (25.0)	11 (4.9)	
Serum AFP (ng/mL)			.125
< 400	141 (62.9)	24 (10.7)	
≥ 400	53 (23.6)	6 (2.7)	
BCLC stage			< .001
A	185 (82.6)	26 (11.6)	
B	9 (4.0)	4 (1.8)	
Etiology			.096
HBV	139 (62.1)	23 (10.3)	
HCV	20 (8.9)	1 (0.4)	
NBNC	35 (15.6)	6 (2.7)	
Fibrosis stage (Batts-Ludwig)			.454
Stage 1, 2	39 (17.4)	7 (3.1)	
Stage 3, 4	155 (69.2)	23 (10.3)	
Microvascular invasion			.983
Not identified	136 (60.7)	21 (9.4)	
Present	58 (25.9)	9 (4.0)	
Tumor number			< .001
< 3	185 (82.6)	26 (11.6)	
≥ 3	9 (4.0)	4 (1.8)	
Edmondson-Steiner grade (worst)			.814
Grade 1, 2	67 (29.9)	10 (4.5)	
Grade 3, 4	127 (56.7)	20 (8.9)	
Edmondson-Steiner grade (most)			.241
Grade 1, 2	128 (57.1)	18 (8.0)	
Grade 3, 4	66 (29.5)	12 (5.4)	
Capsular invasion			.492
Absent	156 (69.6)	25 (11.2)	
Present	38 (17.0)	5 (2.2)	
Early recurrence			.098
Absent	114 (50.9)	15 (6.7)	
Occurs	80 (35.7)	15 (6.7)	

Values are presented as number (%).
CRP, C-reactive protein; AFP, alpha-fetoprotein; BCLC, Barcelona Clinic Liver Cancer; HBV, hepatitis B virus; HCB, hepatitis C virus; NBNC, non-B, non-C hepatocellular carcinoma.

CRP mRNA expression in HCC

We further analyzed CRP protein and mRNA expression in HCCs (n = 12) to see whether CRP expression is regulated at the transcriptional level. Immunoblotting for CRP confirmed variable expression of CRP in HCC cases (Fig. 3A). CRP signals were readily detected in six cases, but not in the remaining six cases. qRT-PCR analysis demonstrated a higher CRP mRNA expression in CRP immunopositive cases than in immunonegative cases (p = .046; ΔCt median of 3.62, range of 2.8–5.98 vs ΔCt median of 8.56, range of 1.07–15) (Fig. 3B).

After confirming the relationship between CRP protein and mRNA expression, we tested if CRP mRNA transcription was dependent on pro-inflammatory mediators. The treatment of Hep3B and SNU-449 cells with IL-6 at the concentration of 50 ng/mL for 6 hours induced a 17.5-fold increase in CRP mRNA expression in Hep3B cells, but CRP mRNA expression was not detected in SNU-449 cells even after IL-6 treatment (Fig. 4).

DISCUSSION

The primary findings of this study are (1) CRP expression is relatively common in HCCs, with variable immunoreactivity in nearly 60% of the cases tested, (2) there is an inverse relationship between diffuse and strong CRP immunoreactivity and cancer-specific patient survival (p = .0047), (3) CRP-positive cases in immunoblotting showed significantly higher CRP mRNA expression, suggesting that increased CRP production is a consequence of transcriptional activation of CRP, and (4) CRP mRNA transcription is induced by IL-6 in Hep3B cells, but not in SNU-449 cells, suggesting that CRP expression marks distinct mo-

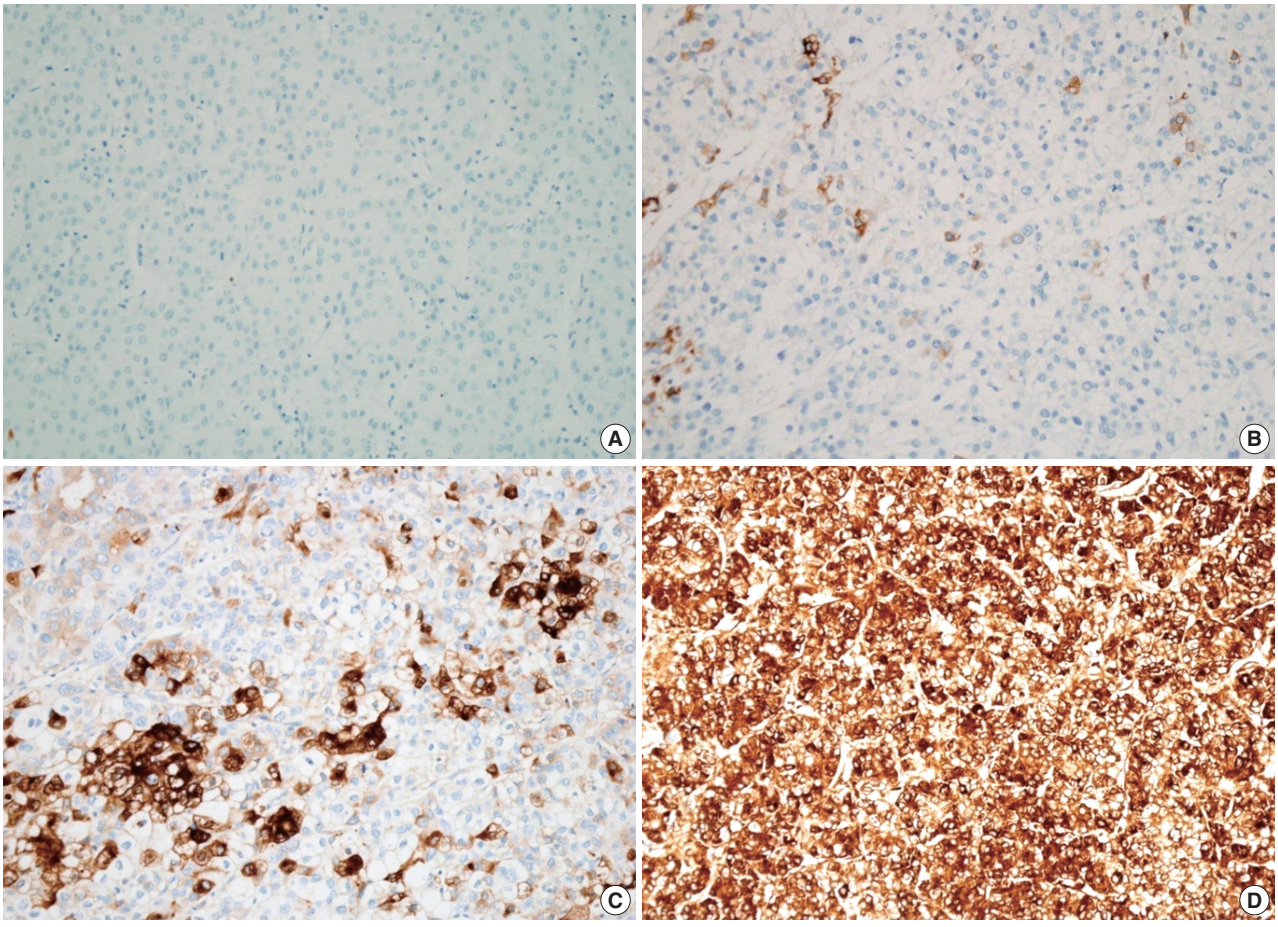

Fig. 1. Cytoplasmic C-reactive protein (CRP) immunoreactivity in hepatocellular carcinoma cases. Immunoreactivity is analyzed using a 4-tier grading system: grade 0 (A), grade 1 (B), grade 2 (C), and grade 3 (D).

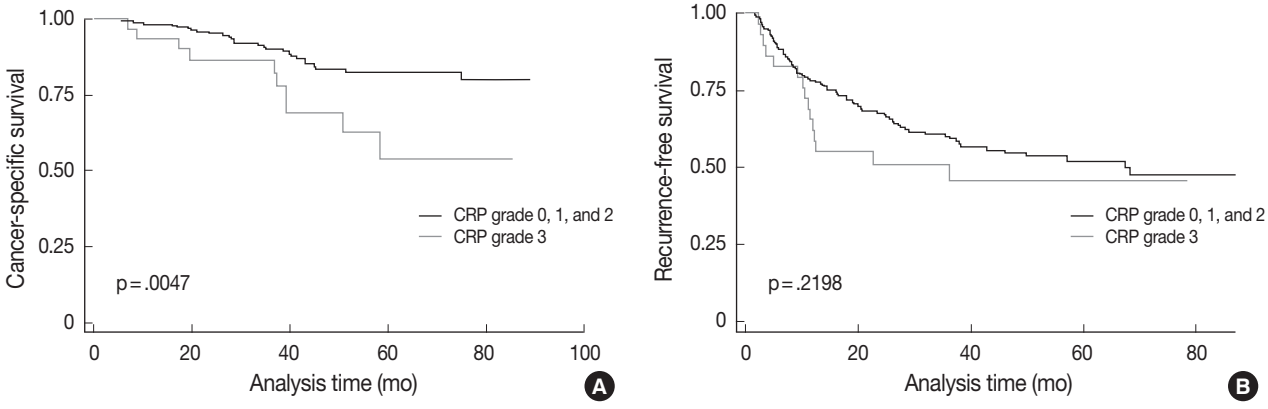

Fig. 2. Clinical significance of C-reactive protein (CRP) immunoreactivity. (A) There is a significant difference in cancer-specific survival between patients with CRP grade 3 hepatocellular carcinomas (HCCs) and those with CRP grade 0, 1, and 2 HCCs. (B) There is no difference in recurrence-free survival between the two groups.

lecular phenotypes among HCCs.

Hepatocellular carcinogenesis represents a classic model of viral etiology associated with chronic inflammation.[23] The elevation of inflammatory biomarkers such as CRP, IL-6, C-peptide, and adiponectin is associated with a higher risk of HCC.[24] Several investigations have addressed the clinical significance of

http://dx.doi.org/10.4132/jptm.2015.01.19

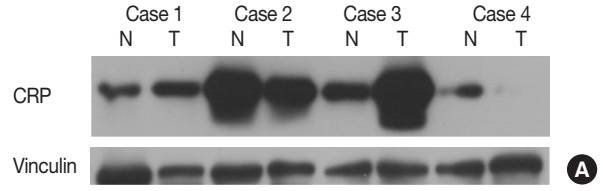

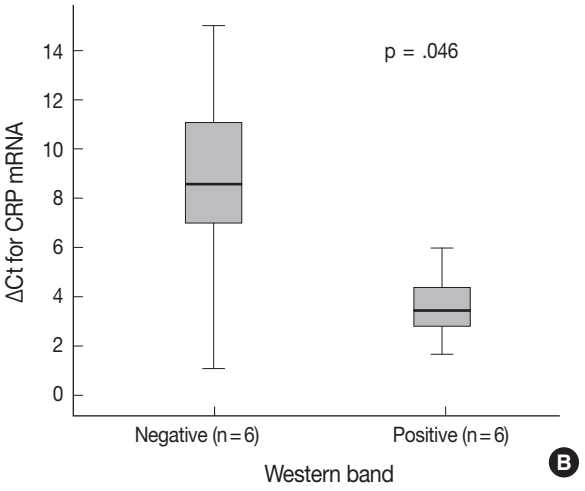

Fig. 3. Correlation between C-reactive protein (CRP) mRNA and protein expression in hepatocellular carcinomas (HCCs). (A) Immunoblotting for CRP protein shows variable expression in HCCs (N, non-neoplastic liver; T, HCC). CRP protein expression is not found in the tumor of case 4, while CRP bands are readily detectable in both non-neoplastic and HCC samples of cases 1, 2, and 3. (B) Quantitative real-time polymerase chain reaction results are shown in box plots of ΔCt for CRP mRNA expression (Ct_CRP–Ct_RPLPO).

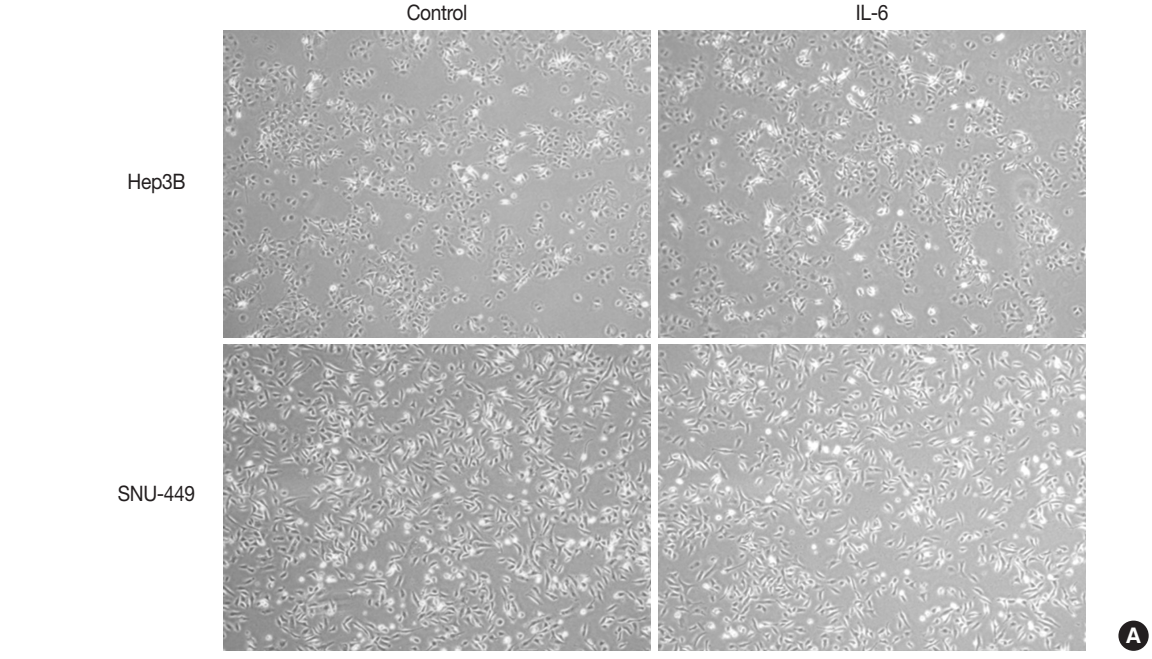

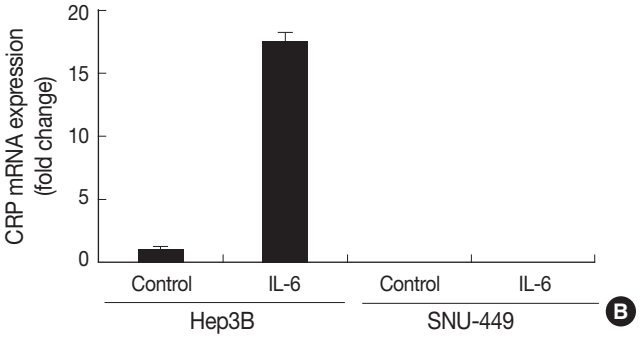

Fig. 4. Induction of C-reactive protein (CRP) mRNA in Hep3B and SNU-449 hepatocellular carcinoma cell lines after interleukin 6 (IL-6) treatment. (A) There are no significant changes in cellular morphology in either cell line after IL-6 treatment. (B) There is a 17.5-fold increase in CRP mRNA expression in IL-6–treated Hep3B cells (50 ng/mL for 6 hours), while CRP mRNA expression is not detected in SNU-449 cells. The y-axis represents fold-changes in CRP mRNA expression following IL-6 treatment.

serum CRP. Serum CRP has been consistently shown to be a key component of inflammation-based prognostication of HCC. Mori *et al.*[25] proposed that a preoperative scoring system based on the preoperative serum concentration of CRP and alpha-fetoprotein has a prognostic value in patients with HCC after hepatectomy. Although the contribution of CRP produced by tumor cells to the elevation of serum CRP cannot be directly assessed, it is very probable that CRP of tumor origin is released

into the systemic circulation. Although we expected certain differences in clinicopathologic characteristics between CRP immunopositive and immunonegative HCCs, a clear difference was found only in the cancer-specific survival of strong CRP immunopositive cases.

One of the major potential drives for CRP overexpression is IL-6, and a role of IL-6 in hepatocellular carcinogenesis has been strongly suggested. When compared to healthy controls, cirrhotic patients and HCC patients had serum IL-6 concentrations that were 4-fold and 25-fold higher, respectively.[26] IL-6 signaling mediated via IL-6 receptors activates STAT3, mitogen-activated protein kinase, and phosphatidylinositol 3-kinase pathways. IL-6–mediated STAT3 activation is known to be a biological link between chronic inflammation and carcinogenesis,[27] and IL-6 confers anti-apoptotic effects to cells. Blocking STAT3 activation using STAT3 siRNA or small molecular STAT3 inhibitor LLL 12 has been shown to abrogate the anti-apoptotic effects of IL-6 against doxorubicin-induced apoptosis in SNU-449 HCC cells, which express a higher level of endogenous IL-6 compared to Hep3B cells.[28] We thought that CRP would be induced in both Hep3B and SNU-449 cells by IL-6 treatment. However, CRP mRNA expression after IL-6 treatment was significantly different between SNU-449 cells and Hep3B cells. Therefore, the observations in HCC tissue samples and the cell lines *in vitro* indicate that the degree of CRP expression involves several mechanisms, which need further elucidation.

A major drawback of this study is that serum CRP or IL-6 levels could not be determined due to a lack of blood samples. Future analyses of the relationship between the CRP-positive HCC phenotype and systemic inflammatory profile will provide a more comprehensive understanding of the biology of HCC. We also could not determine the underlying biochemical mechanisms involved in the differential IL-6-induced responses between Hep3B and SNU-449 cells in terms of induction of CRP mRNA expression. Considering the complexities of IL-6 signaling and CRP transcription, more *in vitro* studies are necessary.

In summary, we report the expression of CRP in HCC for the first time, and provide evidence to support the significance of CRP in HCC based on the clear difference in cancer-specific survival between CRP-positive and -negative cases. Overall findings strongly suggest that CRP is a marker for future molecular phenotyping of HCC.

Conflicts of Interest

No potential conflict of interest relevant to this article was reported.

Acknowledgments

This work was supported by a grant (14-521) from the Asan Institute for Life Sciences, Seoul, Korea.

REFERENCES

1. Lazzarotto C, Ronsoni MF, Fayad L, *et al.* Acute phase proteins for the diagnosis of bacterial infection and prediction of mortality in acute complications of cirrhosis. Ann Hepatol 2013; 12: 599-607.
2. Kushner I, Feldmann G. Control of the acute phase response: demonstration of C-reactive protein synthesis and secretion by hepatocytes during acute inflammation in the rabbit. J Exp Med 1978; 148: 466-77.
3. Volanakis JE, Kaplan MH. Specificity of C-reactive protein for choline phosphate residues of pneumococcal C-polysaccharide. Proc Soc Exp Biol Med 1971; 136: 612-4.
4. Castell JV, Gómez-Lechón MJ, David M, *et al.* Interleukin-6 is the major regulator of acute phase protein synthesis in adult human hepatocytes. FEBS Lett 1989; 242: 237-9.
5. Castell JV, Gómez-Lechón MJ, David M, Fabra R, Trullenque R, Heinrich PC. Acute-phase response of human hepatocytes: regulation of acute-phase protein synthesis by interleukin-6. Hepatology 1990; 12: 1179-86.
6. Yoshizaki K. Pathogenic role of IL-6 combined with TNF-alpha or IL-1 in the induction of acute phase proteins SAA and CRP in chronic inflammatory diseases. Adv Exp Med Biol 2011; 691: 141-50.
7. de Man P, Jodal U, Svanborg C. Dependence among host response parameters used to diagnose urinary tract infection. J Infect Dis 1991; 163: 331-5.
8. Yin G, Hu G, Cang X, *et al.* C-reactive protein: rethinking its role in evaluating the severity of hyperlipidemic acute pancreatitis. Pancreas 2014; 43: 1323-8.
9. Lee CH, Chang JS, Syu SH, *et al.* IL-1beta promotes malignant transformation and tumor aggressiveness in oral cancer. J Cell Physiol 2015; 230: 875-84.
10. Sipos F, Műri I, Constantinovits M, Tulassay Z, Műzes G. Contribution of TLR signaling to the pathogenesis of colitis-associated cancer in inflammatory bowel disease. World J Gastroenterol 2014; 20: 12713-21.
11. Saxena M, Yeretssian G. NOD-like receptors: master regulators of inflammation and cancer. Front Immunol 2014; 5: 327.
12. Castaño-Rodríguez N, Kaakoush NO, Mitchell HM. Pattern-recognition receptors and gastric cancer. Front Immunol 2014; 5: 336.
13. Szkandera J, Stotz M, Absenger G, *et al.* Validation of C-reactive protein levels as a prognostic indicator for survival in a large cohort of pancreatic cancer patients. Br J Cancer 2014; 110: 183-8.

14. Yi JH, Wang D, Li ZY, Hu J, Niu XF, Liu XL. C-reactive protein as a prognostic factor for human osteosarcoma: a meta-analysis and literature review. PLoS One 2014; 9: e94632.
15. Zheng Z, Zhou L, Gao S, Yang Z, Yao J, Zheng S. Prognostic role of C-reactive protein in hepatocellular carcinoma: a systematic review and meta-analysis. Int J Med Sci 2013; 10: 653-64.
16. Nishikawa H, Arimoto A, Wakasa T, Kita R, Kimura T, Osaki Y. Pretreatment C-reactive protein as a prognostic factor for recurrence after surgical resection of hepatocellular carcinoma. Anticancer Res 2013; 33: 1181-8.
17. Bioulac-Sage P, Rebouissou S, Thomas C, *et al.* Hepatocellular adenoma subtype classification using molecular markers and immunohistochemistry. Hepatology 2007; 46: 740-8.
18. Han J, van den Heuvel MC, Kusano H, de Jong KP, Gouw AS. How normal is the liver in which the inflammatory type hepatocellular adenoma develops? Int J Hepatol 2012; 2012: 805621.
19. Bioulac-Sage P, Laumonier H, Cubel G, Rossi JZ, Balabaud C. Hepatic resection for inflammatory hepatocellular adenomas: pathological identification of micronodules expressing inflammatory proteins. Liver Int 2010; 30: 149-54.
20. Fonseca S, Hoton D, Dardenne S, *et al.* Histological and immunohistochemical revision of hepatocellular adenomas: a learning experience. Int J Hepatol 2013; 2013: 398308.
21. Sempoux C, Chang C, Gouw A, *et al.* Benign hepatocellular nodules: what have we learned using the patho-molecular classification. Clin Res Hepatol Gastroenterol 2013; 37: 322-7.
22. Kakar S, Grenert JP, Paradis V, Pote N, Jakate S, Ferrell LD. Hepatocellular carcinoma arising in adenoma: similar immunohistochemical and cytogenetic features in adenoma and hepatocellular carcinoma portions of the tumor. Mod Pathol 2014; 27: 1499-509.
23. Tarocchi M, Polvani S, Marroncini G, Galli A. Molecular mechanism of hepatitis B virus-induced hepatocarcinogenesis. World J Gastroenterol 2014; 20: 11630-40.
24. Aleksandrova K, Boeing H, Nöthlings U, *et al.* Inflammatory and metabolic biomarkers and risk of liver and biliary tract cancer. Hepatology 2014; 60: 858-71.
25. Mori S, Kita J, Kato M, Shimoda M, Kubota K. Usefulness of a new inflammation-based scoring system for prognostication of patients with hepatocellular carcinoma after hepatectomy. Am J Surg 2015; 209: 187-93.
26. Porta C, De Amici M, Quaglini S, *et al.* Circulating interleukin-6 as a tumor marker for hepatocellular carcinoma. Ann Oncol 2008; 19: 353-8.
27. Hodge DR, Hurt EM, Farrar WL. The role of IL-6 and STAT3 in inflammation and cancer. Eur J Cancer 2005; 41: 2502-12.
28. Liu Y, Li PK, Li C, Lin J. Inhibition of STAT3 signaling blocks the anti-apoptotic activity of IL-6 in human liver cancer cells. J Biol Chem 2010; 285: 27429-39.

Journal of Pathology and Translational Medicine 2015; 49: 112-117
http://dx.doi.org/10.4132/jptm.2015.01.31

■ ORIGINAL ARTICLE ■

The Diagnostic Usefulness of HMGA2, Survivin, CEACAM6, and SFN/14-3-3 δ in Follicular Thyroid Carcinoma

Min Hye Jang[1,2] · Kyeong Cheon Jung[2] Hye Sook Min[3]

[1]Department of Pathology, Seoul National University Bundang Hospital, Seongnam; [2]Department of Pathology, Seoul National University College of Medicine, Seoul; [3]Department of Epidemiology and Preventive Medicine, Graduate School of Public Health, Seoul National University, Seoul, Korea

Received: January 5, 2015
Revised: January 29, 2015
Accepted: January 30, 2015

Corresponding Author
Hye Sook Min, M.D.
Department of Epidemiology and Preventive Medicine, Graduate School of Public Health, Seoul National University, 1 Gwanak-ro, Gwanak-gu, Seoul 151-742, Korea
Tel: +82-2-880-2743
Fax: +82-2-762-9105
E-mail: lilloa@snu.ac.kr

Background: Follicular thyroid carcinoma (FTC) is the second most common thyroid malignancy and its differential diagnosis includes follicular adenoma (FA) and adenomatous goiter (AG). Several ancillary markers have been suggested to aid in the diagnosis of FTC, but the successful use of these methods still needs to be validated. **Methods:** In the present study, we verified the immunoexpression of HMGA2, CEACAM6, survivin, and SFN/14-3-3 δ in lesions including 41 AGs, 72 FAs, and 79 FTCs. We evaluated their diagnostic usefulness, combined with galectin 3, Hector Battifora mesothelial 1 (HBME1), cytokeratin 19, and cyclin D1, in diagnosing FTC. **Results:** The expressions of HBME1 (65.8%) and HMGA2 (55.7%) were significantly higher in FTCs than in FAs and AGs ($p < .001$ and $p = .005$, respectively). HBME1 was the only marker that was more frequently expressed in FTCs than in FAs ($p = .021$) and it was more frequently expressed in follicular neoplasms than in AGs ($p < .001$). Among the novel markers, the combination of HMGA2 and HBME1 showed the highest sensitivity (72.2%) and specificity (76.1%) for diagnosing FTC. CEACAM6, survivin, and SFN/14-3-3 δ were barely expressed in most cases. **Conclusions:** Our present results show that only HMGA2 can be beneficial in differentiating FTC using the novel markers.

Key Words: Adenocarcinoma, follicular; Follicular neoplasm; Novel immunohistochemical markers; HMGA2

Follicular thyroid carcinoma (FTC) is the second most common thyroid malignancy with a reported incidence of 5%–20%.[1] Its preoperative diagnosis is not possible, as FTC can only be diagnosed in a surgically-resected specimen.[2,3] However, the differential diagnosis between FTC, follicular adenoma (FA), and adenomatous goiter (AG) is often difficult, even in resected lesions. Occasionally AG has a fibrous capsule and solid proliferation of follicles, requiring detailed microscopic examination for its diagnosis.[4,5] The distinction between benign and malignant follicular-patterned lesions solely depends on the presence of capsular and/or vascular invasion.[4-7] Therefore, all patients with follicular neoplasm (FN) diagnosed with fine needle aspiration are recommended to undergo a thyroid lobectomy for histologic confirmation.[2] If the tumor is diagnosed as FTC, additional resection of the remaining thyroid or lymph node is required.

Previous studies have reported differential expression of several genes in malignant neoplasms, and the use of some of those markers for differential diagnosis has been subsequently validated in formalin-fixed paraffin-embedded (FFPE) tissues.[8-15] DDIT3, ARG2, ITM1, and C1orf24 have been tested as additional diagnostic tools for distinguishing FTC from FA, but none have been proven to be reliable markers.[16,17] CEACAM6, HMGA2, and SFN/14-3-3 δ (stratifin) need to be validated using FFPE thyroid tissues. Additionally, it has been suggested that the expression of survivin is higher in FTC than in FA, but the number of cases was limited in the study (FTC, 11 cases).[11] Galectin 3 (Gal-3), Hector Battifora mesothelial 1 (HBME1), cytokeratin 19 (CK19), and cyclin D1, all of which are well-established diagnostic markers for papillary thyroid carcinoma (PTC), have also been used in differentiating FTC from other benign follicular lesions but the results are controversial.[15,18-20]

In the present study, we evaluated the immunohistochemical expression of HMGA2, CEACAM6, survivin, SFN/14-3-3 δ, Gal-3, HBME1, CK19, and cyclin D1 in lesions including 41 AGs, 72 FAs, and 79 FTCs. We also evaluated their diagnostic

pISSN 2383-7837
eISSN 2383-7845

usefulness in differentiating FTC.

MATEIRALS AND METHODS

Tissue specimens and microarray construction

Formalin-fixed, paraffin-embedded thyroid tissue blocks were retrieved from the archive maintained at the Department of Pathology, Seoul National University Hospital, from 2001 to 2013. A total of 192 cases of thyroid lesions consisting of 41 AGs, 72 FAs, and 79 FTCs were identified, and representative tissue blocks were obtained for all lesions. All cases were surgically resected. The hematoxylin and eosin–stained slides were reviewed in each case to confirm the original diagnosis using the strict criteria of capsular invasion and vascular invasion defined by two pathologists (M.H.J. and H.S.M.). AG cases were selected from the archives from 2001 to 2007, with identification of the follow-up records for confirming their benign nature.

Tissue microarrays were constructed for immunohistochemical staining. A single, large tissue core (4.0 mm in diameter) was obtained from the most representative area of individual cases. Additionally, 74 cores of normal thyroid tissue from each matched thyroid lesion were included for negative controls. This study was approved by the Institutional Review Board of Seoul National University Hospital (E-1302-023-462).

Immunohistochemical analyses

Immunohistochemistry was performed on 4-μm-thick sections of tissue microarray blocks that included 192 surgically-removed samples. Tissue sections were deparaffinized and rehydrated following standard procedures. Heat-induced antigen retrieval was carried out and sections were incubated with primary antibodies for 32 minutes at 37°C at a dilution of 1:50 for HBME1 and cyclin D1, 1:100 for Gal-3 and SFN/14-3-3 δ, 1:200 for CK19, HMGA2 and CEACAM6, and 1:600 for survivin. Monoclonal antibodies were used for Gal-3 (clone 9C4, Novocastra, Newcastle, United Kingdom), HBME1 (clone HBME-1, Dako, Carpinteria, CA, USA), CK19 (clone RCK108, Dako), cyclin D1 (clone SP4, Thermo Fisher Scientific, Waltham, MA, USA), CEACAM6 (clone 9A6, Abcam, Cambridge, MA, USA) and SFN/14-3-3 δ (clone 5D7, Santacruz, Dalla, TX, USA). Polyclonal antibodies were used for HMGA2 (Biocheck, Foster city, CA, USA) and survivin (Novus Biologicals, Littleton, CO, USA). All immunohistochemical staining was carried out in a BenchMark XT autostainer (Ventana Medical Systems, Tucson, AZ, USA) using the DAB detection kit (Ventana Medical Systems).

Immunohistochemical interpretation

The immunohistochemical staining of tissue microarrays was evaluated by two pathologists (M.H.J. and H.S.M.). The immunoreactivity was scored for Gal-3, HBME1, CK19, cyclin D1, HMGA2, CEACAM6, survivin, and SFN/14-3-3 δ by categorizing methods based on the percentage of positive cells: 0 (less than 10%), 1 (10%–25%), 2 (26%–50%), and 3 (more than 50%). In Gal-3, CK19, survivin, and SFN/14-3-3 δ, cytoplasmic staining was considered as positive immunoreactivity. Membranous staining was regarded as positive for HBME1 and CEACAM6, and nuclear expression was regarded as positive for cyclin D1 and HMGA2.

Statistical analysis

The data was analyzed using SPSS ver. 21.0.0 for Windows (SPSS Inc., Chicago, IL, USA). The χ^2 test or Fisher exact test was used to compare the expression of markers between different diagnostic subgroups. A p-value of $<.05$ was considered statistically significant. Sensitivity, specificity, and diagnostic accuracy were calculated using standard formulae for each marker individually, using histological diagnosis as the gold standard.

RESULTS

Clinicopathologic features

The whole series of samples was obtained from 36 males and 156 females, with a median age of 46 years (range, 9 to 76 years). The mean size of FAs and FTCs was 1.83 cm (range, 1.4 to 4.7 cm) and 3.7 cm (range, 0.8 to 7.3 cm), respectively. The FTC series included samples from 17 males and 61 females, with a median age of 42 years (range, 9 to 76 years). There were 19 cases with vascular invasion. There was only one case that metastasized to lung, and one case recurred in neck soft tissue 15 months after a total thyroidectomy. Unfortunately, we could not obtain the clinicopathologic information of the primary tumor of the metastatic FTC. The clinicopathologic characteristics of the 78 primary FTCs are summarized in Table 1.

Immunohistochemical expressions of markers in AGs, FAs, and FTCs

Most markers, including Gal-3, HBME1, cyclin D1, HMGA2, CEACAM6, survivin, and SNF/14-3-3 δ, were not expressed in the 74 normal thyroid tissues. On the contrary, CK19 was expressed as grade 1 (10%–25%) or 2 (26%–50%) in 31.1% of the normal thyroid tissues.

In the AG group (n = 41), most cases showed negative or lim-

ited immunoreactivity (less than grade 1, ≤25%) for all eight markers. Gal-3 was expressed in one case, but it showed relatively diffuse expression (grade 2, 26%–50%). HBME1, CK19, and cyclin D1 were expressed in only a few cases, showing grade 2 or 3 (grade 2: HBME1, 2/41; CK19, 3/41; cyclin D1, 3/41; grade 3: HBME1, 2/41; CK19, 0/41; cyclin D1, 0/41). However, HMGA2 was expressed in more cases, showing grade 2 (6/41) and grade 3 (4/41). All cases with expression of HBME1 (3/41) and HMGA2 (6/41) exhibited a characteristic feature of microfollicular proliferation of various extents, reminiscent of FN, and showed HBME1 and HMGA2 positivity in this area.

In the FA group (n=72), HBME1, cyclin D1, and HMGA2 were expressed in more than 25% of tumor cells (grade 2: HBME1, 12/72; cyclin D1, 24/72; HMGA2, 12/72; grade 3: HBME1, 22/72; cyclin D1, 14/72; HMGA2, 18/72). There was no diffuse staining of CEACAM6, survivin, and SNF/14-3-3 δ. CK19 was expressed only in four cases, either as grade 2 (3/72) or grade 3 (1/72).

The expression of HBME1 and HMGA2 was the highest in the FTC group, followed by that of cyclin D1, which was expressed at a similar frequency with the FA group. However, HBME1 and HMGA2 expression were not significantly different between FTCs without vascular invasion and FTCs with vascular invasion (p=.382 and p=.418, respectively). The frequency of CK19 expression was higher in the FTC group than in the FA group, but the difference was not statistically significant (p=.133). There was no diffuse staining of CEACAM6, survivin, or SNF/14-3-3 δ (Table 2).

Overall, among the novel markers, SFN/14-3-3 δ and CEACAM6 were not expressed in any of the subgroups, and survivin was only expressed in a small percentage of lesions (grade 0, less than 10%) in 14/97 FTCs. Therefore, these three markers were not helpful in distinguishing the diagnostic subgroups. In contrast, HMGA1 was significantly expressed in FTC and FA cases. The represented immunohistochemical expression of all markers is shown in Fig. 1.

Table 1. Clinicopathologic characteristics of 78 FTCs

Characteristic	Value (n=78)
Age (yr)	
Median (range)	42 (9–76)
Sex	
Female	61
Male	17
Location	
Right lobe	37
Left lobe	38
Isthmus	1
Both lobe	2
T category	
T1a	2
T1b	5
T2	37
T3	33
T4	0
N category	
NX	38
N0	37
N1a	1
N1b	2
Tumor size (cm)	
Mean (range)	3.7 (0.8–7.3)
Capsular invasion	
Minimal	67
Widely	11
Vascular invasion	
Absent	59
Present	19
Follow-up duration (yr)	
Mean (range)	3.33 (0.91–8.98)
Distant metastasis	
Absent	77
Present	1
Local recurrence	
Absent	77
Present	1

FTC, follicular thyroid carcinoma.

Diagnostic utilities of markers in differentiating FTC and FN

Next, we compared the expression of each marker between the diagnostic subgroups. As survivin, CEACAM6 and SNF/14-3-3 δ were expressed in only a few cases or were not expressed

Table 2. Immunohistochemistry in AG, FA, FTC and its association with histologic diagnosis

Diagnosis	Gal-3	HBME1	CK19	Cyclin D1	HMGA2
AG (n=41)	1 (2.4)	4 (9.8)	3 (7.3)	4 (9.8)	10 (24.4)
FA (n=72)	4 (5.6)	34 (47.2)	4 (5.6)	38 (52.8)	30 (41.7)
FTC (n=79)	6 (7.6)	52 (65.8)	10 (12.7)	35 (44.3)	44 (55.7)
p-value (FTC vs FA and AG)	.364	<.001	.121	.321	.005
p-value (FTC vs FA)	.748	.021	.133	.298	.085
p-value (FTC and FA vs AG)	.462	<.001	1.000	<.001	.005

Numbers in parentheses indicate percentage of positive cases. p-values are calculated using the χ^2 test or Fisher exact test.
AG, adenomatous goiter; FA, follicular adenoma; FTC, follicular thyroid carcinoma; Gal-3, galectin-3; HBME1, Hector Battifora mesothelial 1; CK19, cytokeratin 19.

http://dx.doi.org/10.4132/jptm.2015.01.31

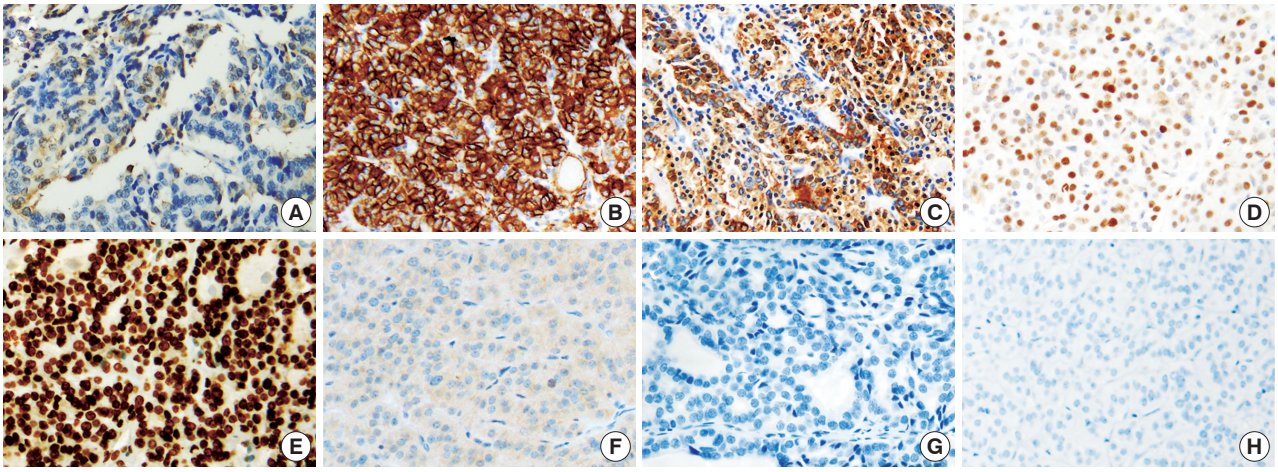

Fig. 1. Representative immunohistochemical results in follicular thyroid carcinoma (FTC). Galectin 3 (A), cytokeratin 19 (C), survivin (F), CEACAM6 (G), and SFN/14-3-3 δ (H) are only occasionally expressed or not expressed. However, Hector Battifora mesothelial 1 (B), HMGA2 (E), and cyclin D1 (D) show diffuse positivity in many FTC cases.

Table 3. Diagnostic values of HBME1/HMGA2 for malignancy (FTC vs FA and AG)

Antibody	Sensitivity (%)	Specificity (%)	PPV (%)	NPV (%)	Diagnostic accuracy (%)
Single marker					
HBME1	65.8	66.4	57.8	73.5	66.1
HMGA2	55.7	64.6	52.4	67.6	60.9
Double markers					
HBME1 and HMGA2	49.4	76.1	52.8	73.8	65.1
HBME1 or HMGA2	72.2	54.9	59.1	68.3	62.0

HBME1, Hector Battifora mesothelial 1; FTC, follicular thyroid carcinoma; FA, follicular adenoma; AG, adenomatous goiter; PPV, positive predictive value; NPV, negative predictive value.

Table 4. Diagnostic values of markers for FN (FTC and FA vs AG)

Antibody	Sensitivity (%)	Specificity (%)	PPV (%)	NPV (%)	Diagnostic accuracy (%)
Single marker					
HBME1	57.0	90.2	96.0	36.3	64.1
Cyclin D1	48.3	90.2	94.8	32.2	57.3
HMGA2	49.0	75.6	88.1	28.7	54.7
Co-expression among 3 markers					
≥1 among HBME1, cyclin D1, HMGA2	80.8	75.6	92.4	51.7	79.7
≥2 among HBME1, cyclin D1, HMGA2	53.6	85.4	93.1	33.3	60.4

FN, follicular neoplasm; FTC, follicular thyroid carcinoma; FA, follicular adenoma; AG, adenomatous goiter; PPV, positive predictive value; NPV, negative predictive value; HBME1, Hector Battifora mesothelial 1.

at all, they were excluded from the statistical analysis for the evaluation of diagnostic utilities.

HBME1 was the only marker that showed differential expression frequency between FTC and FA ($p = .021$) (Table 2). However, it was only expressed in 52 of 79 FTCs (sensitivity, 65.8%) and its specificity remained as 52.8%. When comparing malignant and benign lesions (FTC vs FA and AG), the expression of HBME1 ($p < .001$) and HMGA2 ($p = .005$) was significantly different. In the diagnosis of malignancy, HBME1 showed a slightly better sensitivity (65.8%) and specificity (66.4%) than HMGA2 (sensitivity, 55.7%; specificity, 64.6%).

Additionally, we calculated the sensitivity, specificity, and diagnostic accuracy of the combination of HBME1 and HMGA2 (Table 3). The combined expression of HBME1 or HMGA2 reached the highest sensitivity (72.2%), but the specificity (54.9%) and the diagnostic accuracy (62.0%) were similar or only slightly higher than those of the single markers. The simultaneous expression of HBME1 and HMGA2 increased the specificity up to 76.1%, but its sensitivity (49.4%) was poor.

There were no differences when comparing the diagnostic

utility of the combination of HBME1, cyclin D1 and HMGA2 with those of each single marker in neoplastic lesions (FN including FTC and FA vs AG) (Table 4). As a single marker, HBME1 showed the highest sensitivity (57.0%), and both HBME1 and cyclin D1 showed the highest specificity (90.2%). When more than one marker was expressed among HBME1, cyclin D1, and HMGA2, the sensitivity reached 80.9%, but the specificity decreased.

DISCUSSION

Until now, the entire histologic examination of the fibrous capsule and vasculature after surgery has been the only way to precisely diagnose FTC. Thus, a preoperative diagnosis of FTC is needed in making an accurate preoperative plan and avoiding unnecessary surgery. In this study, we validated the diagnostic utility of HMGA2, CEACAM6, survivin, and SNF/14-3-3 δ with several known markers for distinguishing FTCs, expecting to find out a powerful diagnostic panel.

HMGA2, CEACAM6, and SFN/14-3-3 δ were identified as promising molecular markers that were differentially expressed between benign and malignant thyroid tumors in a previous report by Prasad *et al.*[14] In the immunohistochemical study, HMGA2 and SFN/14-3-3 δ were highly expressed in malignant tumors (HMGA2, $p < .001$, area under the curve [AUC] = 0.84; SFN/14-3-3 δ, $p < .001$, AUC = 0.83). However, CEACAM6 did not show significantly different immunoreactivity.[8] Belge *et al*.[12] suggested that quantifying HMGA2 expression by reverse transcription polymerase chain reaction had a high potential to improve the diagnosis of FNs with a sensitivity of 95.9% and a specificity of 93.9%. In our study, the sensitivity and specificity of HMGA2 for FTC were 55.7% and 64.6%, respectively. However, CEACAM6 was only expressed in infiltrated inflammatory cells (Fig. 1). SFN/14-3-3 δ was only validated in 14 FTC cases in a previous study and thus, the results needed to be verified. Interestingly, its expression was specific for PTC.[8,21] Nevertheless, our study suggested that SFN/ 14-3-3 δ was not an applicable marker for FTC and FN.

Haghpanah *et al.*[11] reported that the cytoplasmic expression of survivin was significantly higher in FTCs than in FAs ($p < .005$), with a high odds ratio (odds ratio, 21.4), but the number of cases was limited (11 FTC cases, 23 FA cases). Recently, Kim *et al.*[22] observed the immunoexpression of survivin in 13/57 FTCs but also in 21/58 FA cases. However, survivin was only expressed in a small proportion (< 10%) of FTCs (14/ 97) in our study (Fig. 1).

Among the well-known markers for PTC that we tested in this study (Gal-3, CK19, and HBME1), HBME1 was the only one expressed at significantly higher levels in the FTC group compared to other groups. The use of HBME1 as a marker of FTC is controversial, and its low specificity has not allowed for the differential diagnosis of FTCs in previous reports.[23,24] Our study yielded a similar result, showing that although the expression of HBME1 was significantly higher in the FTC group, it was expressed in almost half of FAs as well. However, it could differentiate FNs from AGs ($p < .001$), showing positivity in only 4/41 AG cases.

Lastly, our results suggest that the combination use of HBME1 and HMGA2 can be beneficial in the differential diagnosis of FTC. Both markers showed significantly increased expression in FTCs when used alone. When either HBME1 or HMGA2 alone, or both HBME1 and HMGA2 were expressed in lesions, the sensitivity for detecting FTC reached 72.7%. When both markers were simultaneously positive, the specificity reached 76.1%. Therefore, the concurrent use of HBME1 and HMGA2 may be more beneficial than the single use, but it requires a more sophisticated interpretation for FTC diagnosis.

In summary, among all the novel immunohistochemical markers that we tested, HMGA2 was expressed at a higher level in FTCs than in FAs or AGs, but its overall sensitivity was slightly lower than that of HBME1. However, the combination of HMGA2 and HBME1 may be beneficial in differentiating FTCs, as it increased the sensitivity and the specificity for FTCs. Although survivin, CEACAM6, and SFN/14-3-3 δ were initially promising in differentiating malignancy, our results showed that only HMGA2 could help in the diagnosis of FTC.

Conflicts of Interest

No potential conflict of interest relevant to this article was reported.

REFERENCES

1. Kapur U, Wojcik EM. Follicular neoplasm of the thyroid: vanishing cytologic diagnosis? Diagn Cytopathol 2007; 35: 525-8.
2. Wiseman SM, Baliski C, Irvine R, *et al*. Hemithyroidectomy: the optimal initial surgical approach for individuals undergoing surgery for a cytological diagnosis of follicular neoplasm. Ann Surg Oncol 2006; 13: 425-32.
3. McHenry CR, Phitayakorn R. Follicular adenoma and carcinoma of the thyroid gland. Oncologist 2011; 16: 585-93.
4. LiVolsi VA, Baloch ZW. Follicular-patterned tumors of the thyroid:

 http://dx.doi.org/10.4132/jptm.2015.01.31

the battle of benign vs. malignant vs. so-called uncertain. Endocr Pathol 2011; 22: 184-9.
5. Sobrinho-Simões M, Eloy C, Magalhães J, Lobo C, Amaro T. Follicular thyroid carcinoma. Mod Pathol 2011; 24 Suppl 2: S10-8.
6. Mazzaferri EL. Management of a solitary thyroid nodule. N Engl J Med 1993; 328: 553-9.
7. Baloch ZW, LiVolsi VA. Our approach to follicular-patterned lesions of the thyroid. J Clin Pathol 2007; 60: 244-50.
8. Prasad NB, Kowalski J, Tsai HL, *et al.* Three-gene molecular diagnostic model for thyroid cancer. Thyroid 2012; 22: 275-84.
9. Cerutti JM, Delcelo R, Amadei MJ, *et al.* A preoperative diagnostic test that distinguishes benign from malignant thyroid carcinoma based on gene expression. J Clin Invest 2004; 113: 1234-42.
10. Cerutti JM, Latini FR, Nakabashi C, *et al.* Diagnosis of suspicious thyroid nodules using four protein biomarkers. Clin Cancer Res 2006; 12(11 Pt 1): 3311-8.
11. Haghpanah V, Shooshtarizadeh P, Heshmat R, Larijani B, Tavangar SM. Immunohistochemical analysis of survivin expression in thyroid follicular adenoma and carcinoma. Appl Immunohistochem Mol Morphol 2006; 14: 422-5.
12. Belge G, Meyer A, Klemke M, *et al.* Upregulation of HMGA2 in thyroid carcinomas: a novel molecular marker to distinguish between benign and malignant follicular neoplasias. Genes Chromosomes Cancer 2008; 47: 56-63.
13. Chiappetta G, Ferraro A, Vuttariello E, *et al.* HMGA2 mRNA expression correlates with the malignant phenotype in human thyroid neoplasias. Eur J Cancer 2008; 44: 1015-21.
14. Prasad NB, Somervell H, Tufano RP, *et al.* Identification of genes differentially expressed in benign versus malignant thyroid tumors. Clin Cancer Res 2008; 14: 3327-37.
15. Paunovic I, Isic T, Havelka M, Tatic S, Cvejic D, Savin S. Combined immunohistochemistry for thyroid peroxidase, galectin-3, CK19 and HBME-1 in differential diagnosis of thyroid tumors. APMIS 2012; 120: 368-79.
16. Bryson PC, Shores CG, Hart C, *et al.* Immunohistochemical distinction of follicular thyroid adenomas and follicular carcinomas. Arch Otolaryngol Head Neck Surg 2008; 134: 581-6.
17. Sigstad E, Paus E, Bjøro T, *et al.* The new molecular markers DDIT3, STT3A, ARG2 and FAM129A are not useful in diagnosing thyroid follicular tumors. Mod Pathol 2012; 25: 537-47.
18. de Matos PS, Ferreira AP, de Oliveira Facuri F, Assumpção LV, Metze K, Ward LS. Usefulness of HBME-1, cytokeratin 19 and galectin-3 immunostaining in the diagnosis of thyroid malignancy. Histopathology 2005; 47: 391-401.
19. Prasad ML, Pellegata NS, Huang Y, Nagaraja HN, de la Chapelle A, Kloos RT. Galectin-3, fibronectin-1, CITED-1, HBME1 and cytokeratin-19 immunohistochemistry is useful for the differential diagnosis of thyroid tumors. Mod Pathol 2005; 18: 48-57.
20. Papale F, Cafiero G, Grimaldi A, *et al.* Galectin-3 expression in thyroid fine needle cytology (t-FNAC) uncertain cases: validation of molecular markers and technology innovation. J Cell Physiol 2013; 228: 968-74.
21. Lal G, Padmanabha L, Provenzano M, Fitzgerald M, Weydert J, Domann FE. Regulation of 14-3-3sigma expression in human thyroid carcinoma is epigenetically regulated by aberrant cytosine methylation. Cancer Lett 2008; 267: 165-74.
22. Kim YA, Chang M, Park YJ, Kim JE. Detection of survivin and COX-2 in thyroid carcinoma: anaplastic carcinoma shows overexpression of nuclear survivin and low COX-2 expression. Korean J Pathol 2012; 46: 55-60.
23. Park YJ, Kwak SH, Kim DC, *et al.* Diagnostic value of galectin-3, HBME-1, cytokeratin 19, high molecular weight cytokeratin, cyclin D1 and p27(kip1) in the differential diagnosis of thyroid nodules. J Korean Med Sci 2007; 22: 621-8.
24. Saleh HA, Jin B, Barnwell J, Alzohaili O. Utility of immunohistochemical markers in differentiating benign from malignant follicular-derived thyroid nodules. Diagn Pathol 2010; 5: 9.

Journal of Pathology and Translational Medicine 2015; 49: 118-128
http://dx.doi.org/10.4132/jptm.2015.02.05

■ ORIGINAL ARTICLE ■

Pathologic Factors Associated with Prognosis after Adjuvant Chemotherapy in Stage II/III Microsatellite–Unstable Colorectal Cancers

Jung Ho Kim · Jeong Mo Bae[1]
Hyeon Jeong Oh[1] · Hye Seung Lee[2]
Gyeong Hoon Kang[1]

Department of Pathology, SMG-SNU Boramae Medical Center; [1]Department of Pathology, Seoul National University College of Medicine, Seoul; [2]Department of Pathology, Seoul National University Bundang Hospital, Seongnam, Korea

Received: February 4, 2015
Accepted: February 5, 2015

Corresponding Author
Gyeong Hoon Kang, M.D.
Department of Pathology, Seoul National University College of Medicine, 103 Daehak-ro, Jongno-gu, Seoul 110-799, Korea
Tel: +82-2-740-8263
Fax: +82-2-765-5600
E-mail: ghkang@snu.ac.kr

Background: Although there are controversies regarding the benefit of fluoropyrimidine-based adjuvant chemotherapy in patients with microsatellite instability–high (MSI-H) colorectal cancer (CRC), the pathologic features affecting postchemotherapeutic prognosis in these patients have not been fully identified yet. **Methods:** A total of 26 histopathologic and immunohistochemical factors were comprehensively evaluated in 125 stage II or III MSI-H CRC patients who underwent curative resection followed by fluoropyrimidine-based adjuvant chemotherapy. We statistically analyzed the associations of these factors with disease-free survival (DFS). **Results:** Using a Kaplan-Meier analysis with log-rank test, we determined that ulceroinfiltrative gross type ($p = .003$), pT4 ($p < .001$), pN2 ($p = .002$), perineural invasion ($p = .001$), absence of peritumoral lymphoid reaction ($p = .041$), signet ring cell component ($p = .006$), and cribriform comedo component ($p = .004$) were significantly associated with worse DFS in patients receiving oxaliplatin-based adjuvant chemotherapy ($n = 45$). By contrast, pT4 ($p < .001$) and tumor budding-positivity ($p = .032$) were significant predictors of poor survival in patients receiving non-oxaliplatin–based adjuvant chemotherapy ($n = 80$). In Cox proportional hazards regression model-based univariate and multivariate analyses, pT category (pT1-3 vs pT4) was the only significant prognostic factor in patients receiving non-oxaliplatin–based adjuvant chemotherapy, whereas pT category, signet ring cell histology and cribriform comedo histology remained independent prognostic factors in patients receiving oxaliplatin-based adjuvant chemotherapy. **Conclusions:** pT4 status is the most significant pathologic determinant of poor outcome after fluoropyrimidine-based adjuvant chemotherapy in patients with stage II/III MSI-H CRC.

Key Words: Chemotherapy, adjuvant; Colorectal neoplasms; Pathology; Microsatellite instability; Prognosis

In the current management strategy for colorectal cancer (CRC), fluoropyrimidine-based adjuvant chemotherapy is generally recommended for all patients with stage III CRC and for a subset of patients with high-risk stage II CRC.[1] However, some previous studies have reported that in patients with microsatellite instability–high (MSI-H) CRC, adjuvant chemotherapy based on fluorouracil, which is the most commonly used intravenous fluoropyrimidine agent, had little or no benefit.[2] Although the mechanisms underlying and the factors determining this poor response to fluorouracil-based adjuvant chemotherapy in MSI-H CRC patients remain incompletely understood, previous *in vitro* experiments have revealed that intact DNA mismatch repair function is necessary for fluorouracil to induce apoptotic effects on cancer cells.[3,4] This finding supports the observed resistance of patients with MSI-H CRC to fluorouracil-based adjuvant chemotherapy.

MSI-H CRC is characterized by unique pathologic features, including predilections for proximal tumor location, mucinous histology, medullary tumor morphology, signet ring cell tumor component, poor tumor differentiation, tumor-infiltrating lymphocytes, Crohn-like lymphoid reaction and peritumoral lymphoid reaction.[5] Molecularly, MSI-H CRC is caused by DNA mismatch repair deficiency, which is usually due to the inactivation of at least one of the mismatch repair genes, including *MLH1, MSH2, MSH6*, and *PMS2*, by germline mutation or acquired promoter hypermethylation.[2] Recent investigations have also determined that germline *EPCAM* deletion-induced *MSH2* epimutation can be one of the causes of Lynch syndrome-associated MSI-H CRC.[6,7] In addition, it is well known that sporadic MSI-H CRC is closely associated with *MLH1* methylation, CpG island methylator phenotype and *BRAF* V600E mutations.[2] Based on the pathologic and molecular heterogene-

pISSN 2383-7837
eISSN 2383-7845

ity of MSI-H CRC, it is strongly expected that there may be pathologic or molecular factors affecting prognostic heterogeneity and differential chemotherapy responses in MSI-H CRC.[2] In this context, our previous investigation revealed that the concurrent loss of caudal type homeobox 2 (CDX2) and cytokeratin 20 (CK20) expression in tumors indicates an aggressive clinical phenotype that is associated with early death or tumor recurrence in patients with MSI-H CRC.[8] Ricciardiello *et al.*[9] previously reported that in CRC patients, MSI-H status is associated with high expression of thymidylate synthase (TS), the target molecule for fluorouracil. Accordingly, this finding could be a putative underlying mechanism of resistance to fluorouracil chemotherapy in MSI-H CRC patients,[9] although this has not been clearly shown.[10-12] Recently, Dorard *et al.*[13] demonstrated that mutant HSP110 expression and its causal mutation, *HSP110* T_{17} microsatellite deletions, can be prognostic and predictive markers in MSI-H CRC.[13] Furthermore, we have also identified the usefulness of wild-type HSP110 (HSP110wt) immunohistochemistry (IHC) for prognostication in MSI-H CRC.[14]

MSI-H CRC is associated with various features, but definitive pathologic or molecular factors that can be used to predict the response to adjuvant chemotherapy in patients with MSI-H CRC have yet to be fully identified. Therefore, we decided to investigate the comprehensive pathologic features that are potentially associated with postchemotherapeutic prognosis in MSI-H CRC patients. Through this intensive analysis, we anticipated identifying the major determining factors for chemotherapy response in MSI-H CRC patients that would be helpful for predicting patient prognosis and establishing treatment strategies in the clinical setting.

MATERIALS AND METHODS

Study samples

A total of 125 MSI-H CRC tissues were retrospectively collected from the pathology archives of Seoul National University Hospital, Seoul, Korea and Seoul National University Bundang Hospital, Seongnam, Korea. All samples were obtained from patients who underwent curative surgery and subsequent adjuvant chemotherapy for CRC at these institutions between 2004 and 2008. During this time, 2,957 consecutive patients with CRC who were treated at these institutions were subjected to MSI analysis conducted by the molecular pathology division of Seoul National University Hospital; of these patients, 237 were diagnosed as MSI-H. Among them, patients who were determined to be American Joint Committee on Cancer TNM stage I or IV and who had undergone surgery alone or preoperative neoadjuvant chemotherapy or radiation therapy for the treatment of CRC were excluded. Finally, 125 stage II or III MSI-H CRC patients who had received postoperative fluoropyrimidine-based chemotherapy as a first-line adjuvant treatment were included in this study. Of these patients, 51 received fluorouracil/leucovorin, 29 received oral prodrug of fluorouracil (21 capecitabine and 8 tegafur-uracil), 43 received fluorouracil/leucovorin/oxaliplatin and 2 received capecitabine/oxaliplatin. MSI analysis was previously performed in the molecular pathology laboratory of Seoul National University Hospital.[14] Five microsatellite markers (BAT-25, BAT-26, D5S346, D17S250, and D2S123) recommended by the National Cancer Institute were used in the MSI analysis, and MSI-H status was defined as the presence of two or more markers showing instability in tumor DNA compared with normal DNA.

Ethics statement

This study was approved by the Institutional Review Board of Seoul National University Hospital (IRB No. H-1203-072-402). Under the condition of retrospective archival tissue collection and data anonymization, our study was exempt from informed consent of the participants. All patient records/information were anonymized and de-identified prior to analysis.

Surgical pathology analysis

We reviewed the surgical and pathological reports and retrieved data on tumor location, size, multiplicity, and gross type. For survival analysis, all patients were categorized into proximal or distal for tumor location using the splenic flexure as a dividing point and were classified into large or small for tumor size using a cutoff value of the average tumor size (7 cm). Two pathologists (J.H.K. and J.M.B.), who were blinded to the clinicopathologic and molecular data of the cases, independently evaluated the histopathologic features of the 125 MSI-H CRCs by examining hematoxylin and eosin-stained tissue slides using light microscopy. The assessed histopathologic factors included tumor border, pT/pN categories, lymphovascular invasion, perineural invasion, tumor differentiation, tumor budding, peritumoral lymphoid reaction, Crohn-like lymphoid reaction, mucinous, signet ring cell, medullary, serrated, and cribriform comedo tumor components. Conflicting assessment results between the two pathologists were reviewed and discussed, and a consensus was reached. The assessment criteria for histologic parameters used in this study are described below.

Tumor differentiation

Although all MSI-H CRCs are considered low-grade tumors according to the 2010 World Health Organization (WHO) classification,[15] the degree of histomorphologic differentiation for each tumor in this study was graded as one of three differentiation statuses (well, moderately, or poorly differentiated) based on the percentage of gland formation (>95%, 50%–95%, and <49%, respectively).

Tumor budding

Tumor budding status was evaluated as previously described.[16] Tumor budding was defined as a single tumor cell or a cluster composed of <five tumor cells at the invasive margin. Under a light microscopic field with ×200 magnification, the number of tumor buds was counted in the most intensive budding area. A tumor showing five or more buds in this area was determined to be tumor budding-positive.

Peritumoral lymphoid reaction

The peritumoral lymphoid reaction was assessed using the four-tier scoring system suggested by Klintrup *et al.*[17] No increase in lymphoid cells at the invasive margin was scored as 0; a mild and patchy increase in lymphoid cells without destruction of tumor cells by lymphocytes was scored as 1; a band-like infiltration of lymphoid cells at the invasive margin with focal destruction of tumor cells by lymphocytes was scored as 2; and a cup-like intense lymphoid infiltration at the invasive margin with frequent destruction of tumor cells by lymphocytes was scored as 3. Among the 125 cases, four were excluded from the peritumoral lymphoid reaction assessment owing to suboptimal staining or tissue section qualities of peritumoral areas.

Crohn-like lymphoid reaction

Crohn-like lymphoid reaction activity was evaluated using Ueno's criteria.[18] The maximum size of the largest lymphoid aggregate of Crohn-like lymphoid reaction in CRC was measured. Tumors with the largest lymphoid aggregate ≥1 mm were classified into the active reaction group, whereas tumors with the largest lymphoid aggregate <1 mm were classified into the inactive reaction group. Among the 125 cases, four were excluded from the Crohn-like lymphoid reaction assessment owing to suboptimal staining or tissue section qualities of peritumoral areas.

Mucinous histology

The degree of extracellular mucin pools in a tumor was assessed as absent, focal (<50% of tumor area), or diffuse (≥50% of tumor area).

Signet ring cell tumor component

The signet ring cell component in a tumor was assessed as absent, focal (<50% of tumor cells), or diffuse (≥50% of tumor cells).

Medullary tumor component

The medullary component in a tumor was assessed as absent, focal (<50% of tumor cells), or diffuse (≥50% of tumor cells). Medullary features were determined based on the combination of sheet-like growth pattern of large tumor cells, high nuclear/cytoplasmic ratios, abundant amphophilic cytoplasm, vesicular nuclei, prominent nucleoli and frequent tumor-infiltrating lymphocytes.[19]

Serrated tumor component

The serrated component in a tumor was assessed as absent, focal (<50% of tumor cells), or diffuse (≥50% of tumor cells). Serrated morphology was determined based on the combination of glandular serrations, abundant eosinophilic or clear cytoplasm, vesicular nuclei, prominent nucleoli, absence of necrosis and intra- and extracellular mucin.[20]

Cribriform comedo tumor component

The cribriform comedo component in a tumor was assessed as absent, focal (<50% of tumor cells), or diffuse (≥50% of tumor cells). Cribriform comedo histology was defined as cribriform gland architecture with a comedo-like necrosis pattern resembling breast intraductal carcinoma.[21]

Immunohistochemistry

Tissue microarray (TMA) construction and IHC were conducted as previously described.[14] For TMA construction, three tissue cores corresponding to three different areas of cancer were extracted from formalin-fixed, paraffin-embedded tissue blocks of individual cases. Immunostaining with antibodies against MLH1 (Dako, Glostrup, Denmark), MSH2 (Invitrogen, Camarillo, CA, USA), PMS2 (Ventana Medical Systems, Tucson, AZ, USA), MSH6 (Ventana Medical Systems), CDX2 (Ventana Medical Systems), CK20 (Dako), TS (Invitrogen), and HSP110wt (NCL-HSP105, Leica Biosystems, Newcastle upon Tyne, UK) was performed on TMA blocks composed of all 125 MSI-H CRC tissues. Automated immunohistochemical staining was conducted using the BenchMark XT immunostainer (Ventana Medical Systems) according to the manufacturer's protocol. The expres-

http://dx.doi.org/10.4132/jptm.2015.02.05

Table 1. The pathologic features of samples used in this study (stage II/III MSI-H CRCs treated with fluoropyrimidine-based adjuvant chemotherapy)

Variable		Total patients (n = 125)	Patients receiving oxaliplatin-based therapy (n = 45)	Patients receiving non-oxaliplatin–based therapy (n = 80)
Tumor location	Proximal	83 (66)	30 (67)	53 (66)
	Distal	42 (34)	15 (33)	27 (34)
Tumor size	Large (≥ 7 cm)	54 (43)	23 (51)	31 (39)
	Small (< 7 cm)	71 (57)	22 (49)	49 (61)
Tumor multiplicity	Solitary	113 (90)	43 (96)	70 (88)
	Multiple	12 (10)	2 (4)	10 (12)
Gross tumor type	Polypoid	9 (7)	0 (0)	9 (11)
	Ulcerofungating	84 (67)	27 (60)	57 (71)
	Ulceroinfiltrative	32 (26)	18 (40)	14 (18)
Tumor border	Expanding	19 (15)	4 (9)	15 (19)
	Infiltrative	106 (85)	41 (91)	65 (81)
Depth of tumor invasion (pT category)	pT1	1 (1)	0 (0)	1 (1)
	pT2	0 (0)	0 (0)	0 (0)
	pT3	108 (86)	32 (71)	76 (95)
	pT4	16 (13)	13 (29)	3 (4)
Lymph node metastasis (pN category)	pN0	80 (64)	16 (36)	64 (80)
	pN1	26 (21)	15 (33)	11 (14)
	pN2	19 (15)	14 (31)	5 (6)
Lymphovascular invasion	Absent	90 (72)	20 (44)	70 (88)
	Present	35 (28)	25 (56)	10 (13)
Perineural invasion	Absent	117 (94)	39 (87)	78 (98)
	Present	8 (6)	6 (13)	2 (3)
Peritumoral lymphoid reaction	Absent	8 (7)	7 (17)	1 (1)
	Mild (grade 1)	41 (34)	12 (29)	29 (37)
	Moderate (grade 2)	56 (46)	17 (40)	39 (49)
	Marked (grade 3)	16 (13)	6 (14)	10 (13)
Crohn-like lymphoid reaction	Inactive (largest LA size < 1 mm)	66 (55)	31 (74)	35 (44)
	Active (largest LA size ≥ 1 mm)	55 (45)	11 (26)	44 (56)
Tumor differentiation	WD	12 (10)	4 (9)	8 (10)
	MD	86 (69)	27 (60)	59 (74)
	PD	27 (22)	14 (31)	13 (16)
Tumor budding	Negative (< 5 buds)	100 (80)	32 (71)	68 (85)
	Positive (≥ 5 buds)	25 (20)	13 (29)	12 (15)
Mucinous component	Absent	53 (42)	19 (42)	34 (42)
	Focal (< 50%)	45 (36)	14 (31)	31 (39)
	Diffuse (≥ 50%)	27 (22)	12 (27)	15 (19)
Signet ring cell component	Absent	112 (90)	38 (84)	74 (93)
	Focal (< 50%)	8 (6)	3 (7)	5 (6)
	Diffuse (≥ 50%)	5 (4)	4 (9)	1 (1)
Medullary component	Absent	121 (97)	43 (96)	78 (98)
	Focal (< 50%)	0 (0)	0 (0)	0 (0)
	Diffuse (≥ 50%)	4 (3)	2 (4)	2 (3)
Serrated component	Absent	114 (91)	41 (91)	73 (91)
	Focal (< 50%)	11 (9)	4 (9)	7 (9)
	Diffuse (≥ 50%)	0 (0)	0 (0)	0 (0)
Cribriform comedo component	Absent	122 (98)	43 (96)	79 (99)
	Focal (< 50%)	3 (2)	2 (4)	1 (1)
	Diffuse (≥ 50%)	0 (0)	0 (0)	0 (0)
MLH1 expression	Negative	88 (70)	32 (71)	56 (70)
	Positive	37 (30)	13 (29)	24 (30)
MSH2 expression	Negative	35 (28)	17 (38)	18 (23)
	Positive	90 (72)	28 (62)	62 (78)
MSH6 expression	Negative	37 (30)	18 (40)	19 (24)
	Positive	88 (70)	27 (60)	61 (76)
PMS2 expression	Negative	92 (74)	32 (71)	60 (75)
	Positive	33 (26)	13 (29)	20 (25)
CDX2 expression	Negative	15 (12)	8 (18)	7 (9)
	Positive	110 (88)	37 (82)	73 (91)

(continued to the next page)

Table 1. continued

Variable		Total patients (n = 125)	Patients receiving oxaliplatin-based therapy (n = 45)	Patients receiving non-oxaliplatin–based therapy (n = 80)
CK20 expression	Negative	22 (18)	10 (22)	12 (15)
	Positive	103 (82)	35 (78)	68 (85)
HSP110wt expression	Negative (0)	15 (12)	4 (9)	11 (14)
	Weak positive (1+)	20 (16)	12 (27)	8 (10)
	Intermediately positive (2+)	49 (39)	18 (40)	31 (39)
	Strong positive (3+)	41 (33)	11 (24)	30 (38)
TS expression	Low (0/1+)	69 (55)	30 (67)	39 (49)
	High (2+/3+)	56 (45)	15 (33)	41 (51)

Values are presented as number (%).
LA, lymphoid aggregate; WD, well differentiated; MD, moderately differentiated; PD, poorly differentiated; HSP110wt, wild-type HSP110.

sion of CDX2, CK20 and each of the mismatch repair proteins was assessed to be negative (loss) or positive (retained), as previously described.[8] The positivity of CDX2 and mismatch repair proteins was determined when a nuclear staining pattern in tumor cells was observed. CK20 expression was determined to be positive when a cytoplasmic to membranous staining pattern in tumor cells was observed. HSP110wt and TS expression statuses were evaluated semiquantitatively using a four-tier scoring system based on staining intensity (0/1+/2+/3+), as previously described.[14,22] The detailed steps of HSP110wt and TS assessment were as follows. Among the three tissue cores of each tumor case, identical scores for two or more tissue cores determined the overall score for the case. Subsequently, for survival analysis, all cases were dichotomously categorized into negative (0) or positive (1+/2+/3+) for HSP110wt expression status and low (0/1+) or high (2+/3+) for TS expression status. The assessment of all immunohistochemical stainings in this study was performed independently by two pathologists (J.H.K. and J.M.B.), who were blinded to the clinicopathologic and molecular data. Conflicting assessment results between the two pathologists were reviewed and discussed, and a consensus was reached.

Statistical analysis

All statistical analyses in this study were performed using IBM SPSS Statistics ver. 20 (IBM Co., Armonk, NY, USA). By reviewing the medical records of our institutions and using the Micro Data Service System by Statistics Korea, the times of death, tumor recurrence and the last clinical follow-up for disease-free survival (DFS) data were collected. The average DFS time was 1,817 days and ranged from 29 to 3,186 days. The DFS rates were analyzed using the Kaplan-Meier method with the log-rank test. To identify independent prognostic factors, univariate and multivariate survival analyses were performed using the Cox proportional hazards regression model. For survival analysis, all 125 patients included in this study were divided into two groups: those receiving oxaliplatin-based therapy (n = 45; 43 fluorouracil/leucovorin/oxaliplatin, 2 capecitabine/oxaliplatin) and those receiving non-oxaliplatin–based therapy (n = 80; 51 fluorouracil/leucovorin, 21 capecitabine, 8 tegafuruacil). All p-values were two-sided, and statistical significance was determined at $p < .05$.

RESULTS

Pathologic features of study samples

The pathologic and immunophenotypic features of 125 MSI-H CRC patients treated with fluoropyrimidine-based adjuvant chemotherapy are summarized in Table 1. Representative photomicrographs of histopathologic and immunohistochemical features, including tumor budding, mucinous histology, signet ring cell component, medullary component, serrated morphology, cribriform comedo histology, HSP110wt expression and TS expression, are demonstrated in Figs. 1 and 2, respectively.

Survival analysis

In the preliminary survival analysis of patients treated with oxaliplatin- and non-oxaliplatin–based therapies, there were no significant differences in DFS between polypoid and ulcerofungating types, pT1 and pT3, pN0 and pN1, scores 1, 2, and 3 for peritumoral lymphoid reaction, well differentiation and moderate differentiation, focal presence (< 50%) and diffuse presence (≥ 50%) of each tumor component (mucinous, signet ring cell, medullary, serrated, and cribriform comedo components), and 1+, 2+, and 3+ of HSP110wt expression. Therefore, we decided to unify each of these sub-classifications into one category, and consequently, all pathologic variables assessed in this study were dichotomously categorized for subsequent survival analyses (Table 1).

Kaplan-Meier survival analysis with log-rank test revealed that, among the 26 pathologic and immunohistochemical fac-

 http://dx.doi.org/10.4132/jptm.2015.02.05

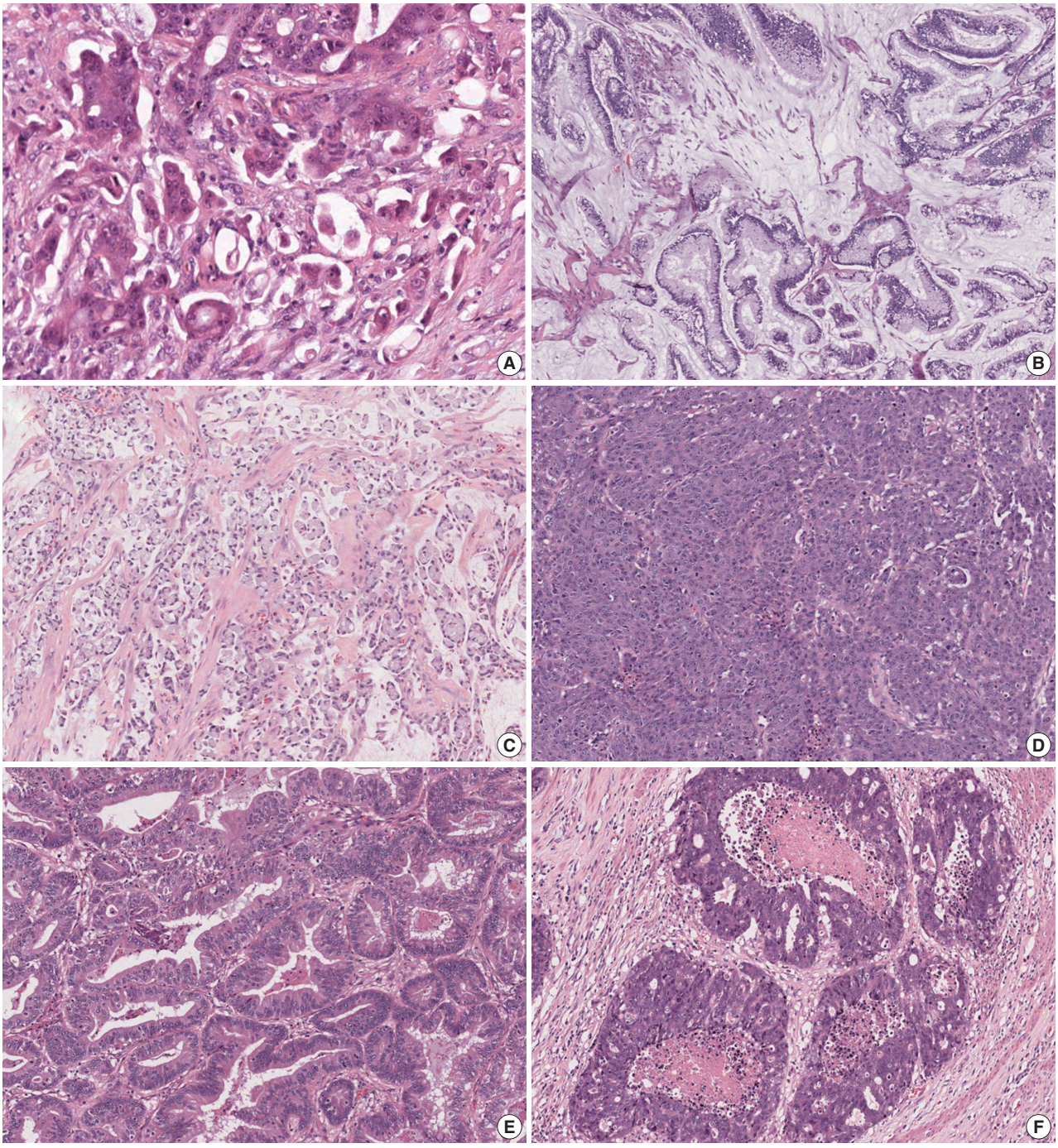

Fig. 1. Histopathologic features in microsatellite instability–high colorectal cancers. (A) A case determined to be tumor budding–positive (buds ≥5). (B) A case classified as mucinous adenocarcinoma. (C) A case classified as signet ring cell carcinoma. (D) A case classified as medullary carcinoma. (E) A case showing a serrated tumor component. (F) A case showing a cribriform comedo-type tumor component.

tors, ulceroinfiltrative gross tumor type (p = .003) (Fig. 3A), pT4 stage (p < .001) (Fig. 3B), pN2 stage (p = .002) (Fig. 3C), presence of perineural invasion (p = .001) (Fig. 3D), absence of peritumoral lymphoid reaction (p = .041) (Fig. 3E), presence of signet ring cell component (p = .006) (Fig. 3F), and presence of cribriform comedo histology (p = .004) (Fig. 3G) were significant factors for poorer DFS in MSI-H CRC patients who were treated with oxaliplatin-based adjuvant chemotherapy. In contrast, pT4 stage (p < .001) (Fig. 4A) and tumor budding-positivity (p = .032) (Fig. 4B) were significantly associated with poor-

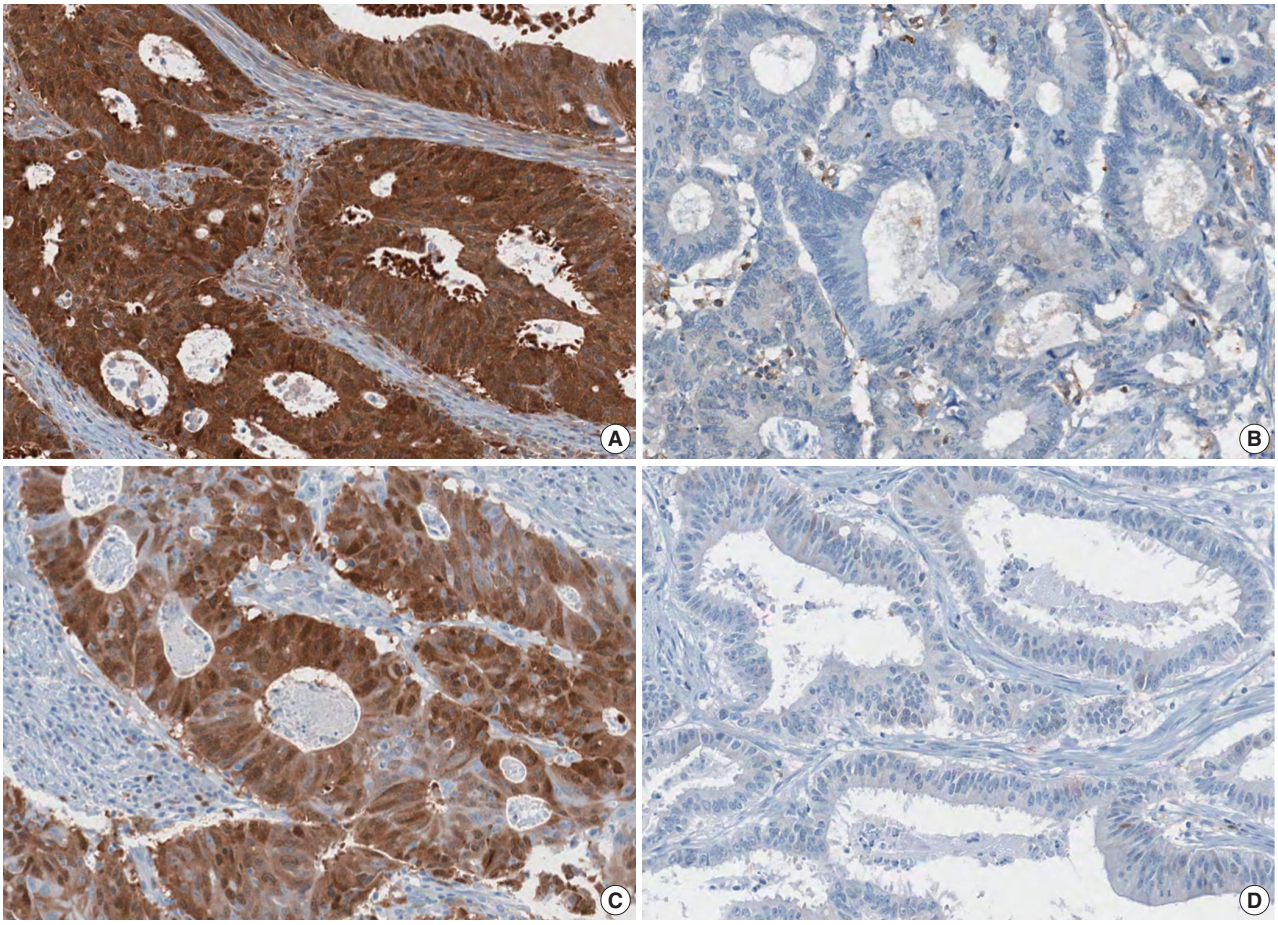

Fig. 2. Immunohistochemical expression of wild-type HSP110 (HSP110wt) and thymidylate synthase (TS) in microsatellite instability–high colorectal cancers. (A) A case showing high-level expression of HSP110wt (score 3+). (B) A case showing HSP110wt-negativity (score 0). (C) A case showing high-level expression of TS (score 3+). (D) A case showing low-level expression of TS (score 0).

er DFS in patients treated with non-oxaliplatin–based chemotherapy. Notably, although a statistical significance in survival differences was not observed, there were no deaths or incidences of CRC recurrence in patients with the HSP110wt-negative phenotype (Figs. 3H, 4C).

Finally, to determine the most significant factor among the pathologic prognosticators, we performed univariate and multivariate survival analyses using the Cox proportional hazards regression model. In univariate analysis, gross tumor type, pT category, pN category, perineural invasion, signet ring cell component and cribriform comedo component were significant prognostic factors in patients treated with oxaliplatin-based therapy (Table 2). By contrast, only the pT category was a significant factor in patients treated with non-oxaliplatin–based therapy (hazard ratio, 17.6; 95% confidence interval, 3.34 to 92.8; p= .001). In multivariate analysis, the pT4 stage, signet ring cell histology and cribriform comedo histology were determined to be independent prognostic factors associated with poor DFS in patients treated with oxaliplatin-based therapy (Table 2).

DISCUSSION

MSI-H is one of the major molecular subtypes of CRC and has been thought to be associated with poor response to fluorouracil-based adjuvant chemotherapy. However, recent evidence has suggested that MSI is not a significant factor for determining postchemotherapeutic prognosis in CRC patients who have been treated with oxaliplatin-based adjuvant chemotherapy.[2] Although controversy may still remain, these findings imply that adding oxaliplatin to fluorouracil-based chemotherapy regimens may be important for overcoming fluorouracil-resistance in MSI-H CRC patients. Therefore, because the pathologic and molecular factors that affect patient prognosis after adjuvant chemotherapy could be fundamentally different depending on

 http://dx.doi.org/10.4132/jptm.2015.02.05

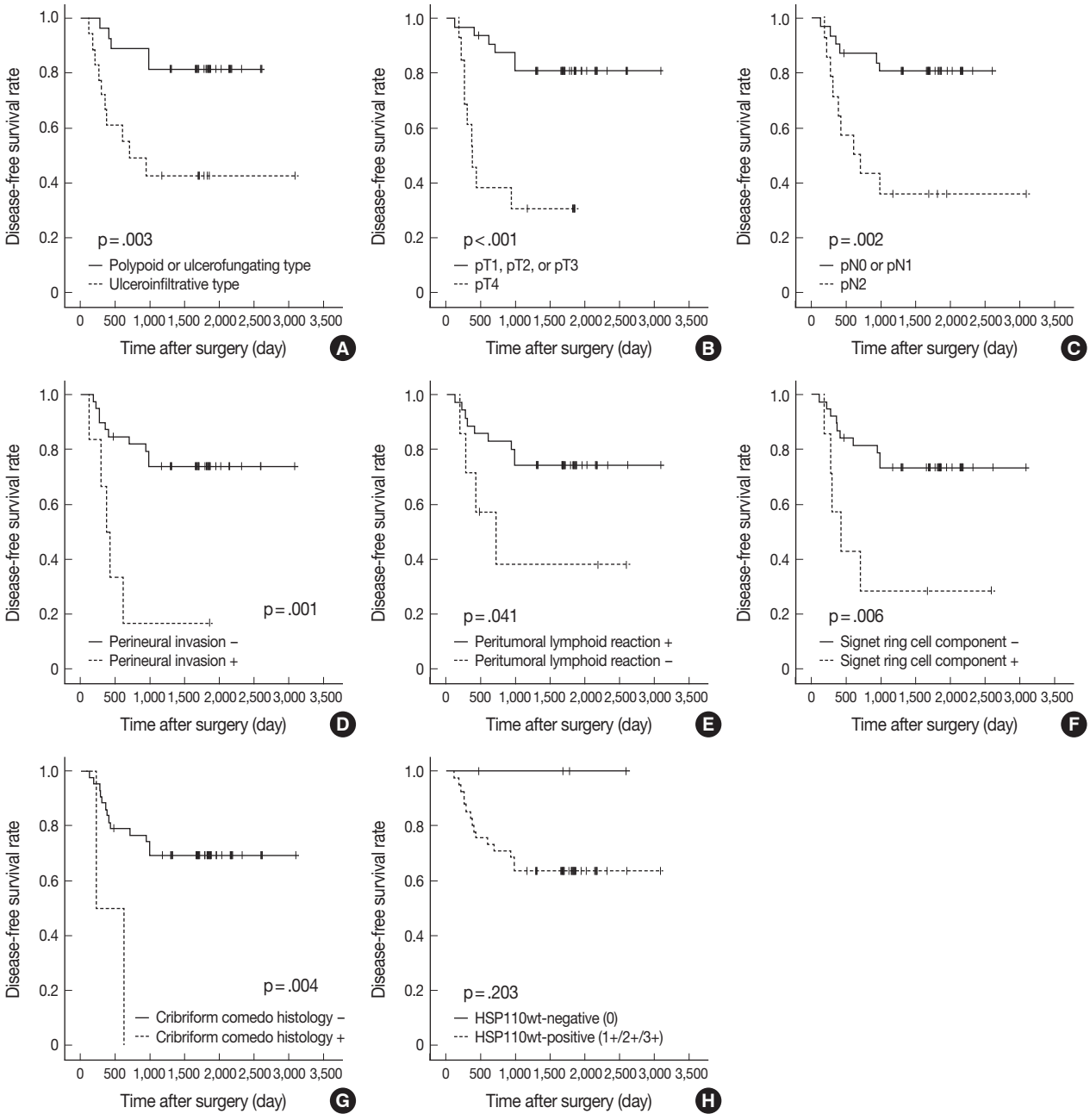

Fig. 3. Kaplan-Meier survival analyses of microsatellite instability–high colorectal cancer patients receiving oxaliplatin-based chemotherapy (n=45). (A-G) The disease-free survival of patients differed significantly according to gross tumor type (A), pT category (B), pN category (C), perineural invasion (D), peritumoral lymphoid reaction (E), signet ring cell component (F), and cribriform comedo component (G). (H) Note the absence of death or tumor recurrence in patients with wild-type HSP110 (HSP110wt)-negative tumors.

the presence or absence of oxaliplatin in their chemotherapy regimens, for survival analysis, all 125 patients with MSI-H CRC in our present study were divided into patient subgroups based on whether they were treated with oxaliplatin- or non-oxaliplatin–based therapy.

In terms of pathology, the depth of tumor invasion (pT category), lymph node metastasis (pN category), gross tumor type, tumor budding, perineural invasion, lymphocytic reactions, and signet ring cell tumor component are known prognostic pathologic factors in CRC.[23] Therefore, it is not surprising that in the present study, these features were confirmed as being significant factors for postchemotherapeutic prognosis in patients with MSI-H CRC. However, several interesting issues regarding the prognostic pathologic features identified in our study

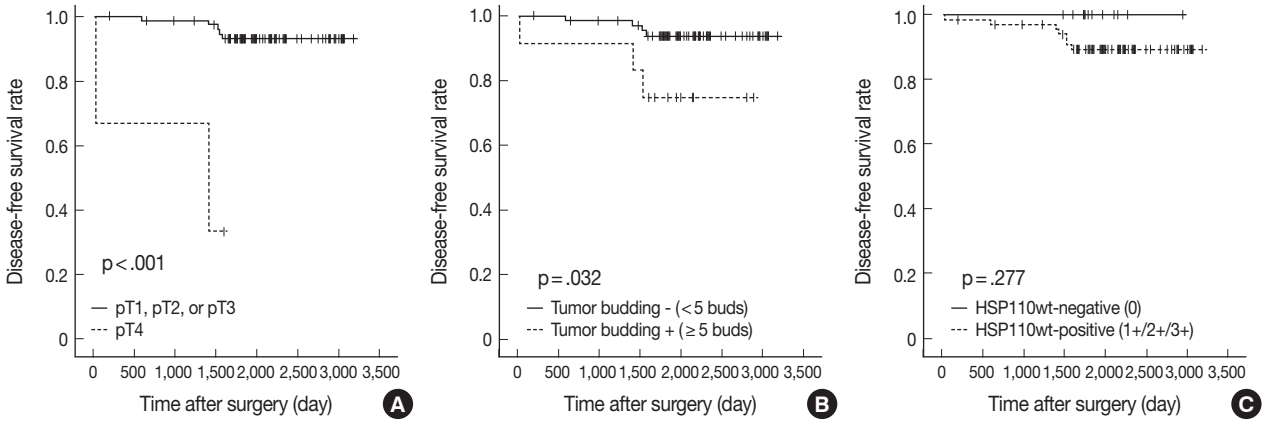

Fig. 4. Kaplan-Meier survival analyses of microsatellite instability-high colorectal cancer patients receiving non-oxaliplatin–based chemotherapy (n=80). (A, B) The disease-free survival of patients differed significantly according to the pT category (A) and tumor budding (B). (C) Note the absence of death or tumor recurrence in patients with wild-type HSP110 (HSP110wt)-negative tumors.

Table 2. Univariate and multivariate survival analyses of stage II/III MSI-H CRC patients treated with oxaliplatin-based adjuvant chemotherapy

Variable	n	Univariate analysis HR (95% CI)	p-value	Multivariate analysis HR (95% CI)	p-value
Gross tumor type			.007		.373
Polypoid/ulcerofungating	27	Reference		Reference	
Ulceroinfiltrative	18	4.4 (1.49-12.97)		1.76 (0.51-6.12)	
Depth of tumor invasion (pT category)			.001		.012
pT1-pT3	32	Reference		Reference	
pT4	13	6.23 (2.19-17.77)		4.91 (1.42-16.95)	
Lymph node metastasis (pN category)			.004		.268
pN0-pN1	31	Reference		Reference	
pN2	14	4.56 (1.61-12.91)		2 (0.59-6.85)	
Perineural invasion			.002		.932
Absent	39	Reference		Reference	
Present	6	5.68 (1.88-17.22)		0.94 (0.25-3.57)	
Signet ring cell component			.011		.035
Absent	38	Reference		Reference	
Present	7	4.09 (1.38-12.13)		4.31 (1.11-16.83)	
Cribriform comedo component			.014		.045
Absent	43	Reference		Reference	
Present	2	6.93 (1.48-32.36)		7.86 (1.04-59.17)	

MSI-H, microsatellite instability–high; CRC, colorectal cancer; HR, Cox hazard ratio; 95% CI, 95% confidence interval of HR.

remain to be addressed.

One of our interesting findings is the potential association between the peritumoral lymphoid reaction and the response to oxaliplatin-based chemotherapy in CRC (Fig. 3E). It has been well documented that host immune reactions against the tumor can determine the prognosis of cancer patients. It has also been reported that peritumoral inflammatory reaction is an independent prognostic factor in patients with CRC.[24] However, there has not been enough evidence to support a relationship between peritumoral inflammatory reaction and treatment response in CRC patients receiving adjuvant chemotherapy. Therefore, our data provide an important and timely indication of the value of peritumoral lymphoid reaction in predicting the response of CRC patients to oxaliplatin-based chemotherapy. According to a previous *in vitro* study, oxaliplatin can induce the immunogenic death of CRC cells,[25] and this finding could account for the favorable prognostic effect of peritumoral lymphoid reaction during oxaliplatin-based chemotherapy in patients with CRC.

Another interesting finding is the prognostic significance of cribriform comedo-type histology in MSI-H CRC patients receiving oxaliplatin-based chemotherapy (Table 2, Fig. 3G). According to a previous study by Chirieac *et al.*,[21] the presence of cribriform comedo gland patterns in microsatellite-stable CRCs was significantly associated with CpG island hypermethylation.

http://dx.doi.org/10.4132/jptm.2015.02.05

However, the detailed prognostic implications of the cribriform comedo morphology in CRC, including both MSI-H and MSI-low/microsatellite-stable phenotypes, have not been studied. To the best of our knowledge, our investigation is the first study reporting the prognostic impact of cribriform comedo histology in CRC, though our study samples were restricted to patients with MSI-H tumors receiving adjuvant chemotherapy. As such, additional efforts to elucidate the clinicopathologic and molecular associations and the prognostic values of cribriform comedo histology in CRC are needed.

Previous studies have suggested a few molecular factors putatively associated with resistance to fluorouracil chemotherapy in CRC, such as TS expression, but the practical predictive value of these factors remains unclear.[26] In addition, although the beneficial effect of fluorouracil-based adjuvant chemotherapy in patients with MSI-H CRC has been doubtful, few established biomarkers can be used to stratify MSI-H CRC patients into chemotherapy-responsive or chemotherapy-nonresponsive subgroups. In this context, recent investigations have reported notable findings regarding *HSP110* T_{17} deletions and HSP110 expression alterations as promising prognostic and predictive markers in MSI-H CRC.[13] In our previous study, we suggested that IHC for HSP110wt could be a useful tool for stratifying prognostic subgroups of patients with MSI-H CRC.[14] Therefore, we also applied HSP110wt immunostaining in the present study to verify the predictive value of this method in MSI-H CRC patients undergoing adjuvant chemotherapy. However, there were no significant survival differences according to HSP110wt expression status in the patient groups receiving either oxaliplatin- or non-oxaliplatin–based therapies (Figs. 3H, 4C). Interestingly, although the results of survival analysis were not statistically significant, all patients with HSP110wt-negative tumors did not experience death or tumor recurrence. This finding was consistent with the results of our previous investigation. In our previous study, among 168 MSI-H CRC patients, there were no deaths or incidences of tumor recurrence in patients with HSP110wt-negative tumors.[14] Collectively, our previous and present data suggest that HSP110wt-negative MSI-H CRCs may be characterized by remarkably favorable prognosis. Although we could not prove the prognostic significance of HSP-110wt expression in our cohort of MSI-H CRC patients receiving adjuvant chemotherapy, the potential associations between *HSP110* mutation/HSP110 expression statuses and responses to chemotherapy in MSI-H CRC should be further evaluated.

The final issue to be addressed is an interpretation of our study results in terms of potential chemotherapy resistance in MSI-H CRC. Interestingly, recent investigations have suggested that the prognostic impact of the pT category has been underestimated in CRC staging. According to the study by Li *et al.*,[27] the pT category is more significantly associated with patient survival than the pN category in CRC. In addition, according to the study by Snaebjornsson *et al.*,[28] pT4 is the most significant determinant of poor survival in stage II/III colon cancer patients. Based on these reports, our conclusion that pT4 status is the most important indicator of poor outcome after adjuvant chemotherapy in stage II/III MSI-H CRC suggests that the adverse prognostic effect of the major high-risk factor (pT4) in stage II/III CRC is not improved after adjuvant chemotherapy in MSI-H CRC. In other words, this finding may reflect poor responses to fluoropyrimidine-based adjuvant chemotherapy in patients with MSI-H CRC.

In summary, regardless of the efficacy of fluoropyrimidine-based adjuvant chemotherapy in MSI-H CRC patients, the depth of tumor invasion can be considered the most significant pathologic factor associated with postchemotherapeutic prognosis in patients with locally advanced MSI-H CRC. In addition, other pathologic factors, including gross tumor type, lymph node metastasis, perineural invasion, peritumoral lymphoid reaction, signet ring cell component, cribriform comedo histology, and HSP110 expression, should be further evaluated as potential predictive factors for response to adjuvant chemotherapy in CRC patients.

Conflicts of Interest

No potential conflict of interest relevant to this article was reported.

Acknowledgments

This study was supported by a grant from the Basic Science Research Program through the National Research Foundation (NRF) funded by the Korean Ministry of Education (2013R1 A1A2059080), a grant from the Korea Health Technology R&D Project funded by the Korean Ministry of Health and Welfare (HI13C1804), the NRF grant funded by the Korean Ministry of Science, ICT and Future planning (2011-0030049), a grant from the Priority Research Centers Program through the NRF (2009-0093820), and a grant from the Korea Health Technology R&D Project through the Korea Health Industry Development Institute funded by the Korean Ministry of Health and Welfare (HI14C1277).

REFERENCES

1. Wolpin BM, Mayer RJ. Systemic treatment of colorectal cancer. Gastroenterology 2008; 134: 1296-310.
2. Kim JH, Kang GH. Molecular and prognostic heterogeneity of microsatellite-unstable colorectal cancer. World J Gastroenterol 2014; 20: 4230-43.
3. Carethers JM, Chauhan DP, Fink D, *et al.* Mismatch repair proficiency and *in vitro* response to 5-fluorouracil. Gastroenterology 1999; 117: 123-31.
4. Arnold CN, Goel A, Boland CR. Role of hMLH1 promoter hypermethylation in drug resistance to 5-fluorouracil in colorectal cancer cell lines. Int J Cancer 2003; 106: 66-73.
5. Jenkins MA, Hayashi S, O'Shea AM, *et al.* Pathology features in Bethesda guidelines predict colorectal cancer microsatellite instability: a population-based study. Gastroenterology 2007; 133: 48-56.
6. Ligtenberg MJ, Kuiper RP, Chan TL, *et al.* Heritable somatic methylation and inactivation of MSH2 in families with Lynch syndrome due to deletion of the 3' exons of *TACSTD1*. Nat Genet 2009; 41: 112-7.
7. Kim JH, Bae JM, Kim KJ, *et al.* Differential features of microsatellite-unstable colorectal carcinomas depending on EPCAM expression status. Korean J Pathol 2014; 48: 276-82.
8. Kim JH, Rhee YY, Bae JM, Cho NY, Kang GH. Loss of CDX2/CK20 expression is associated with poorly differentiated carcinoma, the CpG island methylator phenotype, and adverse prognosis in microsatellite-unstable colorectal cancer. Am J Surg Pathol 2013; 37: 1532-41.
9. Ricciardiello L, Ceccarelli C, Angiolini G, *et al.* High thymidylate synthase expression in colorectal cancer with microsatellite instability: implications for chemotherapeutic strategies. Clin Cancer Res 2005; 11: 4234-40.
10. Sinicrope FA, Rego RL, Halling KC, *et al.* Thymidylate synthase expression in colon carcinomas with microsatellite instability. Clin Cancer Res 2006; 12: 2738-44.
11. Popat S, Wort R, Houlston RS. Inter-relationship between microsatellite instability, thymidylate synthase expression, and p53 status in colorectal cancer: implications for chemoresistance. BMC Cancer 2006; 6: 150.
12. Kim GP, Colangelo LH, Wieand HS, *et al.* Prognostic and predictive roles of high-degree microsatellite instability in colon cancer: a National Cancer Institute-National Surgical Adjuvant Breast and Bowel Project Collaborative Study. J Clin Oncol 2007; 25: 767-72.
13. Dorard C, de Thonel A, Collura A, *et al.* Expression of a mutant HSP110 sensitizes colorectal cancer cells to chemotherapy and improves disease prognosis. Nat Med 2011; 17: 1283-9.
14. Kim JH, Kim KJ, Rhee YY, *et al.* Expression status of wild-type HSP110 correlates with HSP110 T17 deletion size and patient prognosis in microsatellite-unstable colorectal cancer. Mod Pathol 2014; 27: 443-53.
15. Bosman FT, Carneiro F, Hruban RH, Theise ND. WHO classification of tumours of the digestive system. 4th ed. Lyon: IARC Press, 2010.
16. Ueno H, Mochizuki H, Hashiguchi Y, *et al.* Risk factors for an adverse outcome in early invasive colorectal carcinoma. Gastroenterology 2004; 127: 385-94.
17. Klintrup K, Mäkinen JM, Kauppila S, *et al.* Inflammation and prognosis in colorectal cancer. Eur J Cancer 2005; 41: 2645-54.
18. Ueno H, Hashiguchi Y, Shimazaki H, *et al.* Objective criteria for crohn-like lymphoid reaction in colorectal cancer. Am J Clin Pathol 2013; 139: 434-41.
19. Wick MR, Vitsky JL, Ritter JH, Swanson PE, Mills SE. Sporadic medullary carcinoma of the colon: a clinicopathologic comparison with nonhereditary poorly differentiated enteric-type adenocarcinoma and neuroendocrine colorectal carcinoma. Am J Clin Pathol 2005; 123: 56-65.
20. Bettington M, Walker N, Clouston A, Brown I, Leggett B, Whitehall V. The serrated pathway to colorectal carcinoma: current concepts and challenges. Histopathology 2013; 62: 367-86.
21. Chirieac LR, Shen L, Catalano PJ, Issa JP, Hamilton SR. Phenotype of microsatellite-stable colorectal carcinomas with CpG island methylation. Am J Surg Pathol 2005; 29: 429-36.
22. Johnston PG, Fisher ER, Rockette HE, *et al.* The role of thymidylate synthase expression in prognosis and outcome of adjuvant chemotherapy in patients with rectal cancer. J Clin Oncol 1994; 12: 2640-7.
23. Marzouk O, Schofield J. Review of histopathological and molecular prognostic features in colorectal cancer. Cancers (Basel) 2011; 3: 2767-810.
24. Richards CH, Flegg KM, Roxburgh CS, *et al.* The relationships between cellular components of the peritumoural inflammatory response, clinicopathological characteristics and survival in patients with primary operable colorectal cancer. Br J Cancer 2012; 106: 2010-5.
25. Tesniere A, Schlemmer F, Boige V, *et al.* Immunogenic death of colon cancer cells treated with oxaliplatin. Oncogene 2010; 29: 482-91.
26. Ross JS, Torres-Mora J, Wagle N, Jennings TA, Jones DM. Biomarker-based prediction of response to therapy for colorectal cancer: current perspective. Am J Clin Pathol 2010; 134: 478-90.
27. Li J, Guo BC, Sun LR, *et al.* TNM staging of colorectal cancer should be reconsidered by T stage weighting. World J Gastroenterol 2014; 20: 5104-12.
28. Snaebjornsson P, Coupe VM, Jonasson L, Meijer GA, van Grieken NC, Jonasson JG. pT4 stage II and III colon cancers carry the worst prognosis in a nationwide survival analysis: Shepherd's local peritoneal involvement revisited. Int J Cancer 2014; 135: 467-78.

 http://dx.doi.org/10.4132/jptm.2015.02.05

Journal of Pathology and Translational Medicine 2015; 49: 129-135
http://dx.doi.org/10.4132/jptm.2015.01.28

■ ORIGINAL ARTICLE ■

Image-Guided Fine Needle Cytology with Aspiration Versus Non-Aspiration in Retroperitoneal Masses: Is Aspiration Necessary?

Rajiv Kumar Misra · Shaila Mitra Rishav Kumar Jain[1] · Shilpa Vahikar Archana Bundela · Purak Misra[2]

Departments of Pathology and [1]Radiology, B.R.D. Medical College, Gorakhpur; [2]Apollo Hospital, New Delhi, India

Received: March 6, 2014
Revised: January 24, 2015
Accepted: January 28, 2015

Corresponding Author
Shaila Mitra, M.D.
Department of Pathology, B.R.D Medical College, Gorakhpur, 273013 Uttar Pradesh, India
Tel: +91-7379651447
Fax: +91-0551-2501736
E-mail: shaila.prasad14@yahoo.co.in

Background: Although using fine needle cytology with aspiration (FNC-A) for establishing diagnoses in the retroperitoneal region has shown promise, there is scant literature supporting a role of non-aspiration cytology (FNC-NA) for this region. We assessed the accuracy and reliability of FNC-A and FNC-NA as tools for preoperative diagnosis of retroperitoneal masses and compared the results of both techniques with each other and with histopathology. **Methods:** Fifty-seven patients with retroperitoneal masses were subjected to FNC-A and FNC-NA. Smears were stained with May-Grunwald Giemsa and hematoxylin and eosin stain. An individual slide was objectively analysed using a point scoring system to enable comparison between FNC-A and FNC-NA. **Results:** By FNC-A, 91.7% accuracy was obtained in cases of retroperitoneal lymph node lesions followed by renal masses (83.3%). The diagnostic accuracy of other sites by FNC-A varied from 75.0%–81.9%. By FNC-NA, 93.4% diagnostically accurate results were obtained in the kidney, followed by 75.0% in adrenal masses. The diagnostic accuracy of other sites by FNC-NA varied from 66.7%–72.8%. **Conclusions:** Although both techniques have their own advantages and disadvantages, FNC-NA may be a more efficient adjuvant method of sampling in retroperitoneal lesions.

Key Words: Fine needle aspiration; Non-aspiration technique; Retroperitoneal masses

The retroperitoneum has long been an area of interest in the aspect of diagnostic procedure because diagnostic procedures generally used in other sites fall short of providing the requisite access. Considering the numerous and heterogeneous contents of this region, lesions may be encountered in lymph nodes, soft tissues, adrenal glands, kidneys, ureters, and the aorta and its branches.

Two cytodiagnostic techniques are available to obtain cytology samples. They are fine needle cytology with aspiration (FNC-A) and an alternative "non-aspiration technique" (FNC-NA),[1,2] which was developed in France.

Although a large volume of data is available to compare FNC-A and FNC-NA sampling in superficial lesions, no literature is available regarding FNC-NA for retroperitoneal masses. Therefore, we have studied the utility of FNC-NA by comparing it with FNC-A and with histopathology.

MATERIALS AND METHODS

The study was carried out in the Department of Pathology from August 2010 to July 2013 on 57 patients with retroperitoneal masses on ultrasound (USG). After proper workup, including detailed clinical history and examination, FNC-A was performed using a 9 cm, 22–24 gauge spinal needle attached to a 20-mL syringe. FNC-NA was performed with a 22–24 gauge spinal needle without a syringe. Fine needle aspiration sampling was performed as described previously.[3]

FNC-NA was performed by holding the needle directly with the finger tips and inserting it into the target lesion with USG guidance. After reaching the site, the stylet was removed and the needle was moved back and forth in various directions at different depths. Removal of the stylet at this stage avoids contamination of diagnostic material with other tissues of the needle track. The needle was then taken out from the site and connected to a syringe filled with air. Cellular material was then expelled onto a glass slide. Uniform and thinly spread smears were obtained with the superimposition technique.[1]

Both cytotechniques were done at the same time and slides were made by a single operator, avoiding bias in all stages of sampling from patient examination to slide fixation. Smears

pISSN 2383-7837
eISSN 2383-7845

Table 1. Modified scoring system used in the interpretation of cytological features

Criteria	Description		Point score
Background, blood clot	Large amount	Great compromise to diagnosis	0
	Large amount	Diagnosis still possible	0.5
	Moderate	Diagnosis possible	1
	Moderate	Diagnosis evident	1.5
	Minimal	Excellent quality	2
Amount of cellular material	Absent	Diagnosis not possible	0
	Minimal	Diagnosis still possible	0.5
	Moderate	Sufficient for diagnosis	1
	Moderate to abundant	Diagnosis evident	1.5
	Abundant	Diagnosis simple, excellent quality	2
Degree of cellular degeneration	Marked	Diagnosis impossible	0
	Marked	Diagnosis still possible	0.5
	Moderate	Diagnosis possible	1
	Moderate	Diagnosis evident	1.5
	Minimal	Diagnosis easy	2
Degree of cellular trauma	Marked	Diagnosis impossible	0
	Marked	Diagnosis still possible	0.5
	Moderate	Diagnosis possible	1
	Moderate	Diagnosis evident	1.5
	Minimal	Diagnosis easy	2
Retention of appropriate architectures	Minimal to absent	Diagnosis impossible	0
	Minimal	Diagnosis still possible	0.5
	Moderate	Some preservation Follicles, papillae, acini, flat sheets, syncitia, single cells, etc. Diagnosis evident	1
	Moderate	Excellent architectural display closely reflecting histological diagnosis	1.5
	Excellent		2

were stained with May-Grunwald Giemsa and hematoxylin and eosin stain. An individual slide was objectively analysed using a point scoring system[4] to enable comparison between FNC-A and FNC-NA techniques as shown in Table 1. On the basis of the five criteria tabulated, a cumulative score between 0–10 points was allocated to each fine needle specimen, which was then categorized as unsuitable for cytodiagnosis (score, 0–2), suitable for cytodiagnosis (score, 3–6) or diagnostically superior (score, 7–10). Accuracy of the cytological diagnoses was assessed by two different pathologists through comparison with the histological diagnosis All the results so obtained were interpreted statistically using the student's t-test.

RESULTS

Fifty-seven cases of retroperitoneal lesions were studied in patients ranging from 6–80 years of age. Most patients (56.1%) were 50–60 years old; 37 patients (64.9%) were male and 20 (35.0%) were female.

Thirty cases (52.6%) were from the kidney followed by 12 cases (21.0%) from retroperitoneal lymph nodes. Eleven cases (19.2%) were from soft tissues and miscellaneous organs, while only four cases (7.0%) were from the adrenal glands.

Among 30 cases of renal masses, eight (14.0%) were polycystic kidney disease, 16 cases (28.0%) were renal cell carcinoma and six (10.5%) were neuroblastoma. Out of twelve cases of retroperitoneal lymphadenopathy, tuberculous lymphadenitis was found in six cases (10.5%), while non-Hodgkin lymphoma and metastatic seminoma were found in three cases each (5.2%). Out of 11 cases (19.2%) of soft tissue tumours, six cases (10.5%) were diagnosed as liposarcoma, three cases (5.2%) as malignant fibrous histiocytoma, and two cases (3.5%) as fibrosarcoma. All four cases (7.0%) of adrenal mass were pheochromocytoma. The relatively high incidence of neuroblastoma does not reflect the epidemiological incidence of this area, because our center is a referral center and caters to the referred patients from eastern parts of India and Nepal. Although polycystic kidney does not present as a renal mass, a provisional diagnosis of cystic renal lesion was rendered in radiological workup. Therefore, cytological examination was performed to arrive at an accurate diagnosis and to differentiate among cystic lesions such as benign renal cysts, cystic renal cell carcinoma and polycystic kidney.

FNC-A had more blood contamination than FNC-NA smears in all cases and the difference between the techniques was statistically significant in all cases except adrenal masses (Table 2, Fig. 1).

http://dx.doi.org/10.4132/jptm.2015.01.28

Table 2. Comparison of cytological features in the retroperitoneal organs

Site	Background, blood clot	Amount of cellular material	Degeneration	Cell trauma	Maintenance of architectural/cellular arrangement	Average
Kidney (n=30)						
FNC-NA	1.630±0.556	1.060±0.365	1.580±0.648	1.360±0.614	1.260±0.520	6.530±1.846
FNC-A	1.160±0.580	1.260±0.520	1.000±0.574	1.300±0.534	0.520±0.210	5.090±1.246
p-value	<.01	.09	.03	.31	<.01	<.01
Adrenal (n=4)						
FNC-NA	1.00±0.707	0.75±0.830	1.020±0.72	1.000±0.707	0.980±0.707	2.000±1.590
FNC-A	0.75±0.830	0.99±0.810	0.680±0.789	0.750±0.830	0.980±0.707	1.500±1.660
p-value	.66	.69	.55	.25	>.99	.68
RPLN (n=12)						
FNC-NA	1.33±0.346	0.580±0.3	1.200±0.484	1.600±0.648	0.916±0.493	5.960±2.780
FNC-A	0.916±0.277	1.290±0.62	1.023±0.348	1.000±0.578	0.916±0.493	6.500±2.160
p-value	<.01	<.01	.11	.03	>.99	.60
Miscellaneous (n=11)						
FNC-NA	1.020±0.417	0.660±0.486	1.020±0.417	1.020±0.319	0.630±0.298	6.360±1.846
FNC-A	0.59±0.298	1.000±0.574	0.590±0.312	0.520±0.312	0.997±0.660	5.090±1.246
p-value	<.01	.13	.04	.001	.05	.07
Total (n=57)						
FNC-NA	1.105±0.325	1.139±0.464	1.233±0.426	1.267±0.455	1.067±0.456	5.833±1.403
FNC-A	1.102±0.425	1.161±0.611	0.911±0.339	0.642±0.321	1.170±0.488	4.884±1.146
p-value	.26	.82	<.01	<.01	.15	<.01

FNC-NA, fine needle cytology with non-aspiration; FNC-A, fine needle cytology with aspiration; RPLN, retroperitoneal lymph node.

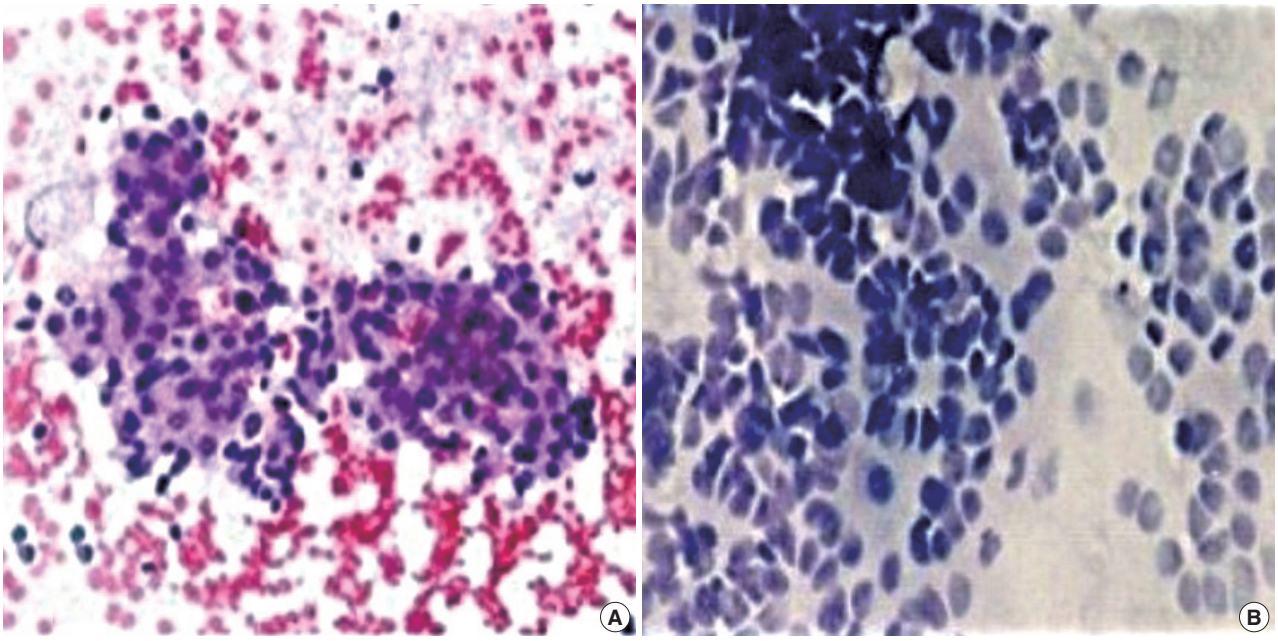

Fig. 1. (A) Fine needle aspiration cytology of neuroblastoma showing sheets and clusters of round, monomorphic tumor cells on a hemorrhagic background. (B) Non-aspiration cytology of neuroblastoma showing clusters and dispersed small, round cells with a high nucleocytoplasmic ratio and scant cytoplasm.

FNC-A smears revealed more dislodged cellular material across the slides than FNC-NA smears but statistical superiority was seen only for retroperitoneal lymph nodes ($p<.01$) (Table 2).

Cellular degeneration was greater in FNC-A in all cases, but this difference was statistically significant for kidney ($p=.03$) and miscellaneous groups ($p=.04$) only.

Greater trauma was observed in FNC-A smears as evidenced by increased blood contamination, clumping of cells, and shrinkage artefacts along with chromatin smearing and smudging while cellular preservation was better in FNC-NA.

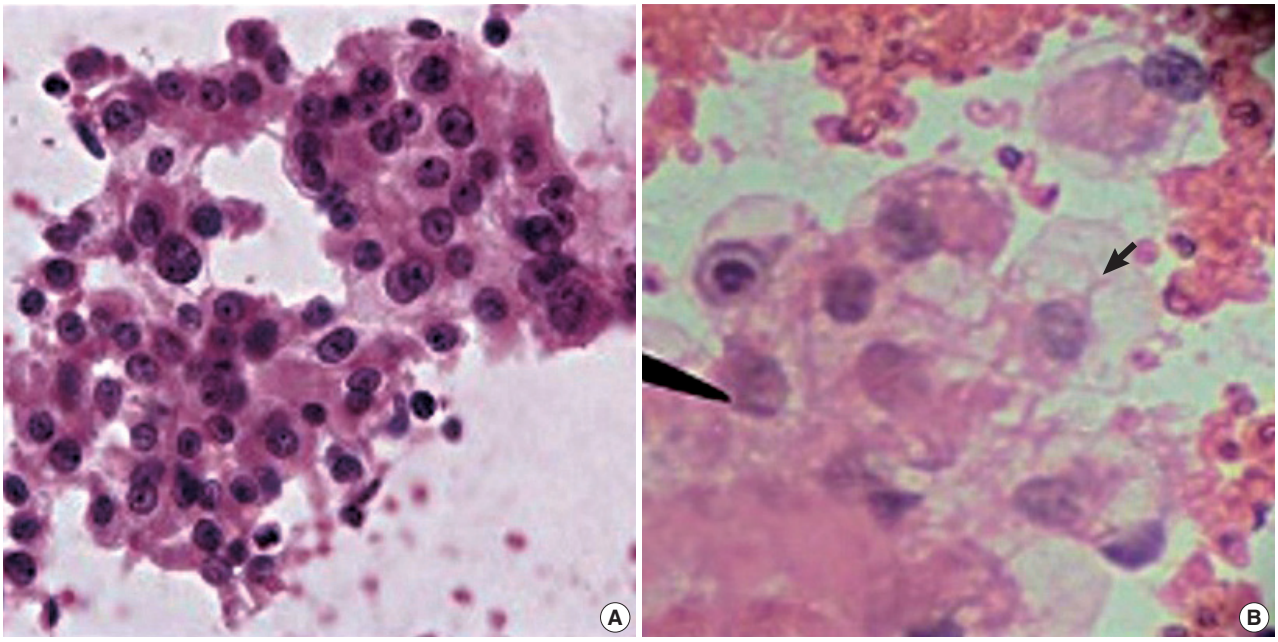

Fig. 2. (A) Fine needle cytology with non-aspiration smear of renal cell carcinoma showing sheets and clusters of cells with abundant, delicate, wispy, finely vacuolated cytoplasm and enlarged nuclei, fine chromatin, prominent nucleoli and thick irregular nuclear border on a relatively clean background. (B) Fine needle cytology with aspiration smear of renal cell carcinoma showing a sheet of cells with abundant vacuolated cytoplasm (arrow) and enlarged nuclei on a haemorrhagic background.

Table 3. Comparison of quality of smears obtained by FNC-A and FNC-NA

Quality of smear	FNC-A	FNC-NA	p-value
Superior (7–10)	20 (35.1)	27 (47.4)	.18
Diagnostic (3–6)	31 (54.4)	20 (35.1)	.03
Superior+Diagnostic (3–10)	51 (89.4)	47 (82.4)	.28
Insufficient (0–2)	6 (10.5)	10 (17.5)	-

Values are presented as number (%).
FNC-A, fine needle cytology with aspiration; FNC-NA, fine needle cytology with non-aspiration.

Table 4. Comparison of sitewise and overall diagnostic accuracy of FNC-NA and FNC-A

Site	Histopathology obtained	Diagnostic accuracy		p-value
		FNC-NA	FNC-A	
Kidney	30	28 (93.4)	25 (83.3)	.42
Adrenal	4	3 (75.0)	3 (75.0)	>.99
RPLN	12	8 (66.7)	11 (91.6)	.31
Miscellaneous	11	8 (72.8)	9 (81.9)	>.05
Total	57	47 (82.4)	48 (84.2)	.80

Values are presented as number (%).
FNC-NA, fine needle cytology with non-aspiration; FNC-A, fine needle cytology with aspiration; RPLN, retroperitoneal lymph node.

When comparing the architectural arrangements of cells in smears obtained by both techniques, such as rosette formations in neuroblastoma, dissociated cells in lymphoma, glandular tissue fragments in adenocarcinoma, and papillary fragments in papillary tumors, the difference was statistically insignificant in all cases except the kidneys where FNC-NA was superior to FNC-A ($p < .01$).

There was a statistically insignificant difference in sampling technique score in all cases except in the kidney, where the FNC-NA score was statistically significant ($p < .01$) (Table 2, Fig. 2).

Smears obtained by FNC-A and FNC-NA techniques were then categorized on the basis of scores obtained (Table 3). FNC-A produced a greater number of diagnostically adequate smears (31 cases, 54.4%) than FNC-NA (20 cases, 35.1%) ($p = .03$). FNC-NA provided more diagnostically "superior quality smears" (27 cases, 47.4%) than FNC-A (20 cases, 35.1%), but the difference was statistically insignificant ($p = .18$). Diagnosis could be made in 51 cases (89.4%) by FNC-A as compared to 47 cases (82.4%) by FNC-NA when combining superior and diagnostic quality scores. FNC-NA had more smears showing inadequate material for diagnosis (10 cases, 17.5%) than FNC-A (6 cases, 10.5%).

The overall diagnostic accuracy was 82.4% in FNC-NA and 84.2% in FNC-A ($p = .08$). Accuracy of 91.7% was obtained in retroperitoneal lymph node lesions while 83.3% accuracy was obtained in renal masses by FNC-A. The diagnostic accuracy of other sites by FNC-A varied from 75.0%–81.9%. Diagnostically accurate results of 93.4% were obtained in the kidney and

http://dx.doi.org/10.4132/jptm.2015.01.28

75.0% diagnostically accurate results were obtained in adrenal masses by FNC-NA. The diagnostic accuracy of other sites by FNC-NA varied from 66.7%–72.8%, with lowest being in the retroperitoneal lymph nodes (Table 4).

DISCUSSION

FNC-A is widely accepted as the primary method for diagnosis of palpable masses.[5] In 1930, Martin and Ellis[3] first presented a tumor diagnosis by needle aspiration and termed it "aspiration biopsy." Franzen *et al.*[6] in 1955 introduced a special syringe holder and thus improved the technique.[7,8]

FNC-NA was developed in France by Brifford *et al.*[1] in 1982. It avoids aspiration and relies on capillary pressure to suck cells inside the needle core. The French authors termed this technique as "cytopuncture." It has been shown that with the application of an objective scoring system, FNC-NA produces a comparable cellular yield, and has a similar diagnostic accuracy to the classic fine needle aspiration technique.[9-11] Many studies have proved that FNC-NA seems to be better for diagnosing malignant lesions while FNC-A appeared better for diagnosing benign lesions.[12-14] Malignant cells, being fragile, are more prone to degeneration and trauma of suction. The application of suction to draw cells through a fine needle traumatizes fragile cells, resulting in artifacts that can lead to diagnostic error. They opined that FNC-NA was more patient friendly, gave more cellular yield with less blood contamination and improved quality of the smears. FNC-A was considered as the procedure of choice for cystic lesions as the fluid could be collected for cytological evaluation. According to them better diagnostic results could be obtained if both the techniques are used together.[9,11-15]

The function of negative pressure is not to tear the cells from the tissue but to hold the tissue against the sharp cutting edge of the needle. Santos and Leiman[16] explained the scientific basis of the FNC-NA technique. This technique which employs the insertion of a fine needle into a lesion without attachment of a syringe, depends on the property of capillary tension in a narrow channel (outer diameter of needle, 0.6 mm). A fluid in a narrow channel is governed by the formula $h = 2T/pgr$, where h is the height attained, T is the surface tension of the fluid, p is the density of that fluid, g is the gravity and r is the radius. They performed a more exhaustive comparative analysis using both FNC-A and FNC-NA techniques on 50 thyroid lesions. In their study, diagnostically superior material was obtained in 22 (44.0%) of the non-aspiration samples versus four of aspiration samples (8.0%) ($p = .0033$). This is probably because in FNC-NA, concentrated cellular material that was less distorted by blood had better preservation of architecture and excellent picture quality.

Zajdela *et al.*[17] 1987, studied a large series of mammary tumors in order to compare the results of FNC-A with those of FNC-NA. In their study FNC-A was employed in all the cases prior to 1981, and after that FNC-NA was used. Therefore, these techniques were not used together on the same tumours or patient populations. With FNC-NA, more precise entry into the mass was possible and this is particularly important in locations like the orbit and thyroid, to avoid injury to the eyeball and trachea.[18]

Other workers[19-21] tried to explain the reason for the lesser degree of blood contamination by FNC-NA. They reported that this could be because the specimen is obtained by a spontaneous capillary action without much trauma to tissues. Thus, it gives a clean and clear picture to the cytopathologist. In FNC-A, significant quantity of blood is aspirated, especially in vascular organs.

Cellular yield was more or less comparable for both techniques except in the kidneys, where FNC-NA was significantly better. USG-guided percutaneous FNC-A of renal masses was first reported by Kristensen *et al.*[21] The present findings are consistent with findings of Renshaw *et al.*[22] However, Mair *et al*.[4] and Zajdela *et al*.[17] did not find any significant difference in the smears prepared by both techniques. Jayaram and Gupta[23] observed that cellularity was higher in aspiration smears than in non-aspiration smears in goiters. Zhou *et al.*[24] mentioned that FNC-A may be more suitable than FNC-NA for sampling nodules that measure from 5.1 to 10.0 mm and > 20.0 mm. Stewart *et al.*[25] directly compared FNC-A and needle core biopsy in 141 patients undergoing image guided sampling of abdominal lesions and noticed that FNC-A cytology was more sensitive and accurate than biopsy.

Available literature on cellular trauma, degeneration and retention of architecture revealed less cellular degeneration and cellular trauma in FNC-NA as compared to FNC-A.[14,15] The high suction pressure that is maintained during FNC-A causes some increase in cellular trauma.[26,27] In FNC-NA, since suction pressure is not used, concentrated cellular material shows better preservation of the architecture with less traumatic distortion and less contamination by blood. FNC-NA smears showed better retention of architecture and excellent picture quality, whereas FNC-A smears had good quantity of material. Ghosh *et al.*[28] also observed the same findings in their study of FNC-NA on thyroid lesions. Better preservation of architecture and excellent picture quality was the only parameter in which FNC-NA scored

much better than FNC-A, as reported by other authors.[14,15,18,28]

Low cellularity and fibrous lesions appear to be a main cause of FNC-NA failure. However Zajdela *et al.*[17] found that the frequency of insufficient cellular yield was less by FNC-NA (5.5%) than FNC-A (6.0%).

In this study, non-aspiration sampling was used as the first sampling method in all cases. This design was based on the interventional radiology literature, which suggests that if both methods are to be used, the less traumatic method (i.e., non-aspiration sampling) must precede the negative pressure method (FNC-A) to ensure the initial samples will contain less bloody material and be more amenable to rapid staining and analysis. The drawback of using this technique was that initial biopsies with non-aspiration sampling may have caused tissue damage and bleeding, putting subsequently collected FNC-A specimens at a disadvantage.

In most cases, sufficient diagnostic material was dislodged over the slide by FNC-A, thereby increasing its diagnostic accuracy ($p = .03$). Out of 57 cases of retroperitoneal lumps, diagnosis was made in greater number of cases by FNC-A compared to FNC-NA, while the quality of smears was superior in FNC-NA.

We used a long, 24-gauge lumbar puncture needle of 24-gauge instead of a short hypodermic needles with good results, as cells are detached by the cutting edge of the needle and conducted into the lumen by capillary force. The caliber of the needle is more important than the length as noted by the physical principle that ascent of fluid into a narrow channel is governed by the formula $h = 2T/pgr$.

In retroperitoneal masses, USG-guided FNC-NA may be a more efficient adjuvant method of sampling. Non-aspiration (FNC-NA) provides "superb quality" of smears with superior diagnostic value and is less traumatic, simple, and easy to perform with better patient compliance. It also produces better quality of cellularity and less field obscurity by blood, and allows for much better control of the needle while in the lesion. In addition, direct contact with the needle allows a more sensitive fingertip feeling of the consistency of the tumor tissue during sampling. Preferably, FNC-NA should be performed initially, followed by FNC-A in order to attain a clear and accurate cytological diagnosis. In highly cellular lesions where abundant material was obtained, FNC-NA was most likely to be diagnostically superior, although FNC-A can also diagnose most lesions. In less cellular lesions, however, FNC-A was most likely to be diagnostically superior to FNC-NA. In addition, simple benign lesion or abscesses can be drained by aspiration for therapeutic purposes.

Conflicts of Interest

No potential conflict of interest relevant to this article was reported.

REFERENCES

1. Briffod M, Gentile A, Hebert H. Cytopuncture in the follow-up of breast carcinoma. Acta Cytol 1982; 26: 195-200.
2. Zajdela A, de Maublanc MA, Schlienger P, Haye C. Cytologic diagnosis of orbital and periorbital palpable tumors using fine-needle sampling without aspiration. Diagn Cytopathol 1986; 2: 17-20.
3. Martin HE, Ellis EB. Biopsy by needle puncture and aspiration. Ann Surg 1930; 92: 169-81.
4. Mair S, Dunbar F, Becker PJ, Du Plessis W. Fine needle cytology: is aspiration suction necessary? A study of 100 masses in various sites. Acta Cytol 1989; 33: 809-13.
5. Orell SR, Sterrett GF, Whitaker D. Fine needle aspiration cytology. 4th ed. Philadelphia: Elsevier Churchill Livingstone, 2005; 125-64.
6. Franzen S, Giertz G, Zajicek J. Cytological diagnosis of prostatic tumours by transrectal aspiration biopsy: a preliminary report. Br J Urol 1960; 32: 193-6.
7. Zajicek J, Franzén S, Jakobsson P, Rubio C, Unsgaard B. Aspiration biopsy of mammary tumors in diagnosis and research: a critical review of 2,200 cases. Acta Cytol 1967; 11: 169-75.
8. Kate MS, Kamal MM, Bobhate SK, Kher AV. Evaluation of fine needle capillary sampling in superficial and deep-seated lesions. An analysis of 670 cases. Acta Cytol 1998; 42: 679-84.
9. Kamal MM, Arjune DG, Kulkarni HR. Comparative study of fine needle aspiration and fine needle capillary sampling of thyroid lesions. Acta Cytol 2002; 46: 30-4.
10. Gadkari RU, Pangarkar M, Dandige S, Munshi M, Kher A. Efficacy of fine needle capillary sampling in the diagnosis of stage III and IV cervical carcinoma. Acta Cytol 1999; 43: 114-6.
11. Pothier DD, Narula AA. Should we apply suction during fine needle cytology of thyroid lesions? A systematic review and meta-analysis. Ann R Coll Surg Engl 2006; 88: 643-5.
12. Suen KC, Quenville NF. Fine needle aspiration biopsy of the thyroid gland: a study of 304 cases. J Clin Pathol 1983; 36: 1036-45.
13. Jayaram N, Chetan M, Prasad SR, Ramaprasad AV. Thyroiditis: thyroid function and cytologic correlation: a study of 66 cases. J Cytol 1996; 13: 21-4.
14. Raghuveer CV, Leekha I, Pai MR, Adhikari P. Fine needle aspiration cytology versus fine needle sampling without aspiration: a prospective study of 200 cases. Indian J Med Sci 2002; 56: 431-9.

 http://dx.doi.org/10.4132/jptm.2015.01.28

15. Pinki P, Alok D, Ranjan A, Chand MN. Fine needle aspiration cytology versus fine needle capillary sampling in cytological diagnosis of thyroid lesion. Iran J Pathol 2015; 10: 47-53.
16. Santos JE, Leiman G. Nonaspiration fine needle cytology: application of a new technique to nodular thyroid disease. Acta Cytol 1988; 32: 353-6.
17. Zajdela A, Zillhardt P, Voillemot N. Cytological diagnosis by fine needle sampling without aspiration. Cancer 1987; 59: 1201-5.
18. Rajasekhar A, Sundaram C, Chowdhary T, Charanpal M, Ratnakar KS. Diagnostic utility of fine-needle sampling without aspiration: a prospective study. Diagn Cytopathol 1991; 7: 473-6.
19. Rizvi SA, Husain M, Khan S, Mohsin M. A comparative study of fine needle aspiration cytology versus non-aspiration technique in thyroid lesions. Surgeon 2005; 3: 273-6.
20. Haddadi-Nezhad S, Larijani B, Tavangar SM, Nouraei SM. Comparison of fine-needle-nonaspiration with fine-needle-aspiration technique in the cytologic studies of thyroid nodules. Endocr Pathol 2003; 14: 369-73.
21. Kristensen JK, Bartels E, Jorgensen HE. Percutaneous renal biopsy under the guidance of ultrasound. Scand J Urol Nephrol 1974; 8: 223-6.
22. Renshaw AA, Granter SR, Cibas ES. Fine-needle aspiration of the adult kidney. Cancer 1997; 81: 71-88.
23. Jayaram G, Gupta B. Nonaspiration fine needle cytology in diffuse and nodular thyroid lesions: a study of 220 cases. Acta Cytol 1991; 35: 789-90.
24. Zhou JQ, Zhang JW, Zhan WW, *et al.* Comparison of fine-needle aspiration and fine-needle capillary sampling of thyroid nodules: a prospective study with emphasis on the influence of nodule size. Cancer Cytopathol 2014; 122: 266-73.
25. Stewart CJ, Coldewey J, Stewart IS. Comparison of fine needle aspiration cytology and needle core biopsy in the diagnosis of radiologically detected abdominal lesions. J Clin Pathol 2002; 55: 93-7.
26. Hamburger JI, Hamburger SW. Fine needle biopsy of thyroid nodules: avoiding the pitfalls. N Y State J Med 1986; 86: 241-9.
27. Lowhagen T, Sprenger E. Cytologic presentation of thyroid tumors in aspiration biopsy smear. A review of 60 cases. Acta Cytol 1974; 18: 192-7.
28. Ghosh A, Misra RK, Sharma SP, Singh HN, Chaturvedi AK. Aspiration vs nonaspiration technique of cytodiagnosis: a critical evaluation in 160 cases. Indian J Pathol Microbiol 2000; 43: 107-12.

Journal of Pathology and Translational Medicine 2015; 49: 136-143
http://dx.doi.org/10.4132/jptm.2015.01.03

■ ORIGINAL ARTICLE ■

Accuracy of Core Needle Biopsy Versus Fine Needle Aspiration Cytology for Diagnosing Salivary Gland Tumors

In Hye Song · Joon Seon Song
Chang Ohk Sung · Jong-Lyel Roh[1]
Seung-Ho Choi[1] · Soon Yuhl Nam[1]
Sang Yoon Kim[1] · Jeong Hyun Lee[2]
Jung Hwan Baek[2] · Kyung-Ja Cho

Departments of Pathology, [1]Otorhinolaryngology, and [2]Radiology, Asan Medical Center, University of Ulsan College of Medicine, Seoul, Korea

Received: October 24, 2014
Revised: December 16, 2014
Accepted: January 3, 2015

Corresponding Author
Kyung-Ja Cho, M.D.
Department of Pathology, Asan Medical Center, University of Ulsan College of Medicine, 88 Olympic-ro 43-gil, Songpa-gu, Seoul 138-736, Korea
Tel: +82-2-3010-4545
Fax: +82-2-472-7898
E-mail: kjc@amc.seoul.kr

Background: Core needle biopsy is a relatively new technique used to diagnose salivary gland lesions, and its role in comparison with fine needle aspiration cytology needs to be refined. **Methods:** We compared the results of 228 ultrasound-guided core needle biopsy and 371 fine needle aspiration procedures performed on major salivary gland tumors with their postoperative histological diagnoses. **Results:** Core needle biopsy resulted in significantly higher sensitivity and more accurate tumor subtyping, especially for malignant tumors, than fine needle aspiration. No patient developed major complications after core needle biopsy. **Conclusions:** We recommend ultrasound-guided core needle biopsy as the primary diagnostic tool for the preoperative evaluation of patients with salivary gland lesions, especially when malignancy is suspected.

Key Words: Salivary gland neoplasms; Biopsy, large-core needle; Biopsy, fine-needle; Parotid gland; Submandibular gland

In recent decades, fine needle aspiration cytology (FNAC) has been established as an efficient diagnostic tool for superficial masses, including salivary gland lesions. FNAC is technically simple, safe, fast, and cost-effective. However, FNAC traditionally demonstrates relatively low sensitivity in comparison with its high specificity for diagnosing salivary gland tumors. According to a previous meta-analysis by Schmidt *et al.*,[1] the average sensitivity and specificity determined in 6,169 cases were 80% and 97%, respectively. Recent studies report that the sensitivity and specificity of FNAC range between 64%–90% and 86%–100%, respectively.[2-8] The low sensitivity of FNAC can be attributed to several factors, but is primarily due to the difficulty of diagnosing low-grade carcinomas by cellular morphology alone.

Core needle biopsy (CNB) is a relatively new technique for diagnosing salivary gland lesions. Since intact tissue cores can be retrieved using ultrasound-guided CNB, improved specimen adequacy is expected. The sensitivity and specificity of salivary gland CNB are reportedly 92%–94% and 99%–100%, respectively.[9-12] Preoperative evaluation of salivary gland lesions should provide the clinicians with a treatment plan including the type and extent of surgical intervention needed. For this purpose, differentiating benign from malignant tumors is crucial, and moreover, information on the grade and specific type of the tumor will further aid in the choice of therapeutic procedures.

With the aim of establishing the most accurate diagnostic tool as new techniques emerge, we compared the diagnostic accuracy and accurate tumor subtyping rates of CNB and FNAC performed for the preoperative evaluation of salivary gland tumors.

MATERIALS AND METHODS

Between July 2008 and June 2013, 708 tumors in the major salivary glands were surgically resected from 705 patients at Asan Medical Center in Seoul, Korea. Of these 708 cases, 562 cases

pISSN 2383-7837
eISSN 2383-7845

had undergone in-house preoperative FNAC and/or ultrasound-guided CNB (US-CNB) procedures 1–3 times previously. The FNAC procedures were performed by pathologists on 371 occasions, using traditional methods with 23-gauge syringes. Two hundred and twenty-eight CNB procedures were performed by radiologists under ultrasound guidance, using a 1.1- or 1.6-cm excursion, 18-gauge, double-action, spring-activated needle (TSK Ace-cut, Create Medic, Yokohama, Japan) after administering local anesthesia with 1% lidocaine. Of these, 33 cases had undergone FNAC followed by US-CNB. No patients developed immediate or delayed complications after the procedure. We compared the diagnoses determined by preoperative FNAC without image guidance and US-CNB with the postoperative histological diagnoses. In addition, specimen adequacy, sensitivity, specificity, positive predictive value (PPV), negative predictive value (NPV), numbers of false-negative and -positive cases, and accurate tumor subtyping rate were analyzed. Tumor subtyping was considered accurate when one exact tumor type was diagnosed, favored, suggested, or suspected. The t test was used to evaluate differences in continuous data. The chi-squared test was used to assess the associations between categorical groups. The two-group proportion test was used to compare FNAC and CNB. All tests were two-sided, and $p < .05$ was considered statistically significant. Statistical analyses were performed using Stata/IC statistical software ver. 12 (StataCorp. Ltd., College Station, TX, USA).

RESULTS

Characteristics of the examined cases

The locations of the 562 surgical cases included parotid gland (n = 472), submandibular gland (n = 88), and sublingual gland (n = 2). Histologic diagnoses included 103 malignant and 459 benign tumors. Malignant tumors included 21 mucoepidermoid carcinomas, 17 salivary duct carcinomas, 17 carcinoma ex pleomorphic adenomas, 12 adenoid cystic carcinomas, 10 acinic cell carcinomas, 7 basal cell adenocarcinomas, 5 adenocarcinomas not otherwise specified, 3 epithelial-myoepithelial carcinomas, 3 squamous cell carcinomas, 2 oncocytic carcinomas, 1 cystadenocarcinoma, 3 malignant lymphomas, 1 rhabdomyosarcoma, and 1 undifferentiated pleomorphic sarcoma. Benign tumors included 305 pleomorphic adenomas, 96 Warthin tumors, 37 basal cell adenomas, 7 myoepitheliomas, 3 oncocytomas, 1 lymphadenoma, 5 neurogenic tumors (4 schwannomas and 1 neurofibroma), 3 vascular tumors (2 hemangiomas and 1 lymphangioma), and 2 lipomas.

When the general characteristics of the CNB and FNAC groups were compared to exclude selection bias, the proportion of malignancy, location, laterality, and multiplicity were not significantly different between the two groups (Table 1). One significant difference was the tumor size. The average size of tumors in the FNAC group was bigger than that in the CNB group ($p = .006$), which can be explained by the fact that generally patients with larger palpable tumors are sent to the Pathology Department for FNAC.

Specimen adequacy

Regarding the specimen adequacy of the 228 CNB specimens and 371 FNAC samples, the unsatisfactory rate tended to be lower following CNB (2.6%) than FNAC (6.2%) (Table 2). A total of 33 cases underwent CNB after FNAC. Adenoid cystic carcinoma, salivary duct carcinoma, and oncocytoma showed high rates for multiple diagnostic procedures (3/12, 3/17, and 1/3, respectively).

Accuracy

The sensitivity of detecting malignant tumors using the CNB method was significantly higher (88.2%) than that with FNAC (58.2%) ($p = .006$) (Table 3). The specificity, PPV, and NPV of CNB were slightly higher than those of FNAC, without significant differences.

False-negative and -positive cases

A total of 29 false-negative cases and 5 false-positive cases are listed in Table 4. False-negative results by CNB were restricted to cases of basal cell adenocarcinoma, carcinoma ex pleomorphic adenoma, and epithelial-myoepithelial carcinoma, while false-negative results by FNAC were found in a wide range of tumors

Table 1. General characteristics of salivary gland tumors according to CNB and FNAC

Characteristic		CNB (n = 228)	FNAC (n = 371)	p-value
Malignant:benign tumor		54:174	62:309	.479
Size (mean ± SD, cm)		2.57 ± 1.22	2.85 ± 1.21	.006
Site	Parotid	171 (75.0)	329 (88.7)	.150
	SMG	56 (24.6)	40 (10.8)	
	SLG	1 (0.4)	2 (0.5)	
Laterality	Left	126 (55.2)	193 (52.0)	.687
	Right	100 (43.9)	175 (47.2)	
	Bilateral	2 (0.9)	3 (0.8)	
Multiplicity		14 (6.1)	13 (3.5)	.560

Values are presented as number (%) unless otherwise indicated.
CNB, core needle biopsy; FNAC, fine needle aspiration cytology; SD, standard deviation; SMG, submandibular gland; SLG, sublingual gland.

Table 2. Unsatisfactory rates and repeated diagnostic procedure rates of salivary gland tumors according to histologic diagnoses

Histologic diagnoses		Unsatisfactory rates		Rates for multiple procedures
		CNB	FNAC	
Malignancy	ACC	0/9	1/6	3/12
	AciCC	1/4	0/7	1/10
	ANOS	0/2	1/3	0/5
	BADC	0/2	1/5	0/7
	CPA	0/5	1/13	1/17
	CystADC	-	1/2	0/1
	EMC	0/2	0/2	1/3
	MEC	1/15	1/7	1/21
	OC	-	0/2	0/2
	SCC	1/3	0/1	1/3
	SDC	0/10	1/10	3/17
	ML	0/1	0/2	0/3
	RMS	0/1	-	0/1
	UPS	-	0/1	0/1
Subtotal		3/54 (5.6)	7/62 (11.3)	
Benign	PA	1/117	10/199	11/305
	WT	2/33	3/70	6/96
	BA	0/16	0/24	2/37
	LA	0/1	-	0/1
	ME	0/2	0/6	1/7
	Oncocytoma	0/2	1/2	1/3
	NT	0/3	1/3	1/5
	VT	-	0/3	0/3
	Lipoma	-	1/2	0/2
Subtotal		3/174 (1.7)	16/309 (5.2)	
Total		6/228 (2.6)	23/371 (6.2)	

Values in parentheses are presented as percentage.
CNB, core needle biopsy; FNAC, fine needle aspiration cytology; ACC, adenoid cystic carcinoma; AciCC, acinic cell carcinoma; ANOS, adenocarcinoma, not otherwise specified; BADC, basal cell adenocarcinoma; CPA, carcinoma ex pleomorphic adenoma; CystADC, cystadenocarcinoma; EMC, epithelial-myoepithelial carcinoma; MEC, mucoepidermoid carcinoma; OC, oncocytic carcinoma; SCC, squamous cell carcinoma; SDC, salivary duct carcinoma; ML, malignant lymphoma; RMS, rhabdomyosarcoma; UPS, undifferentiated pleomorphic sarcoma; PA, pleomorphic adenoma; WT, Warthin tumor; BA, basal cell adenoma; LA, lymphadenoma; ME, myoepithelioma; NT, neurogenic tumor; VT, vascular tumor.

including adenoid cystic carcinoma, acinic cell carcinoma, adenocarcinoma not otherwise specified, mucoepidermoid carcinoma, oncocytic carcinoma, and malignant lymphoma (Fig. 1). No high-grade carcinomas (e.g., salivary duct carcinoma) were diagnosed as false-negatives by either method. False-positive results from neither method exhibited specific patterns; they might be the result of misinterpretation of pathologic findings, with or without artifacts.

Accurate tumor subtyping

The accurate tumor subtyping rates of the salivary gland tumors were significantly higher with CNB (88.3%) than with FNAC (70.7%) ($p < .001$) (Table 5). Immunohistochemical studies for tumor subtyping were performed in 11 CNB samples: CD117 in adenoid cystic carcinoma; smooth muscle actin, calponin, and p63 in pleomorphic adenoma; and S100 protein in

Table 3. Accuracy of preoperative CNB and FNAC for diagnosing salivary gland tumors

Characteristic	CNB	FNAC	p-value
Total No. of cases	228	371	-
No. of adequate specimens, n (%)	222 (97.4)	348 (93.8)	-
No. of unsatisfactory specimens, n (%)	6 (2.6)	23 (6.2)	.078
No. of adequate malignant cases	51	55	-
No. of preop. Dx as malignancy	45	32	-
No. of adequate benign cases	171	293	-
No. of preop. Dx as benign	170	289	-
Sensitivity (%)	88.20	58.20	.006
Specificity (%)	99.40	98.60	.742
Positive predictive value (%)	97.80	88.90	.253
Negative predictive value (%)	96.60	92.60	.121

CNB, core needle biopsy; FNAC, fine needle aspiration cytology; preop., preoperative; Dx, diagnosis.

Table 4. False-negative and -positive results determined by preoperative CNB and FNAC

Histologic diagnoses	CNB	FNAC
Malignancy (false-negative results)		
ACC	-	PA (n=1), benign cyst (n=1), mucocele (n=1)
AciCC	-	Oncocytoma (n=1)
ANOS	-	WT (n=1)
BADC	BA (n=2)	BA (n=2), benign cyst (n=1)
CPA	PA (n=2)	PA (n=7)
EMC	BA (n=1), PA (n=1)	PA (n=1), benign lesion (n=1)
MEC	-	PA (n=2), benign cyst (n=1), mucocele (n=1)
OC	-	Oncocytoma vs WT (n=1)
ML	-	Benign lymphoid lesion (n=1)
Benign (false-positive results)		
PA	MEC (n=1)	CPA (n=1), LG malignancy (n=1)
ME	-	ACC (n=2)

CNB, core needle biopsy; FNAC, fine needle aspiration cytology; ACC, adenoid cystic carcinoma; PA, pleomorphic adenoma; AciCC, acinic cell carcinoma; ANOS, adenocarcinoma, not otherwise specified; WT, Warthin tumor; BADC, basal cell adenocarcinoma; BA, basal cell adenoma; CPA, carcinoma ex pleomorphic adenoma; EMC, epithelial-myoepithelial carcinoma; MEC, mucoepidermoid carcinoma; OC, oncocytic carcinoma; ML, malignant lymphoma; ME, myoepithelioma; LG, low grade.

http://dx.doi.org/10.4132/jptm.2015.01.03

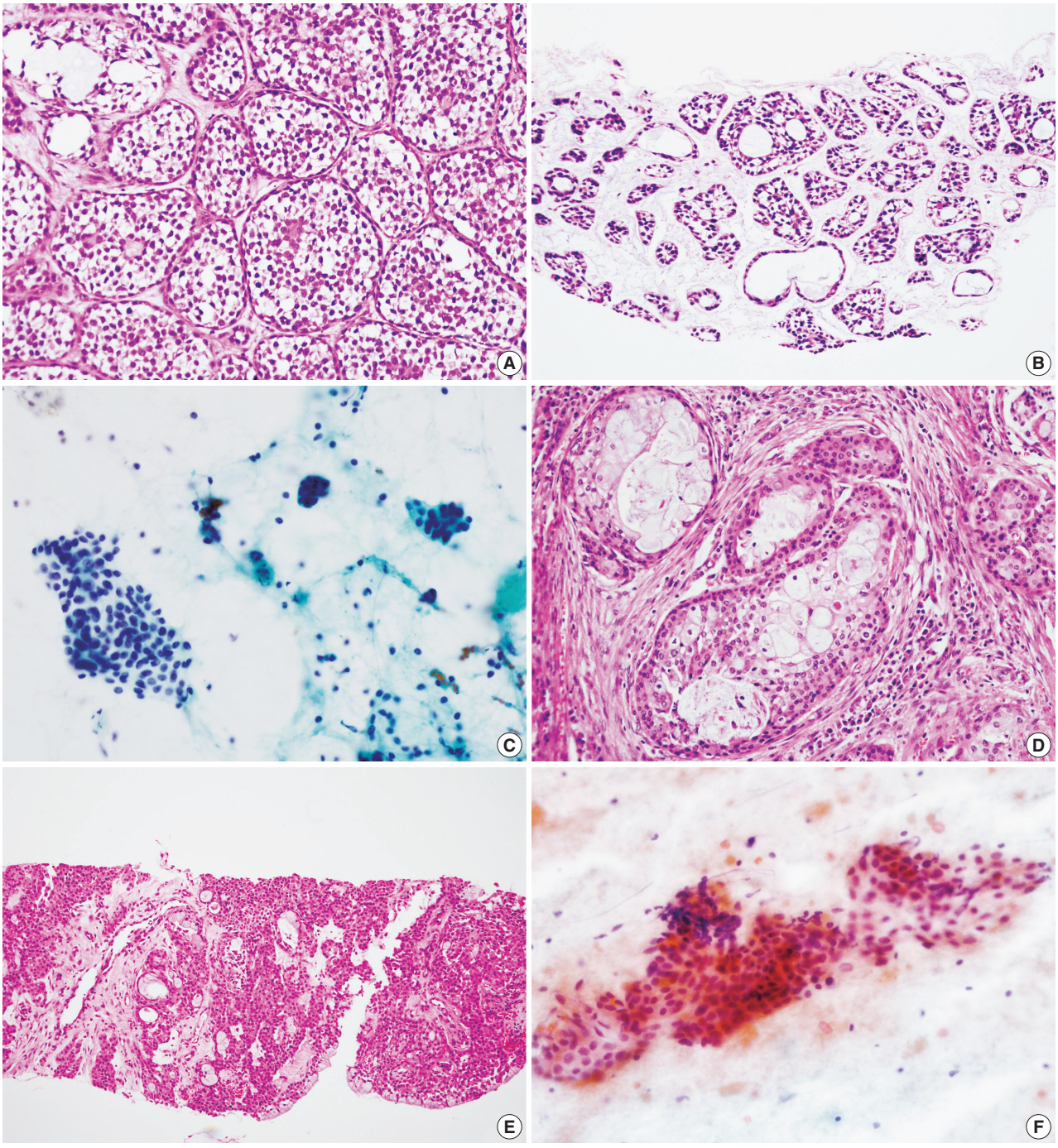

Fig. 1. Examples of low grade carcinomas diagnosed as false-negatives by fine needle aspiration cytology. (A) Adenoid cystic carcinoma in surgical specimens. (B) Core needle biopsy shows similar architectural findings. (C) Low cellularity and lack of obvious cellular atypia in fine needle aspiration cytology were interpreted as pleomorphic adenoma. (D) Mucoepidermoid carcinoma in surgical specimens. (E) Core needle biopsy shows intermediate and mucous cells. (F) Cystic background and presence of oncocytoid components in fine needle aspiration cytology led to the misdiagnosis of Warthin tumor.

neurogenic tumor. Tumor typing rates of benign tumors by CNB and FNAC were 91.8% and 80.5%, respectively (p = .003). For malignant tumors, accurate tumor subtyping was achieved in 39 of 51 CNB cases (76.5%), but in only 10 of 55 FNAC cases (18.2%) (p = .002). For a few special entities, both methods faced diagnostic difficulties. Since the diagnosis of basal cell adeno-

Table 5. Accurate tumor subtyping rates of salivary gland tumors determined by preoperative CNB and FNAC

Histologic diagnoses		CNB	FNAC	p-value
Malignancy	ACC	9/9	2/5	
	AciCC	3/3	4/7	
	ANOS	2/2	0/2	
	BADC	0/2	0/4	
	CPA	2/5	0/12	
	CystADC	-	0/1	
	EMC	0/2	0/2	
	MEC	12/14	2/6	
	OC	-	0/2	
	SCC	2/2	0/1	
	SDC	7/10	1/9	
	ML	1/1	1/2	
	RMS	1/1	-	
	UPS	-	0/2	
Subtotal		39/51 (76.5)	10/55 (18.2)	.002
Benign	PA	111/116	170/189	
	WT	31/31	53/66	
	BA	12/16	10/24	
	LA	0/1	-	
	ME	0/2	2/6	
	Oncocytoma	1/2	0/2	
	NT	2/3	1/2	
	VT	-	0/3	
	Lipoma	-	0/1	
Subtotal		157/171 (91.8)	236/293 (80.5)	.003
Total		196/222 (88.3)	246/348 (70.7)	<.001

Values in parentheses are presented as percentage.
CNB, core needle biopsy; FNAC, fine needle aspiration cytology; ACC, adenoid cystic carcinoma; AciCC, acinic cell carcinoma; ANOS, adenocarcinoma, not otherwise specified; BADC, basal cell adenocarcinoma; CPA, carcinoma ex pleomorphic adenoma; CystADC, cystadenocarcinoma; EMC, epithelial-myoepithelial carcinoma; MEC, mucoepidermoid carcinoma; OC, oncocytic carcinoma; SCC, squamous cell carcinoma; SDC, salivary duct carcinoma; ML, malignant lymphoma; RMS, rhabdomyosarcoma; UPS, undifferentiated pleomorphic sarcoma; PA, pleomorphic adenoma; WT, Warthin tumor; BA, basal cell adenoma; LA, lymphadenoma; ME, myoepithelioma; NT, neurogenic tumor; VT, vascular tumor.

carcinoma and oncocytic carcinoma requires extracapsular invasion by definition, none of these cases could be diagnosed using either CNB or FNAC (Fig. 2). Similarly, the diagnosis of carcinoma ex pleomorphic adenoma was not possible without concomitant carcinoma and pleomorphic adenoma components, even by CNB. The diagnosis of epithelial-myoepithelial carcinoma was difficult by either method, most likely due to its resemblance to pleomorphic adenoma, its low-grade nature, and a low index of suspicion (Fig. 2).

DISCUSSION

In 1999, Buckland *et al.*[13] introduced US-CNB using an 18-gauge needle, instead of fine needle aspiration using a 23-gauge needle, to evaluate salivary gland lesions. They reported satisfactory results based on their experiences of diagnosing and treating parotid gland masses in up to 220 patients.[14-17] The technique was soon adopted by other groups as well; small series of CNB results for salivary gland tumors have been reported from several countries, including the UK, Taiwan, Japan, and Germany.[11,12,18-20]

Our current study of 228 CNB and 371 FNAC procedures demonstrates the superiority of CNB over FNAC for diagnosing salivary gland tumors in terms of adequacy (97.4% vs 93.8%), sensitivity (88.2% vs 58.2%), specificity (99.4% vs 98.6%), PPV (97.8% vs 88.9%), NPV (96.6% vs 92.6%), and accurate tumor subtyping (88.3% vs 70.7%). Among these measures, differences in the sensitivity and tumor typing rate were statistically significant. These results are based on the histological confirmation of surgically treated cases. Although this type of design tends to lead to verification bias,[21] we did not include follow-up cases because our aims were to compare the accuracy of the two tests for specific diagnoses. As a result, the sensitivities of both methods may have been overestimated due to verification bias.[21] Even if the bias affected both methods, the sensitivity of CNB appears to be markedly improved, which can be attributed to the ability to recognize tumor structures by histological examination in CNB and not just cellular morphology alone as in FNAC.

The diversity and rarity of salivary gland carcinomas tend to provide diagnostic challenges for pathologists. Diagnosis of malignancy can be difficult when the cells in question pose no significant cytologic atypia. In addition, pathologists' experience and knowledge can affect the accuracy of FNAC. In our current study, no high-grade carcinomas, including salivary duct carcinoma and squamous cell carcinoma, were diagnosed as false-negatives using FNAC; however, low-grade carcinomas, including adenoid cystic carcinoma, acinic cell carcinoma, mucoepidermoid carcinoma, epithelial-myoepithelial carcinoma, and adenocarcinoma not otherwise specified, were occasionally misinterpreted as benign lesions. The PPV and NPV, which are not affected by verification bias, were also higher in CNB than in FNAC, though the differences were not statistically significant.

The difficulties of diagnosing basal cell adenocarcinoma, oncocytic carcinoma, and carcinoma ex pleomorphic adenoma apply to not only FNAC, but also to CNB when invasive and/or malignant foci are not sampled. For example, we misinterpreted two epithelial-myoepithelial carcinomas as pleomorphic adenoma in one and basal cell adenoma in the other, and one pleomorphic adenoma as mucoepidermoid carcinoma in CNB. Sali-

http://dx.doi.org/10.4132/jptm.2015.01.03

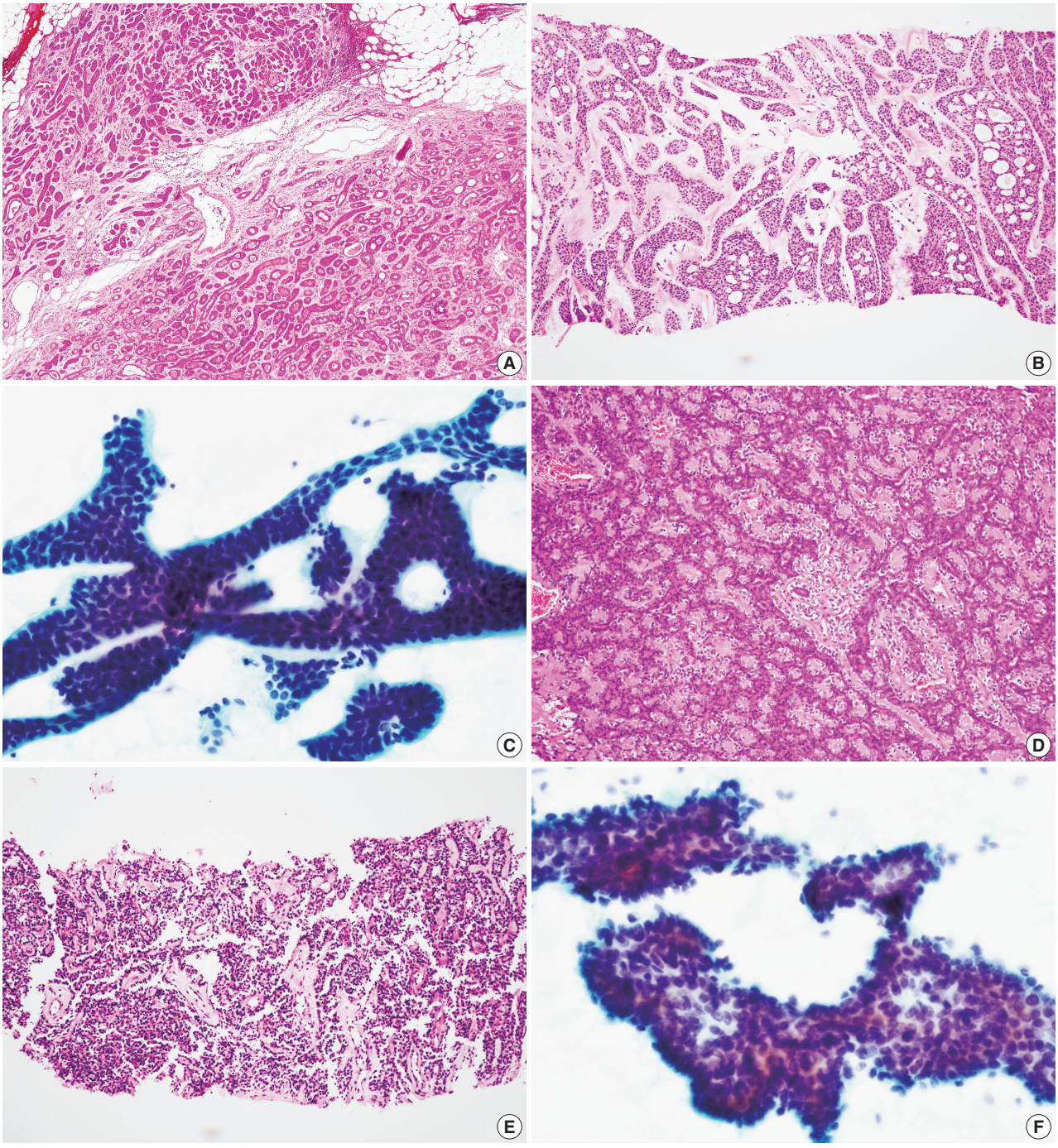

Fig. 2. Difficult samples for both core needle biopsy and fine needle aspiration. (A) Surgical specimen of basal cell adenocarcinoma shows extracapsular invasion which cannot be confirmed in core needle biopsy (B) or fine needle aspiration cytology (C). (D) Epithelial-myoepithelial structures of epithelial-myoepithelial carcinoma can be mistaken for those of pleomorphic adenoma in both core needle biopsy (E) and fine needle aspiration cytology (F), because of the lack of obvious cellular atypia.

vary gland tumors are diverse and also analogous with specific architectural patterns such as epithelial-myoepithelial structures which are present in various benign and malignant tumors. Interpreting a limited number of cores can be difficult, even for experienced pathologists. Nonetheless, accurate tumor subtyping rates were generally higher for CNB than for FNAC (88.3% vs 70.7%). In particular, malignant tumors were more often accurately classified using CNB than FNAC (76.5% vs 18.2%) in

comparison to the benign tumors (91.8% vs 80.5%). Both high- and low-grade carcinomas could be more specifically diagnosed by CNB than by FNAC.

Some clinicians prefer FNAC because it has technical advantages such as simplicity of the procedure, safety, cost-effectiveness, and the lack of need for ultrasound assistance. However, the CNB procedure is generally well tolerated under local anesthesia, and the actual complication rate of CNB appears to be far less than expected. The major complications of salivary gland biopsy include facial nerve injury and tumor seeding along the biopsy track. However, experienced radiologists can avoid facial nerve injury by tracing the main intraparotid vessels or the parotid duct, which can be easily identified on ultrasound.[14,18] Tumor seeding was once considered a significant complication when performing large needle biopsy on cancers, and the needle diameter and number of passes are assumed to be related to this risk.[22] However, such evidence is lacking in the case of salivary gland tumors. Two cases of tumor seeding following needle biopsy of the salivary gland using 14–16-gauge needles have been previously reported, but a few reports of tumor seeding following FNAC have also been reported more recently.[23,24] However low the risk, some authors have suggested surgical removal of the biopsy track at the time of surgery.[12,25]

No studies on the use of 18-gauge CNB to assess the salivary glands, including our present series, have reported these major complications. The minor complications that have been reported following salivary gland CNB include subclinical hematoma,[11,12,14-16,18,20] temporary facial weakness after local anesthesia,[11] and the formation of salivary fistulas.[17] Fistula developed after post-biopsy acute parotitis and did not present with tumor seeding.[17] Increased awareness of this rare complication would help provide better patient care and follow-up.

In conclusion, CNB is an accurate and safe method for diagnosing salivary gland lesions, and provides significant superiority in accurate tumor subtyping in comparison to FNAC. We recommend CNB as the primary diagnostic tool for preoperatively evaluating salivary gland masses, especially when malignancy is suspected.

Conflicts of Interest

No potential conflict of interest relevant to this article was reported.

REFERENCES

1. Schmidt RL, Hall BJ, Wilson AR, Layfield LJ. A systematic review and meta-analysis of the diagnostic accuracy of fine-needle aspiration cytology for parotid gland lesions. Am J Clin Pathol 2011; 136: 45-59.
2. Kim BY, Hyeon J, Ryu G, *et al*. Diagnostic accuracy of fine needle aspiration cytology for high-grade salivary gland tumors. Ann Surg Oncol 2013; 20: 2380-7.
3. Tryggvason G, Gailey MP, Hulstein SL, *et al.* Accuracy of fine-needle aspiration and imaging in the preoperative workup of salivary gland mass lesions treated surgically. Laryngoscope 2013; 123: 158-63.
4. Nguansangiam S, Jesdapatarakul S, Dhanarak N, Sosrisakorn K. Accuracy of fine needle aspiration cytology of salivary gland lesions: routine diagnostic experience in Bangkok, Thailand. Asian Pac J Cancer Prev 2012; 13: 1583-8.
5. Huang YT, Jung SM, Ko SF, *et al.* Diagnostic efficacy of ultrasonography-guided fine needle aspiration biopsy in evaluating salivary gland malignancy. Chang Gung Med J 2012; 35: 62-9.
6. Kechagias N, Ntomouchtsis A, Valeri R, *et al.* Fine-needle aspiration cytology of salivary gland tumours: a 10-year retrospective analysis. Oral Maxillofac Surg 2012; 16: 35-40.
7. Piccioni LO, Fabiano B, Gemma M, Sarandria D, Bussi M. Fine-needle aspiration cytology in the diagnosis of parotid lesions. Acta Otorhinolaryngol Ital 2011; 31: 1-4.
8. Cho HW, Kim J, Choi J, *et al.* Sonographically guided fine-needle aspiration biopsy of major salivary gland masses: a review of 245 cases. AJR Am J Roentgenol 2011; 196: 1160-3.
9. Schmidt RL, Hall BJ, Layfield LJ. A systematic review and meta-analysis of the diagnostic accuracy of ultrasound-guided core needle biopsy for salivary gland lesions. Am J Clin Pathol 2011; 136: 516-26.
10. Novoa E, Gurtler N, Arnoux A, Kraft M. Role of ultrasound-guided core-needle biopsy in the assessment of head and neck lesions: a meta-analysis and systematic review of the literature. Head Neck 2012; 34: 1497-503.
11. Pfeiffer J, Ridder GJ. Diagnostic value of ultrasound-guided core needle biopsy in patients with salivary gland masses. Int J Oral Maxillofac Surg 2012; 41: 437-43.
12. Huang YC, Wu CT, Lin G, Chuang WY, Yeow KM, Wan YL. Comparison of ultrasonographically guided fine-needle aspiration and core needle biopsy in the diagnosis of parotid masses. J Clin Ultrasound 2012; 40: 189-94.
13. Buckland JR, Manjaly G, Violaris N, Howlett DC. Ultrasound-guided cutting-needle biopsy of the parotid gland. J Laryngol Otol 1999; 113: 988-92.
14. Kesse KW, Manjaly G, Violaris N, Howlett DC. Ultrasound-guided biopsy in the evaluation of focal lesions and diffuse swelling of the parotid gland. Br J Oral Maxillofac Surg 2002; 40: 384-8.

 http://dx.doi.org/10.4132/jptm.2015.01.03

15. Howlett DC, Menezes LJ, Lewis K, Moody AB, Violaris N, Williams MD. Sonographically guided core biopsy of a parotid mass. AJR Am J Roentgenol 2007; 188: 223-7.
16. Breeze J, Andi A, Williams MD, Howlett DC. The use of fine needle core biopsy under ultrasound guidance in the diagnosis of a parotid mass. Br J Oral Maxillofac Surg 2009; 47: 78-9.
17. Sriskandan N, Manjaly G, Howlett DC. Re: Breeze J, Andi A, Williams MD, Howlett DC. The use of fine needle core biopsy under ultrasound guidance in the diagnosis of a parotid mass [Br. J. Oral Maxillofac. Surg. 2009;47(1):78-9]. Br J Oral Maxillofac Surg 2009; 47: 493-4.
18. Wan YL, Chan SC, Chen YL, *et al.* Ultrasonography-guided core-needle biopsy of parotid gland masses. AJNR Am J Neuroradiol 2004; 25: 1608-12.
19. Taki S, Yamamoto T, Kawai A, Terahata S, Kinuya K, Tonami H. Sonographically guided core biopsy of the salivary gland masses: safety and efficacy. Clin Imaging 2005; 29: 189-94.
20. Pratap R, Qayyum A, Ahmed N, Jani P, Berman LH. Ultrasound-guided core needle biopsy of parotid gland swellings. J Laryngol Otol 2009; 123: 449-52.
21. Schmidt RL, Jedrzkiewicz JD, Allred RJ, Matsuoka S, Witt BL. Verification bias in diagnostic accuracy studies for fine- and core needle biopsy of salivary gland lesions in otolaryngology journals: a systematic review and analysis. Head Neck 2014; 36: 1654-61.
22. Roussel F, Nouvet G. Evaluation of large-needle biopsy for the diagnosis of cancer. Acta Cytol 1995; 39: 449-52.
23. Witt BL, Schmidt RL. Ultrasound-guided core needle biopsy of salivary gland lesions: a systematic review and meta-analysis. Laryngoscope 2014; 124: 695-700.
24. Douville NJ, Bradford CR. Comparison of ultrasound-guided core biopsy versus fine-needle aspiration biopsy in the evaluation of salivary gland lesions. Head Neck 2013; 35: 1657-61.
25. Howlett DC. Diagnosing a parotid lump: fine needle aspiration cytology or core biopsy? Br J Radiol 2006; 79: 295-7.

Journal of Pathology and Translational Medicine 2015; 49: 144-147
http://dx.doi.org/10.4132/jptm.2014.02.10

■ CASE STUDY ■

Oncocytic Lipoadenoma: A Rare Case of Parotid Gland Tumor and Review of the Literature

Chen-lin Chi · Tseng-tong Kuo[1]
Li-yu Lee[1]

Depatment of Pathology, Buddhist Dalin Tzu Chi Hospital, Chiayi; [1]Department of Pathology, Chang Gung Memorial Hospital, and Chang Gung University College of Medicine, Taoyuan, Taiwan

Received: September 26, 2013
Revised: February 6, 2014
Accepted: February 10, 2014

Corresponding Author
Li-yu Lee, M.D.
Department of Pathology, Chang Gung Memorial Hospital, 5 Fu Hsin Street, Kwei San, Taoyuan, Taiwan
Tel: +886-3-328-1200 (ext. 2722)
Fax: +886-3-328-0147
E-mail: r22068@cgmh.org.tw

Oncocytic lipoadenoma is a rare tumor, with only 18 cases having been reported since the first in 1998. We encountered a case of oncocytic lipoadenoma presenting as a slowly growing parotid mass in a 71-year-old man. This tumor is characteristically comprised of a mixture of oncocytes and adipocytes. The present case is one of five reported cases of oncocytic lipoadenoma showing sebaceous differentiation. The results of immunohistochemical study with DOG1 antibody supported the origination of this tumor in the striated duct.

Key Words: Parotid gland; Lipoadenoma; Oncocytic cell; Sebaceous differentiation; DOG1

Oncocytic lipoadenoma is a rare entity, with only 18 cases having been reported in the literature. Oncocytic lipoadenoma is a benign encapsulated tumor composed of oncocytes and adipocytes, occurring mostly in parotid glands or less frequently in submandibular glands. We herein present a case of parotid oncocytic lipoadenoma with sebaceous differentiation and immunohistochemical study.

CASE REPORT

A 71-year-old man presented with a four-year history of a right infra-auricular mass. The mass measured 4×3 cm and was nontender and movable. Head and neck computed tomography revealed a mass with heterogenous density and a fatty component (Fig. 1A). Partial parotidectomy was performed, revealing a solitary well-defined mass measuring 4.2×3.5×2.5 cm with a thin capsule. The cut surface was tan with yellow areas (Fig. 1B).

Microscopically, the mass was encapsulated and surrounded by normal parotid tissue (Fig. 1C). The tumor comprised oncocytic cells and fat cells with mature adipose tissue occupying about 50% to 60% of the tumor. The oncocytic cells were arranged in an acinar or glandular pattern (Fig. 2A) and contained abundant eosinophilic cytoplasm. Some oncocytic cells were smaller in size, with darker cytoplasm and pyknotic nuclei. Scattered sebaceous glands were also present (Fig. 2B). No pleomorphism, mitosis, necrosis, or capsular invasion was observed.

Immunohistochemically, the oncocytic cells were strongly positive for AE1/AE3 (1:1,000, Dako, Glostrup, Denmark) and cytokeratin 7 (1:1,000, Dako). Peripheral cells were stained by p63 (1:1,000, Dako) and cytokeratin 5/6 (1:200, Dako). Epithelial membrane antigen (1:200, Dako) stained the luminal surface and sebaceous glands. The oncocytic cells were negative for smooth muscle actin (1:1,000, Dako) and calponin (1:1,000, Dako). Cytokeratin 14 (1:400, Biogenex, The Hague, The Netherlands) expression was restricted to sites of sebaceous differentiation. An apical-luminal pattern of DOG1 (1:200, Leica, Newcastle upon Tyne, UK) staining was observed in the normal serous acini, while the tumor cells were negative (Fig. 2C, D). Based on the microscopic findings, we rendered a diagnosis

pISSN 2383-7837
eISSN 2383-7845

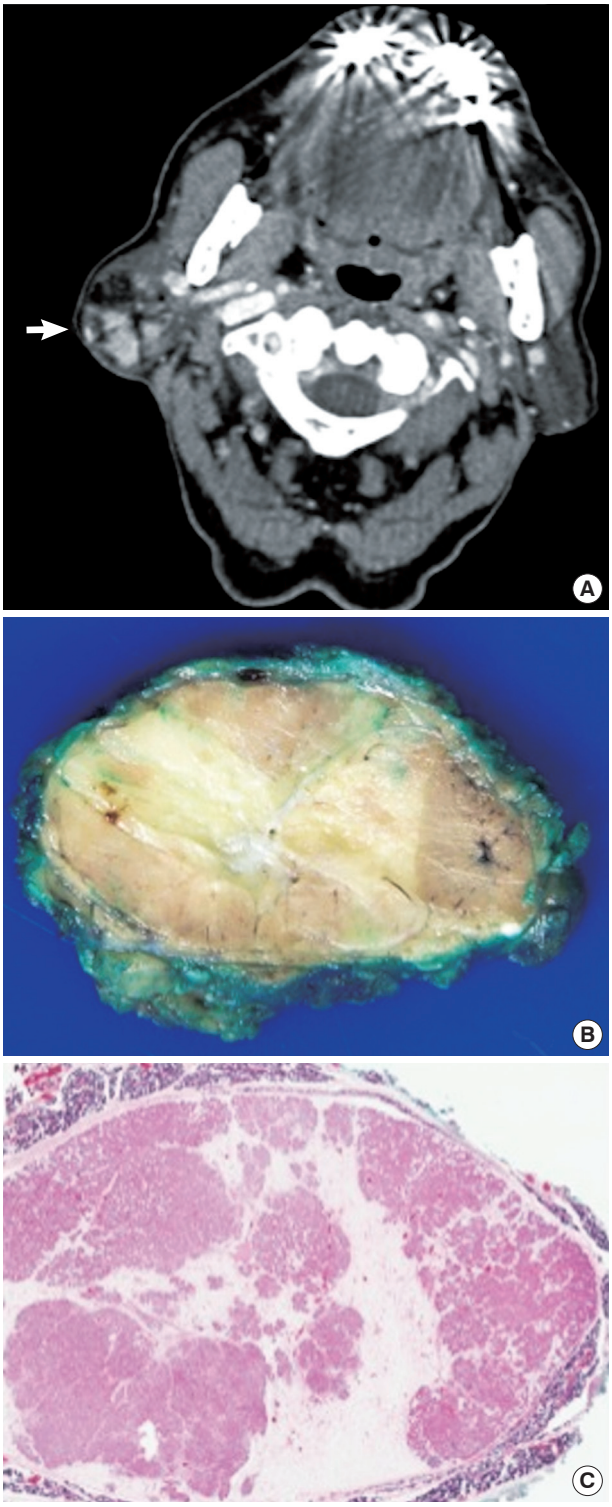

Fig. 1. Oncocytic lipoadenoma. (A) Computed tomography reveals a heterogeneous tumor with a fat component (arrow). (B) Grossly, the cut surface is a mixture of tan and yellow components. (C) The scanning view shows an encapsulated tumor with biphasic components and surrounded by normal acini.

of oncocytic lipoadenoma with sebaceous differentiation. No recurrence was present after a 19-month follow-up.

DISCUSSION

Oncocytic lipoadenoma was first reported by Hirokawa *et al.* in 1998.[1] This rare tumor was not mentioned as an entity in the 2005 World Health Organization (WHO) histologic classification of tumors of salivary glands. In the English literature, 18 cases have been reported (Table 1).[1-12] There is no gender predilection, and the patient ages range from 7 to 89 years (median of 55.5 years). All reported cases demonstrated benign clinical courses after excision. The universal microscopic finding in the literature was an encapsulated tumor comprising a mixture of oncocytic cells and fat cells. So-called dark cells were also common. Uncommon findings as sclerotic and polycystic changes ascribed to chronic involution, squamous metaplasia, lymphoid stroma, and metaplastic bone formation have been reported.[1,2] The presence of mitochondria in those oncocytic cells was confirmed by both immunohistochemical and ultrastructural studies.[7] Phosphotungstic acid hematoxylin staining and antimitochondrial antibody were utilized to demonstrate the presence of mitochondria.[3,6-8] Ultrastructural studies also provided evidence that oncocytic lipoadenoma may be derived from striated ductal cells based on similar histological features.[7] DOG1 expression was found in both normal and neoplastic counterparts of intercalated ducts and acinar cells, whereas striated duct cells were negative.[13] The oncocytic cells in our case were negative for DOG1, which supports the contention that striated ductal cells were the origin of this tumor.

Differential diagnoses include sialolipoma, oncocytoma, oncocytosis, sclerosing polycystic adenosis, and oncocytic metaplasia. The latter two entities do not form a discrete tumor mass. Sialolipomas comprise ductal, acinar, basal, and myoepithelial cell components.[14] Oncocytomas are also encapsulated tumors with immunohistochemical findings identical to those of oncocytic lipoadenomas, but they lack adipose tissue as their component cells. In addition, 20% of patients with oncocytomas have a history of radiation exposure.[15] The presence of sclerotic and polycystic change can be reminiscent of sclerosing polycystic adenosis, but oncocytic lipoadenomas lack xanthomatous and apocrine change, which is commonly seen in sclerosing polycystic adenosis. In addition, the presence of acini in sclerosing polycystic adenosis can be aided by DOG1 antibody.

Sebaceous differentiation is not an uncommon finding in salivary glands and can be found in sebaceous lymphadenoma, se-

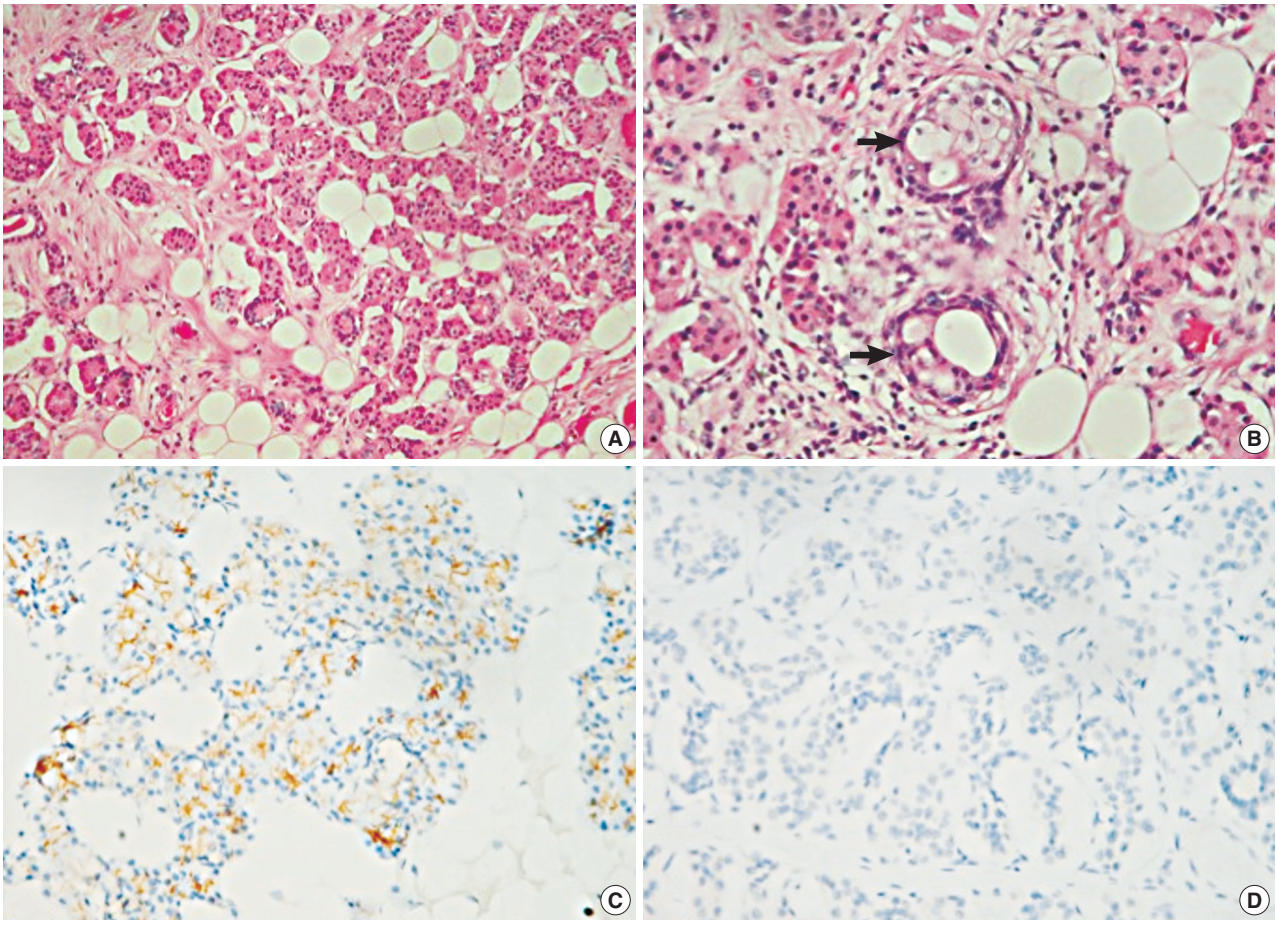

Fig. 2. (A) Oncocytic cells are arranged in an acinar or glandular pattern. (B) The arrows indicate foci of sebaceous differentiation. DOG1 expression is seen in normal parotid acinar cells (C) but not oncocytic cells (D).

Table 1. Clinical summary of the reported cases of oncocytic lipoadenoma

Reference	Gender	Age (yr)	Location	Size (cm)	Sebaceous differentiation	Follow-up
Agaimy *et al.*[2]	M	63	Parotid gland	4.5	Present	NED, 6 mo
Agaimy *et al.*[2]	M	29	Parotid gland	4.5	Present	NED, 141 mo
Agaimy *et al.*[2]	F	54	Parotid gland	2.9	Absent	NED, 18 mo
Agaimy *et al.*[2]	F	7	Parotid gland	N/A	Present	N/A
Agaimy *et al.*[2]	F	89	Parotid gland	4.2	Present	N/A
Agaimy *et al.*[2]	M	55	Parotid gland	2.7	Present	NED, 13 mo
Aouad *et al.*[3]	M	38	Parotid gland	4	N/A	N/A
Chahwala *et al.*[4]	F	50	Parotid gland	14	N/A	N/A
Devadoss *et al.*[5]	F	50	Parotid gland	13.5	N/A	NED, 24 mo
Hirokawa *et al.*[1]	F	66	Submandibular gland	11	N/A	NED, 30 mo
Ilie *et al.*[6]	M	64	Parotid gland	3.5	Present	NED, 24 mo
Kato and Horie[7]	F	57	Parotid gland	4.5	N/A	N/A
Klieb and Perez-Ordonez[8]	F	47	Parotid gland	3	Present	NED, 6 mo
McNeil *et al.*[9]	M	73	Parotid gland	N/A	Present	N/A
Mitsimponas *et al.*[10]	F	55	Parotid gland	2.7	Present	NED, 12 mo
Pusiol *et al.*[11]	M	73	Submandibular gland	9	Present	N/A
Tokyol *et al.*[12]	M	56	Parotid gland	7	N/A	NED, 6 mo
Present case	M	71	Parotid gland	4	Present	NED, 19 mo

M, male; NED, no evident with disease; F, female; N/A, not available.

http://dx.doi.org/10.4132/jptm.2014.02.10

baceous adenoma, pleomorphic adenoma, oncocytoma, sialoblastoma, and Warthin tumor.[15,16] The majority of the reported oncocytic lipoadenomas including our case exhibit sebaceous differentiation.

Lipoadenomas are similar to adenolipomas of the breast, thyroid, and skin in that they all demonstrate a histological mixture of epithelial components and adipose tissue. In contrast to adenolipoma, which is considered to be a hamartoma, oncocytic lipoadenoma is believed to be a true neoplasm. Ilie *et al.*[6] identified a t(12;14) translocation in their case. An altered *HMGA2* gene rearrangement is more commonly seen in lipoma, pleomorphic adenoma, and leiomyoma.[6] The cytogenetic findings support oncocytic lipoadenoma as a distinct neoplasm.

Conflicts of Interest

No potential conflict of interest relevant to this article was reported.

REFERENCES

1. Hirokawa M, Shimizu M, Manabe T, Ito J, Ogawa S. Oncocytic lipoadenoma of the submandibular gland. Hum Pathol 1998; 29: 410-2.
2. Agaimy A, Ihrler S, Märkl B, *et al.* Lipomatous salivary gland tumors: a series of 31 cases spanning their morphologic spectrum with emphasis on sialolipoma and oncocytic lipoadenoma. Am J Surg Pathol 2013; 37: 128-37.
3. Aouad R, Matar N, Sader-Ghorra C, Haddad A. Pathology quiz case 1. Oncocytic lipoadenoma of the parotid gland. Arch Otolaryngol Head Neck Surg 2008; 134: 446, 8.
4. Chahwala Q, Siddaraju N, Singh N, Goneppanavar M, Basu D. Fine needle aspiration cytology of oncocytic lipoadenoma of the parotid gland: report of a rare case. Acta Cytol 2009; 53: 437-9.
5. Devadoss CW, Murugan P, Basu D, Jagdish S. Oncocytic lipoadenoma of the parotid gland: a rare case report. J Clin Diagn Res 2012; 6: 1076-8.
6. Ilie M, Hofman V, Pedeutour F, Attias R, Santini J, Hofman P. Oncocytic lipoadenoma of the parotid gland: immunohistochemical and cytogenetic analysis. Pathol Res Pract 2010; 206: 66-72.
7. Kato M, Horie Y. Oncocytic lipoadenoma of the parotid gland. Histopathology 2000; 36: 285-6.
8. Klieb HB, Perez-Ordoñez B. Oncocytic lipoadenoma of the parotid gland with sebaceous differentiation. Study of its keratin profile. Virchows Arch 2006; 449: 722-5.
9. McNeil ML, Bullock MJ, Trites JR, Hart RD, Taylor SM. Oncocytic lipoadenoma of the parotid gland with sebaceous differentiation in a 73-year-old male. J Otolaryngol Head Neck Surg 2010; 39: E48-50.
10. Mitsimponas KT, Agaimy A, Schlittenbauer T, Nkenke E, Neukam FW. Oncocytic lipoadenoma of the parotid gland: a report of a new case and review of the literature. Int J Clin Exp Pathol 2012; 5: 1000-6.
11. Pusiol T, Franceschetti I, Scialpi M, Piscioli I. Oncocytic sialolipoma of the submandibular gland with sebaceous differentiation: a new pathological entity. Indian J Pathol Microbiol 2009; 52: 379-82.
12. Tokyol C, Dilek FH, Aktepe F, Ayçiçek A, Altuntaş A. Oncocytic lipoadenoma of the parotid gland: a case report with fine needle aspiration cytology findings. Kulak Burun Bogaz Ihtis Derg 2010; 20: 146-9.
13. Chenevert J, Duvvuri U, Chiosea S, *et al.* DOG1: a novel marker of salivary acinar and intercalated duct differentiation. Mod Pathol 2012; 25: 919-29.
14. Nagao T, Sugano I, Ishida Y, *et al.* Sialolipoma: a report of seven cases of a new variant of salivary gland lipoma. Histopathology 2001; 38: 30-6.
15. Brandwein MS, Huvos AG. Oncocytic tumors of major salivary glands: a study of 68 cases with follow-up of 44 patients. Am J Surg Pathol 1991; 15: 514-28.
16. Barnes L. Pathology and genetics of head and neck tumours: World Health Orginization of tumors. Lyon: IARC Press, 2005: 209-281.

Journal of Pathology and Translational Medicine 2015; 49: 148-155
http://dx.doi.org/10.4132/jptm.2014.10.13

■ CASE STUDY ■

Fallopian Metaplastic Papillary Tumour: An Atypical Transdifferentiation of the Tubal Epithelium?

Miguel Fdo. Salazar[1,2]
Isaías Estrada Moscoso[1]
Lorena Troncoso Vázquez[1]
Nubia Leticia López García[2]
Paola Andrea Escalante Abril[2]

[1]Anatomical Pathology Division, "Dr. Manuel Gea González" General Hospital; [2]Pathology Unit, Mexico General Hospital, Mexico City, Mexico

Received: August 3, 2014
Revised: September 22, 2014
Accepted: October 13, 2014

Corresponding Author
Miguel Fdo. Salazar, M.D.
División de Anatomía Patológica, Hospital General "Dr. Manuel Gea González", Calzada de Tlalpan 4800, Col. Sección XVI, Delegación Tlalpan, C.P. 14080, D.F. México
Tel: +52-4000-3000 (ext. 3302)
E-mail: k7nigricans@hotmail.com

A metaplastic papillary tumor of the Fallopian tube is an extremely uncommon condition, with odd and confusing features that make it difficult to categorize as benign or borderline. Here, we summarize all the published cases to date and document the case of a 41-year-old woman diagnosed with this alteration after her last childbirth and ensuing tubal ligation. One of the tubes was bulky and filled with a caramel-like substance encircling a blurry spot. Light microscopy detailed a slender stalk covered by eosinophilic, columnar plump cells, showing atypical nuclei and focal budding. Mitotic figures were absent. The immunohistochemistry panel was positive for pan-cytokeratin, epithelial membrane antigen, cyclin D1, and hormone receptors. Additionally, a proliferation index of less than 5% was rated using Ki-67. The true nature of this tumor (reactive vs neoplastic) is uncertain. Nonetheless, its association with pregnancy suggests an adaptive change, likely similar to the atypical transdifferentiation proposed for Arias-Stella reaction.

Key Words: Metaplastic papillary tumour; Fallopian tubes; Arias-Stella reaction; Cell transdifferentiation

Metaplastic papillary tumors of the Fallopian tube represent an extremely unusual finding particularly related to pregnancy and with morphological features that make precise histopathological classification difficult. At present, nearly ten case reports are documented worldwide (Table 1).[1-7]

CASE REPORT

The patient, a 41-year-old woman with a non-relevant past medical history, concluded her fourth pregnancy by cesarean delivery owing to macrosomic product (July 2013). Tubal ligation was performed on postoperative day one by the Kroener fimbriectomy method, which coursed uneventfully and without any remarkable findings. The specimens obtained were sent for routine histopathological assessment, and the patient was discharged after full recovery. To date she is healthy and without any complaints.

Both distal tubes and fimbriae were identified; the large tube was bulky with a nodular appearance (3.5×2×1.3 cm) (Fig. 1A). Transverse sections taken from this dilated duct revealed an overfilled lumen with a caramel-like substance surrounding an ill-defined peripheral spot, which, when seen under a magnifying glass, showed a fractal pattern similar to a snowflake (Fig. 1B). Histologically, this hazy frame was sketched by a slender stalk with progressively branching papillae lined by columnar non-ciliated cells with plump eosinophilic cytoplasm showing focal pseudostratification and budding (Fig. 1C, D). The nuclei of these cells were centrally located, enlarged, and rounded or oval. The nuclei displayed a variable appearance, either dense and hyperchromatic, or vesicular with a prominent nucleolus, and sometimes having coarse chromatin, membrane foldings, pseudoinclusions or grooves. Mitotic activity was not identified.

Despite the presence of luminal extracellular mucin, several subnuclear mucin-filled vacuoles were also identified, occasionally expanding into cyst-like structures (Fig. 2A). Periodic acid–Schiff and Alcian blue stains highlighted the extracellular and

pISSN 2383-7837
eISSN 2383-7845

Table 1. Metaplastic papillary tumor case list

Case No.	Year	Author (country)	Clinical data overview			Histopathological finding
			Landscape	Evolution and treatment	Follow-up	
1	1978	Starr *et al.*[2] (USA)	26-Year-old woman (G2P1)	Normal delivery and immediate postpartum tubal ligation Total abdominal hysterectomy and bilateral salpingo-oophorectomy performed due to report of malignancy	Check-up every 3 months during a non-specified period No anomalies reported	Interpretation as grade 1 primary adenocarcinoma of the Fallopian tube
2–5	1980	Saffos *et al*.[1] (USA)	Four women between 27 to 33 years of age (multiparous; non-specified number of pregnancies) One patient had used oral contraceptives several years previously	Normal delivery and tubal ligation in every case Two patients had total abdominal hysterectomies with bilateral salpingo-oophorectomies because of uncertainty about the malignancy of the lesions	No evidence of disease in three patients after different times of evaluation (1 year 6 months, 2 years and 6 years postoperatively) One of the cases was lost during follow-up	Original description of the tumour: *oncocytic* and *mucinous* epithelia Mucinous component (intracytoplasmic vacuoles) reactive for mucicarmine stain Only one mitosis noticed in one of the cases
6	1988	Keeney and Thrasher[3] (USA)	27-Year-old Mexican woman (G3P1A1) Hypothyroidism requiring L-tiroxine therapy	Premature rupture of foetal membranes with subsequent caesarean delivery Simultaneous tubal ligation	Without disease after 4 years of follow-up	No gross abnormalities Description of a luminal acidophilic secretion mucicarmine-positive Recognition of only one tripolar mitosis First ultrastructural description by means of transmission electron microscopy
7	1989	Bartnik *et al*.[4] (USA)	23-Year-old woman (G3P2) Respiratory and urinary tract infections treated with ampicillin during the second and third trimesters	Vaginal delivery and tubal ligation (Pomeroy technique)	Postoperative recovery and discharge	Gross description of a pale-yellow mucoid material (extracellular mucin within the tubal lumen) No mitotic activity First description of the cell immunophenotype: CK (+) and EMA (+) Minimal chronic salpingitis observed in both tubes
8	1999	Pang[5] (Taiwan)	52-Year-old non-pregnant Taiwanese woman (G5P3A2) Consumption of progesterone-only oral contraceptives when she was 26 years old Complaint of lower abdominal fullness Bilateral hydrosalpinx by ultrasonography	Laparoscopic resection of both Fallopian tubes	Non-available information	Tumour localized in the right salpinx Intracellular mucin reactive for PAS, alcian blue and mucicarmine stains Extracellular mucine present on the surface of some papillae Simultaneous finding of degenerated, partially calcified chorionic villi in both Fallopian tubes (bilateral ectopic pregnancies)
9	2003	Solomon *et al*.[6] (USA)	26-Year-old woman (G5P3A1) Last pregnancy conceived while using oral contraceptives Unexplained serum FP elevation during the 15th week of gestation	Labor induction at 39 weeks using oxytocin Vaginal delivery and bilateral tubal ligation via Pomeroy procedure on postpartum day 1	No complaints after her 6-week postpartum visit	Involvement of the left Fallopian tube by an exophytic, papillary lesion mucicarmine (+), EMA (+) and CK AE_1/AE_3 (+) Associated chronic salpingitis and focal decidualization in the ipsilateral tube
10	2011	D'Adda *et al*.[7] (Italy)	31-Year-old woman at her 40th week of gestation	Caesarean delivery due to podalic version	Non-available information	Microsatellital analysis of eight chromosomal regions involved in ovarian carcinogenesis: molecular profile probably similar to a subset of minimally altered low-grade borderline serous tumours

CK, cytoketarin; EMA, epithelial membrane antigen; PAS, periodic acid–Schiff.

intracellular mucin, while the intracytoplasmic vacuoles were stained with Mayer's mucicarmine (Fig. 2B–D).

Immunoperoxidase stains demonstrated an intensely positive reaction for cytokeratin cocktail (CK AE_1/AE_3) in the membrane and cytoplasm (Fig. 3A) of cells, as well as for epithelial membrane antigen (EMA) with weak cytoplasmic expression and lu-

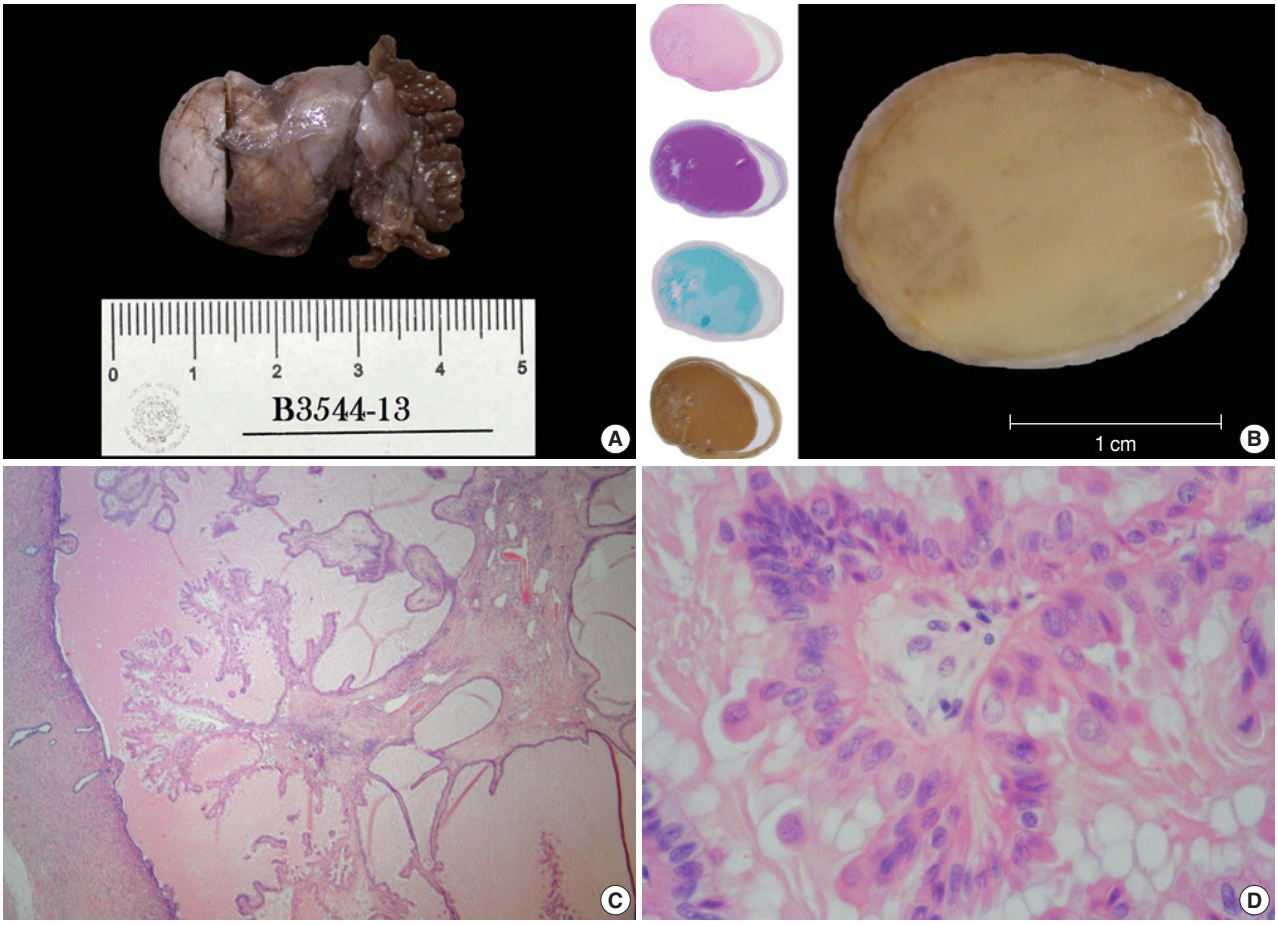

Fig. 1. Gross features/oxyphil metaplastic components. (A) Tubal ligation specimen. (B) Transverse cut surface. A crystallized syrup-like substance with a striking resemblance to a regional candy known as «*acitrón*» fills the lumen; there is also a left marginal blur with a snowflake-like appearance. The left column displays whole-mount sections stained with hematoxylin and eosin, periodic acid–Schiff, Alcian blue, and mucicarmine. (C) Panoramic photomicrograph showing a peninsular papillary framework in a lake of extracellular mucin. The stalk has a loose stroma and contains a small number of inflammatory cells (lymphocytes and neutrophils). (D) High magnification photomicrograph of the oncocytic epithelium. There is mild stratification and cell budding.

minal border reinforcement (Fig. 3B). Detection of progesterone receptors (PR) was markedly positive in 95% of cells, while estrogen receptors (ER) and androgen receptors were moderately and weakly positive in 70% and 10% of cells, respectively (Fig. 3C–E). The proliferation index labeled with Ki-67 was rated in approximately 3% of cells (Fig. 3F). Surprisingly, cyclin D1 staining was observed in nearly 90% of cells (Fig. 3G). No reaction was detected toward a variety of factors, including carcinoembryonic antigen (CEA), human chorionic gonadotropin, human epidermal growth factor receptor 2 (HER2/Neu), or B-cell lymphoma 2 protein (Bcl-2).

Accordingly, the proliferation was diagnosed as a metaplastic papillary tumor of the Fallopian tube, with a note to the clinician about the benign behavior of the alteration.

DISCUSSION

In the 1980s, a group led by Saffos and Scully described an unusual epithelial tumor incidentally discovered in four cases involving tubal ligation after delivery (early puerperium).[1] The morphology detailed in their report describes a papillary stalk lined by atypical oxyphil columnar cells with pseudostratification, budding elements, and focal adenomatous changes involving intramucosal mucin-filled vacuoles, nonetheless, lacking invasion or mitotic activity. According to these features, the team coined a description of this singular pathological entity as a metaplastic papillary tumor of the Fallopian tube. Furthermore, they noticed a striking similarity with serous borderline ovarian tumors, as well as a close association with pregnancy. This led the team to speculate about either a neoplastic nature of the tumor

http://dx.doi.org/10.4132/jptm.2014.10.13

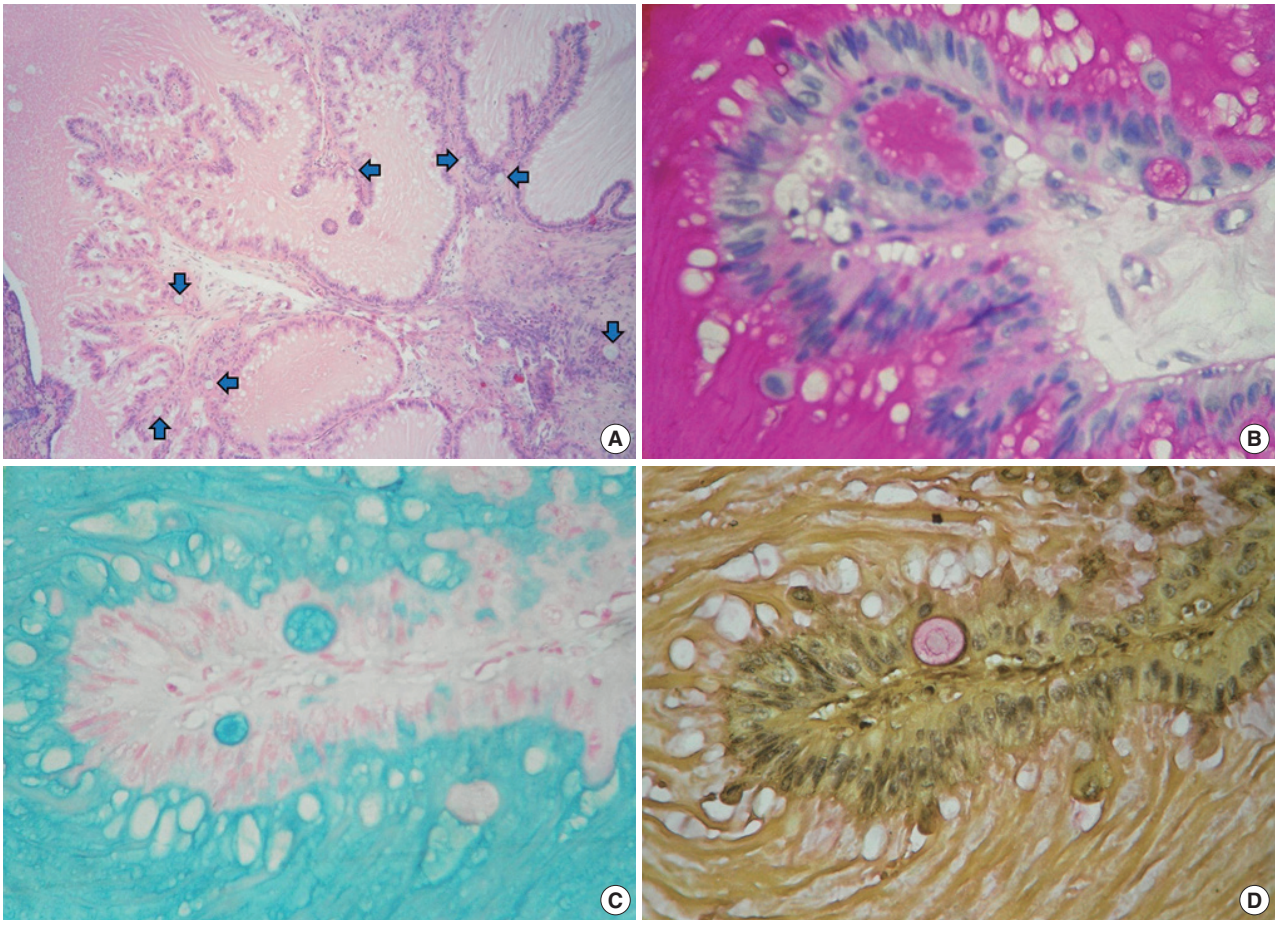

Fig. 2. Mucinous metaplastic components. (A) Some amphophilic mucin-filled cysts are noticeable beneath the epithelium (blue arrows). (B) Periodic acid–Schiff. (C) Alcian blue. (D) Mayer's mucicarmine.

or an adaptive response analogous to Arias-Stella reaction. Interestingly, these characteristics had led Starr *et al.*[2] to report in a study two years earlier (1978) about a similar papillary lesion as a primary carcinoma of the Fallopian tube. Even more intriguing is the fact that some authors claimed to observe a single multipolar mitosis in one of the cases reported.[3] Though ensuing reports failed to provide new insights about the origins of this type of tumor, they accurately detail ultrastructural characteristics of the tumors: luminal border microvilli, sporadic cilia, glycogen particles, "empty" vacuoles, abundant parallel wavy filaments ~6.5 nm in diameter, numerous mitochondria, and a limited amount of rough endoplasmic reticulum.[3,4] Reports are also specific about the immunoprofiles: cytokeratin and epithelial membrane antigen positive, and CEA negative—the latter certainly not different from normal tubal epithelium.[4] Curiously, one paper from 1999 provides evidence for refutation in regard to the inexorable connection of this type of tumor with an immediate postpartum period, demonstrating bilateral partially calcified chorionic villi in addition to the papillary tumor, in a 52-year-old patient.[5] This particular finding represents unequivocal proof of two previous, dateless ectopic pregnancies, but also brings up questions concerning the timing of the tumor. One particular question is whether the tumor had been quiescent for years or whether it was a newly coincidental discovery. A more recent (2003) communication on the subject compiled the data published during previous years, and stressed the importance of recognizing these tumors as benign and the importance of reporting them as such to clinicians in order to prevent drastic surgical resections among postpartum patients.[6]

As discussed above, a schism prevails concerning the histogenesis of this condition (whether it is reactive or neoplastic), though most authors support the second option (a low-grade borderline tumor). In this regard, the work of D'Adda *et al.*[7] is a noteworthy advance in the understanding of this entity, as the study molecularly compares a case of metaplastic papillary tumor with four borderline ovarian tumors and two ovarian ade-

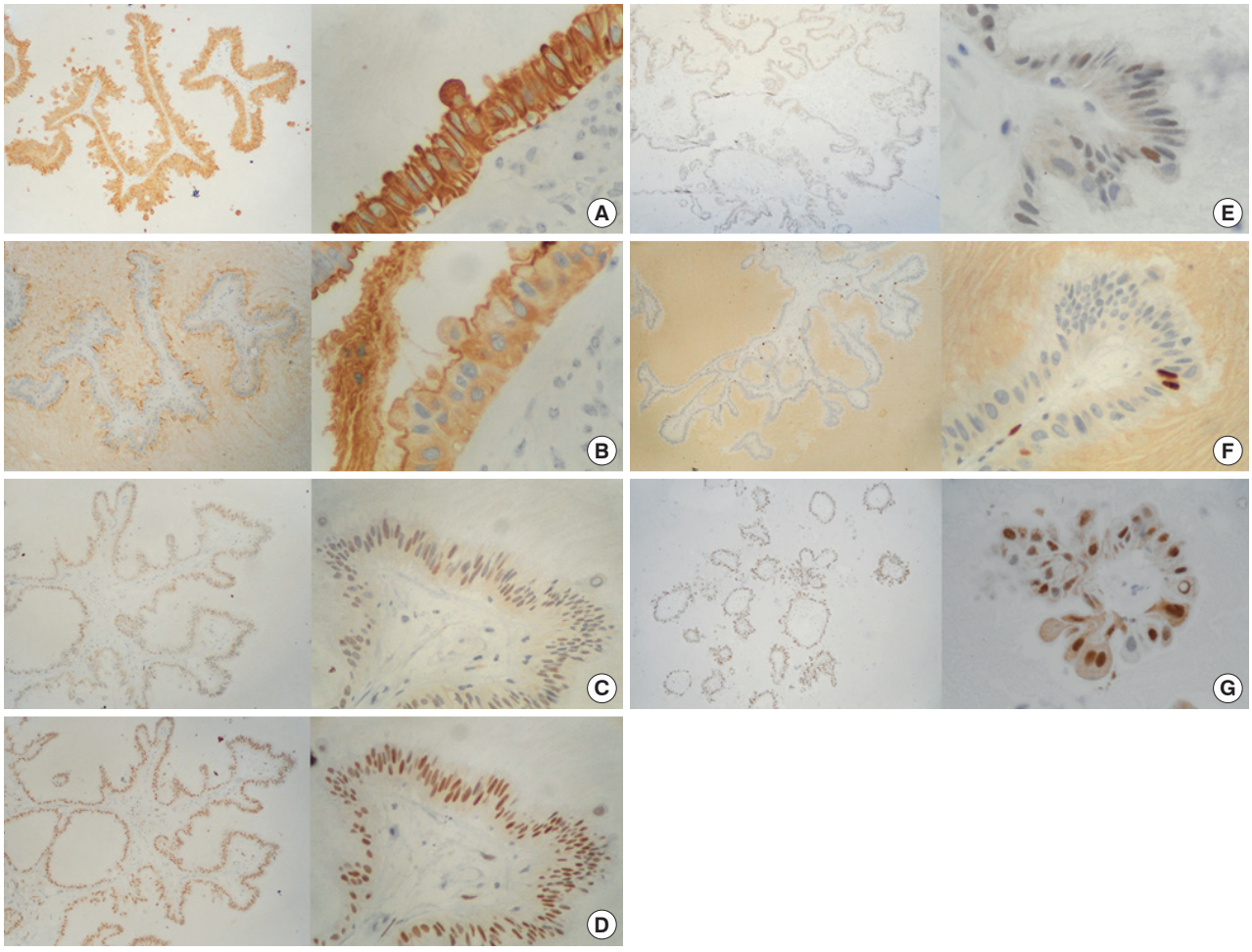

Fig. 3. Immunohistochemistry panel. (A) Cytokeratin AE_1/AE_3 (+++/+++) in 100% of cells. (B) Epithelial membrane antigen (+++/+++) in 100% of cells. (C) Estrogen receptor (++/+++) in ~70% of cells. (D) Progesterone receptor (+++/+++) in ~95% of cells. (E) Androgen receptor (+/+++) in ~10% of cells. (F) Ki-67 (+++/+++) in ~3% of cells. (G) Cyclin-D1 (+++/+++) in ~90% of cells.

nocarcinomas using microsatellite markers directed toward chromosomal regions involved in ovarian carcinogenesis (myc-l1, cdkn2a/cdkn2b, pten, tp53, and dmd). According to their findings, the metaplastic papillary tumor, together with one of the borderline tumors, showed no alterations. Thus the study concluded that the metaplastic papillary tumor might share morphologic and molecular similarities with a subset of minimally altered borderline/atypical proliferative tumors.

On the other hand, there are numerous tubal epithelium reactive changes described under different circumstances: cyclic variations in the height and proportion of cells, hyperplasia (mild stratification and papillary tufts), adenomatous hyperplasia (small glandular intramucosal clefts), and metaplasia (squamous, transitional, oncocytic and mucinous). All of these have been known to be associated with inflammation (acute and chronic salpingitis), neoplastic conditions (endometrial carcinoma), hormonal effects (estrogen secreting ovarian tumors or exogenous administration), or even with no particular etiology.[1-4,6,8] Similarly, as some scholars have proposed, we are quite possibly facing a non-conventional phenomenon analogous to the so-called Arias-Stella reaction in the sense that the tumor might represent some kind of transformation that takes place under similar physiological conditions[1,3] (as a consequence of antagonistic stimuli acting synchronously—namely, estrogen (ciliogenic and proliferative activity) and progesterone (secretory activity)—either in equal proportion or with an inclination toward one of the stimuli). A seminal review written by Arias-Stella[9] calls attention to a phenomenon known as transdifferentiation,[10] which implies the transformation of a mature somatic cell into a different somatic cell preserving its maturity (as opposed to metaplasia, which involves the reprogramming of stem cells). Furthermore, a more dramatic and perplexing process called atypical transdifferentia-

 http://dx.doi.org/10.4132/jptm.2014.10.13

tion, involving polyploidy, lack of aneuploidy, and the absence of progression as signature traits,[9] denotes a singular adaptive cellular change said to be found in tissues strained under opposing hormonal influences, consecutively inducing an increment in the content of DNA. The exhaustive analysis throughout this report caused Arias-Stella to conclude definitively that the reaction which has come to carry his name stands for a distinctive example of atypical transdifferentiation, which can be extrapolated to the atypical cells in seminal vesicles, epididymis and duct deferens, the monstrous cells in large solitary luteinized follicle cysts of pregnancy and puerperium, and to the bizarre benign cells in dyshormonogenetic goiter.[9] Accordingly, we reference the immunoprofile reported for an endometrial Arias-Stella reaction, involving intense and homogenous reactions for CK7 and EMA with increased membranous locations in hypersecretory patterns, positivity for ER and PR, with a higher estrogen weighting (though weaker in comparison to the normal functional phase and hyperplasia) and positive reactions for Ki-67 and proliferating cell nuclear antigen (though less than hyperplasia or the proliferative phase); as well as the reported ultrastructural characteristics: few organelles, sparse particles resembling RNA granules, clearly visible Golgi apparatus, vesicles of endoplasmic reticulum, numerous mitochondrial crests, Palade grains—ribosomes—and, without exception, parallel rows of rough endoplasmic reticulum, which is a trait said to be common among neoplasms of Müllerian origin.[9]

In the present work, we tried to test the expression of steroid hormone receptors in the oncocytic epithelium in order to confirm the feasibility of hormonal long-acting effects. According to our results, variegation in hormone receptor expression shows the following gradient: progesterone > estrogen > androgen. This ranking suggests a higher progesterone dosing, which corresponds with the secretory effect observed. What is more, we appraised a very low Ki-67 proliferation index (~3%), which is consistent with the non-observation of mitotic activity. Nevertheless, it should be mentioned that tubal epithelium normally expresses ER and PR as well as shows a Ki-67 labeling index lower than 5%. The secretory cells of tubal epithelium are typically also positive for the markers HMFG2 and PAX8, while Wilms' tumor gene product (WT-1) is frequently and diffusely expressed in normal Fallopian epithelium.[8,11] Because at some point in our analysis we presumed a similarity of some of the oncocytic cells with the so-called columnar cell change with atypia or flat epithelial atypia of the breast, we tried to test additional markers such as cyclin D1 and Bcl-2.[12,13] To our great surprise, nuclear immunostaining of the former marker was indeed observed. As a cell cycle marker that interacts with CDK4, CDK6 and tumor suppressor protein RB, we expect to recognize overexpression (~90%) of cyclin D1 in correspondence with both mitotic activity and the Ki-67 proliferation index. This, however, is not the case. We believe our observation of this phenomenon in this particular case is similar to the high frequency of cyclin D1 expression seen in either parathyroid adenomas or hyperplastic parathyroid glands.[14]

The differential diagnoses to consider are Fallopian tube papilloma, papillary tubal hyperplasia, serous borderline tumor of the Fallopian tube, and extension from a borderline ovarian tumor. Fallopian tube papilloma is a complex papillary proliferation with an orderly degree of branching that resembles an exaggeration of normal tubal mucosa.[8] In contrast to a metaplastic papillary tumor, Fallopian tube papilloma maintains normal endosalpingeal cell types. Papillary tubal hyperplasia is a recently recognized entity, which is characterized by papillary tufting and detached small round clusters of bland epithelium that are frequently—but not always—associated with psammona bodies.[15] Despite focal stratification of the epithelium can be seen, there is usually a single layer containing ciliated and secretory cells as well as intraepithelial lymphocytes. Occasionally, however, there can be slightly larger cells with eosinophilic cytoplasm. Serous borderline tumors of the Fallopian tube are exceedingly rare lesions with a complex papillary configuration lined by ciliated, hobnail and mesothelium-like cells displaying stratification, budding, and focal nuclear atypia. Occasionally, cells with abundant eosinophilic cytoplasm may also be present in serous borderline tumors of the Fallopian tube.[8,16,17] Mitotic activity is not common. Finally, extension from an adjacent ovarian serous borderline tumor seems to be a reasonable option, which is difficult to rule out, and far more common than either a metaplastic papillary tumor or a tubal borderline malignancy.[8,16] Undeniably, our patient fits in the age group reported for this lesion, and intriguingly, a minority of affected women are pregnant at the time of diagnosis. The surgeon in the present case, however, did not report any external ovarian anomalies during the course of the bilateral Kroener fimbriectomy. Nevertheless, this statement remains debatable as exophytic papillae are seen in the outer surface of nearly 70% of ovarian serous borderline tumors. We did not perform immunoperoxidase staining of WT-1, because, as endosalpingeal mucosa and ovarian surface epithelium normally express this marker,[8,11] the marker loses its diagnostic utility to differentiate a Fallopian serous borderline tumor from its ovarian counterpart. Though some authors claim that metaplastic papillary tumors are microscopic

findings,[7,8,16] a couple of reports challenge this assumption by demonstrating that subtle macroscopic changes can be observed. By way of example, a study by Bartnik *et al.*[4] describes exudation of pale-yellow mucoid material from an affected tube, while Saffos *et al.*[1] illustrate a whole-mount transverse Fallopian section with a conspicuous papillary projection, which, if had been carefully examined, would surely have been grossly apparent as a tumor.

Carrying a good prognosis, Fallopian metaplastic papillary tumors are truly exceptional and remarkable findings in light of their appearance in tubal ligation products and direct relationship to pregnancy. The baroque morphology of a metaplastic papillary tumor challenges up-to-date histopathological taxonomy, and unfortunately, neither electron microscopy, immunohistochemistry, nor molecular biology have completely unveiled the roots of the condition. As interestingly quoted by Keeney and Thrasher in their report[3] "*…despite [the fact that] light microscopy does not reveal an actual differentiation to another cell type, examination through electron microscopy strongly suggests a metaplastic process at an ultrastructural level with an incomplete transition towards a recognizable cell phenotype*…." This statement undoubtedly leads us to inquire whether this metaplastic tumor could be an overly exaggerated example of atypical transdifferentiation, drawn forth by hormonal influences in an appropriate physiological environment. Indeed, we believe this could be the case.

Lastly, as neoplastic changes have not been entirely demonstrated in the condition of metaplastic papillary tumors, we suggest not referring to the alterations as either tumors or lesions (specifically because the condition has been proved to be harmless). Perhaps designation as a Fallopian metaplastic papillary polyp—implying a convex branching axis towards a lumen—is more suitable nomenclature for the characteristics we describe herein.

In summary, we report the 11th known case of a patient with a metaplastic papillary tumor of the Fallopian tube, and provide brief insight about the topic.

Conflicts of Interest

No potential conflict of interest relevant to this article was reported.

REFERENCES

1. Saffos RO, Rhatigan RM, Scully RE. Metaplastic papillary tumor of the Fallopian tube: a distinctive lesion of pregnancy. Am J Clin Pathol 1980; 74: 232-6.
2. Starr AJ, Ruffolo EH, Shenoy BV, Marston BR. Primary carcinoma of the Fallopian tube: a surprise finding in a postpartum tubal ligation. Am J Obstet Gynecol 1978; 132: 344-5.
3. Keeney GL, Thrasher TV. Metaplastic papillary tumor of the Fallopian tube: a case report with ultrastructure. Int J Gynecol Pathol 1988; 7: 86-92.
4. Bartnik J, Powell WS, Moriber-Katz S, Amenta PS. Metaplastic papillary tumor of the Fallopian tube. Case report, immunohistochemical features, and review of the literature. Arch Pathol Lab Med 1989; 113: 545-7.
5. Pang LC. Hydrosalpinx due to asymptomatic bilateral tubal pregnancies associated with metaplastic papillary tumor of the Fallopian tube. South Med J 1999; 92: 725-7.
6. Solomon AC, Chen PJ, LiVolsi VA. Pathologic quiz case: an incidental finding in the Fallopian tube. Fallopian tube, left, tubal ligation: metaplastic papillary tumor of Fallopian tube. Arch Pathol Lab Med 2003; 127: e363-4.
7. D'Adda T, Pizzi S, Bottarelli L, Azzoni C, Manni S, Giordano G. Metaplastic papillary tumor of the salpinx: report of a case using microsatellite analysis. Int J Gynecol Pathol 2011; 30: 532-5.
8. Vang R, Wheeler JE. Diseases of the Fallopian tube and paratubal region. In: Kurman RJ, Ellenson LH, Ronnett BM, eds. Blaustein´s pathology of the female genital tract. 6th ed. New York: Springer, 2011; 529-78.
9. Arias-Stella J. The Arias-Stella reaction: facts and fancies four decades after. Adv Anat Pathol 2002; 9: 12-23.
10. Selman K, Kafatos FC. Transdifferentiation in the labial gland of silk moths: is DNA required for cellular metamorphosis? Cell Differ 1974; 3: 81-94.
11. Rabban JT, Soslow RA, Zaloudek CZ. Immunohistology of the female genital tract. In: Dabbs DJ, ed. Diagnostic immunohistochemistry: theranostic and genomic applications. 3rd ed. Philadelphia: Saunders Elsevier, 2010; 690-762.
12. Kurman RJ, Vang R, Junge J, Hannibal CG, Kjaer SK, Shih IM. Papillary tubal hyperplasia: the putative precursor of ovarian atypical proliferative (borderline) serous tumors, noninvasive implants, and endosalpingiosis. Am J Surg Pathol 2011; 35: 1605-14.
13. Alvarado-Cabrero I. Pathology of the Fallopian tube and broad ligament. In: Nucci MR, Oliva E, eds. Gynecologic pathology: foundations in diagnostic pathology. Philadelphia: Churchill Linvingstone, 2009; 331-66.
14. Krasevic M, Stankovic T, Petrovic O, Smiljan-Severinski N. Serous borderline tumor of the Fallopian tube presented as hematosalpinx: a case report. BMC Cancer 2005; 5: 129.
15. Feeley L, Quinn CM. Columnar cell lesions of the breast. Histopathology 2008; 52: 11-9.

16. Walker RA, Hanby A, Pinder SE, Thomas J, Ellis IO; National Coordinating Committee for Breast Pathology Research Subgroup. Current issues in diagnostic breast pathology. J Clin Pathol 2012; 65: 771-85.

17. DeLellis RA, Shin SJ, Treaba DO. Immunohistology of endocrine tumors. In: Dabbs DJ, ed. Diagnostic Immunohistochemistry. Theranostic and Genomic Applications. 3rd ed. Philadelphia: Saunders Elsevier, 2010; 291-339.

Journal of Pathology and Translational Medicine 2015; 49: 156-158
http://dx.doi.org/10.4132/jptm.2013.08.08

■ BRIEF CASE REPORT ■

Angiomyomatous Hamartoma of Popliteal Lymph Node: An Unusual Entity

Asit Ranjan Mridha · Richa Ranjan · Prateek Kinra · Ruma Ray · Shah Alam Khan[1] · Gamanagatti Shivanand[2]

Departments of Pathology, [1]Orthopaedics, and [2]Radiodiagnosis, All India Institute of Medical Sciences, New Delhi, India

Angiomyomatous hamartoma (AMH) of the lymph node is characterized by partial replacement of normal nodal parenchyma by disorganized blood vessels and smooth muscle cells with or without adipose tissue within a fibrous stroma. Inguinal and femoral lymph nodes are commonly involved,[1-3] while popliteal lymph node involvement is uncommon.[4,5] We report a rare case of AMH of the popliteal lymph node in a young patient with a clinical diagnosis of Baker's cyst.

CASE REPORT

An 18-year-old male presented with pain and swelling in the left popliteal fossa lasting 3 years. The swelling slowly increased in size. There was no history of any trauma, fever, tuberculosis, weight loss, or chronic illness. A clinical diagnosis of Baker's cyst was made without any imaging studies. The lesion was operated on under local anesthesia. The swelling persisted, however, and physical examination revealed a 1.5 cm-sized, mildly tender, non-reducible, firm mass in the left popliteal fossa. An magnetic resonance imaging (MRI) scan revealed a 1.5×1.0-cm soft tissue mass close to the popliteal blood vessels without encasing them (Fig. 1A, B). No cyst was seen. The radiological differential diagnoses offered were benign neoplasm and pseudotumor. The left popliteal fossa was explored again and a firm, soft tissue mass loosely adherent to the popliteal blood vessels was identified and excised. The postoperative period was uneventful. Hematoxylin and eosin–stained sections revealed a lymph node with partial replacement of the parenchyma from the hilum to the cortex by fibrous tissue containing several irregular blood vessels of varying sizes, interspersed with spindle cells and smooth muscle cells (Fig. 2A, B). Mature adipose tissue infiltration was seen in a small area near the hilum of the lymph node (Fig. 2C). The capsule was thickened. The subcapsular and medullary sinuses were obliterated. Cortical lymphoid tissue showed variable atrophy. Immunohistochemistry with a primary antibody against smooth muscle actin (SMA; 1:400, Thermo Scientific, Waltham, MA, USA) demonstrated smooth muscle cells in the blood vessel walls and in the stromal tissue (Fig. 2D, E). The rich vascularity of the lesion was highlighted by CD34 antibodies (1:100, Diagnostic BioSystems, Pleasanton, CA, USA) (Fig. 2F). A diagnosis of AMH of the lymph node was made.

DISCUSSION

Angiomyomatous hamartoma of the lymph node was first described by Chan *et al.*[1] in 1992 as a distinctive vascular hamartomatous lesion that primarily occurs in inguinal and femoral lymph nodes.[2,3] Occasional cases have been reported in popliteal and cervical lymph nodes.[4,5] Patients may present with painless or painful swelling.[4] Painful lesions in the popliteal fossa require careful evaluation because a number of non-neoplastic and neoplastic lesions can mimic this entity.[6] Baker's cyst results from herniation of the synovial membrane through the posterior capsule of the knee joint or by an escape of synovial fluid through an anatomic bursa next to the semimembranosus or gastrocnemius muscle. Baker's cysts are usually diagnosed by physical and radiological examination between the semimembranosus and medial head of the gastrocnemius.[7] Sometimes it is difficult to differentiate a Baker's cyst from other causes of posterior knee pain, and the differential clinical diagnosis of a Baker's cyst can include arterial aneurysm or tortuous blood vessels in the popli-

Corresponding Author
Asit Ranjan Mridha, M.D.
Department of Pathology, All India Institute of Medical Sciences, Ansari Nagar, New Delhi 110029, India
Tel: +91-11-26593227, Fax: +91-11-26588641, E-mail: asit_aiims@yahoo.co.in

Received: May 10, 2013 **Revised:** August 6, 2013
Accepted: August 8, 2013

pISSN 2383-7837
eISSN 2383-7845

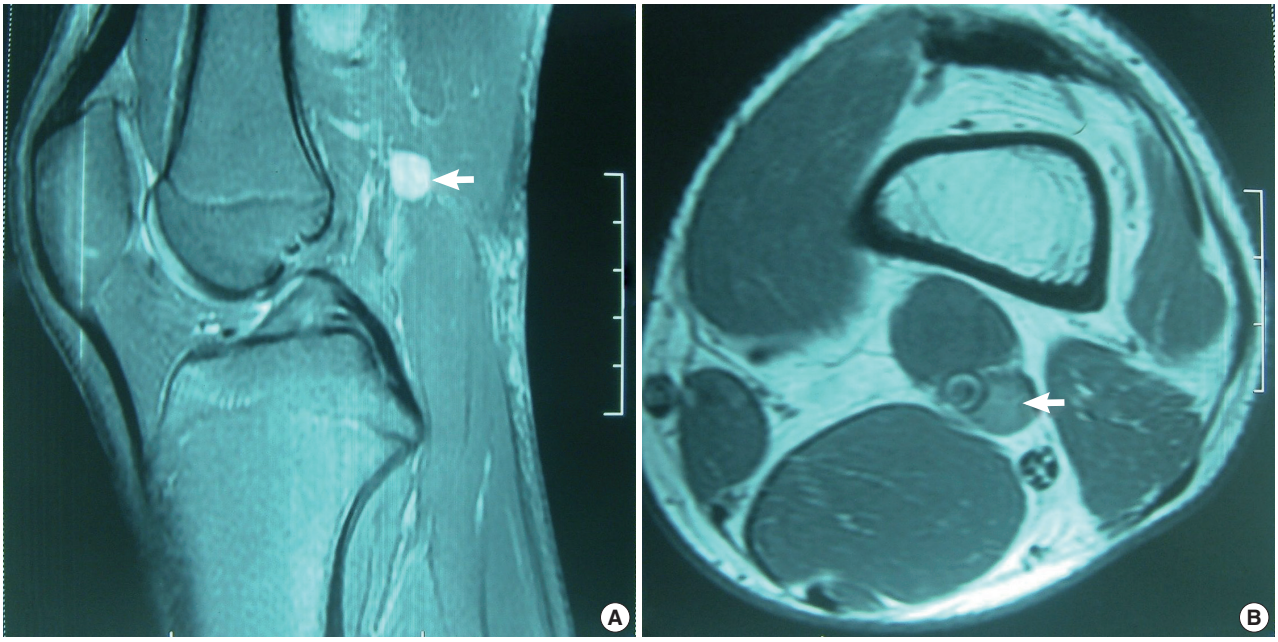

Fig. 1. Axial T1- (A), sagittal T2-weighted (B) magnetic resonance imaging scans showing a well-circumscribed lesion with heterogeneous signal intensity in the soft tissues in close proximity to the popliteal blood vessels (arrows).

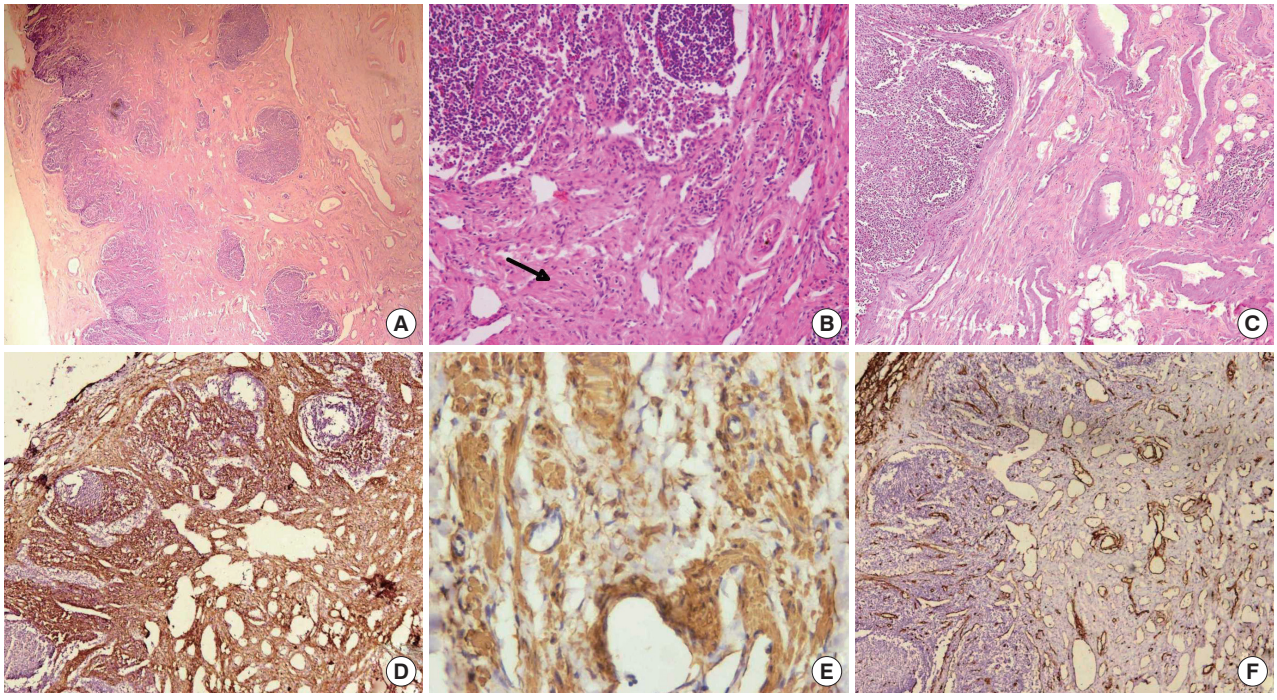

Fig. 2. Photomicrograph showing partial replacement of lymph nodal parenchyma by several disorganized vascular channels in a fibrocollagenous stroma and smooth muscle cells (arrow) (A, B); thick-walled blood vessels and adipocytes in nodal hilum (C). (D, E) Immunohistochemical stain with smooth muscle actin antibodies demonstrating smooth muscle in the blood vessel wall and the stroma. (F) CD34 immunostain highlighting the rich vascularity of the lesion.

teal fossa, deep vessel thrombosis, adipose tissue or tumor.[8] The best imaging for evaluation of a popliteal cyst is MRI as it helps in localizing the cyst and any other internal derangements.[9] In the index case the initial misdiagnosis of Baker's cyst was due

to the presence of painful swelling in the popliteal fossa and the diagnosis was based on physical examination alone. No radiological investigation was done prior to the initial surgery. To the best of our knowledge, to date only twenty-nine cases of AMH of the lymph node have been reported in the literature.[3] This is the third documented case in a popliteal lymph node. Mauro *et al*.[4] reported a case of AMH of the popliteal lymph node which presented with pain in the posterior knee in a 41-year-old male. The second case was reported by Prusac *et al.*[5] in a 14-year-old boy who presented with a right popliteal mass and right leg edema. In both cases, MRI scans revealed mass lesions with heterogeneous signal intensity. The index case also showed similar radiologic features. The radiologic diagnosis of AMH of the lymph node is usually a hemangioma or a tumor.[4,5] In our case, the MRI scan findings suggested a benign tumor or pseudotumor. Microscopically, AMH is characterized by disorganized blood vessels and smooth muscle cells in a collagenous stroma with or without adipose tissue. Our case showed a small area of adipose tissue near the hilum of the lymph node. Histopathological differential diagnosis of AMH includes lymphangiomyomatosis, leiomyomatosis, and angiomyolipoma of the lymph node.[10] Nodal lymphangiomyomatosis occurs exclusively in women and is histologically characterized by the presence of smooth muscle cells forming fascicles and sheets around anastomosing ectatic vascular spaces, resulting in a pericytomatous pattern. Histologically smooth muscle cells are plumper, with lighter/clear cytoplasm, and sclerosis is absent. Nodal leiomyomatosis resembles leiomyoma and is made up of a proliferation of compact bundles of smooth muscle cells with an insignificant vascular component. Angiomyolipoma of the lymph node shows an epithelioid appearance, hypercellularity, pleomorphism, prominent perivascular arrangement and positivity for melanoma associated antigen human melanoma black 45. Our index case did not show ec-static vessels, pleomorphism or hemangiopericytoma like patterns. Adipose cells are known to occur as a significant component in a number of vasoproliferative lesions, such as nodal hemangioma, intramuscular hemangioma (infiltrative angiolipoma) and angiolipomatous hamartoma associated with Castleman's disease. It has been suggested that all cases of AMH of the lymph node with a significant adipose tissue component should be termed angiomyolipomatous hamartoma.[10] The pathogenesis of this lesion is unclear. A possible explanation is that AMH represents a vascular and smooth muscle proliferative response to chronic impairment of nodal lymphatic flow or to previous nodal inflammation.[3]

Lesions in the popliteal fossa should be evaluated carefully, especially when associated with pain. The treatment depends on the type of lesion. Radiological investigation is mandatory for proper characterization. Histopathological examination will confirm this unusual benign entity that is managed surgically.

Conflicts of Interest

No potential conflict of interest relevant to this article was reported.

REFERENCES

1. Chan JK, Frizzera G, Fletcher CD, Rosai J. Primary vascular tumors of lymph nodes other than Kaposi's sarcoma. Analysis of 39 cases and delineation of two new entities. Am J Surg Pathol 1992; 16: 335-50.
2. Piedimonte A, De Nictolis M, Lorenzini P, Sperti V, Bertani A. Angiomyomatous hamartoma of inguinal lymph nodes. Plast Reconstr Surg 2006; 117: 714-6.
3. Catania VD, Manzoni C, Novello M, Lauriola L, Coli A. Unusual presentation of angiomyomatous hamartoma in an eight-month-old infant: case report and literature review. BMC Pediatr 2012; 12: 172.
4. Mauro CS, McGough RL 3rd, Rao UN. Angiomyomatous hamartoma of a popliteal lymph node: an unusual cause of posterior knee pain. Ann Diagn Pathol 2008; 12: 372-4.
5. Prusac IK, Juric I, Lamovec J, Culic V. Angiomyomatous hamartoma of the popliteal lymph nodes in a patient with Klippel-Trenaunay syndrome: case report. Fetal Pediatr Pathol 2011; 30: 320-4.
6. English S, Perret D. Posterior knee pain. Curr Rev Musculoskelet Med 2010; 3: 3-10.
7. Torreggiani WC, Al-Ismail K, Munk PL, *et al*. The imaging spectrum of Baker's (Popliteal) cysts. Clin Radiol 2002; 57: 681-91.
8. Beaman FD, Peterson JJ. MR imaging of cysts, ganglia, and bursae about the knee. Radiol Clin North Am 2007; 45: 969-82.
9. Fritschy D, Fasel J, Imbert JC, Bianchi S, Verdonk R, Wirth CJ. The popliteal cyst. Knee Surg Sports Traumatol Arthrosc 2006; 14: 623-8.
10. Ram M, Alsanjari N, Ansari N. Angiomyomatous hamartoma: a rare case report with review of the literature. Rare Tumors 2009; 1: e25.

 http://dx.doi.org/10.4132/jptm.2013.08.08

Journal of Pathology and Translational Medicine 2015; 49: 159-162
http://dx.doi.org/10.4132/jptm.2013.10.02

■ BRIEF CASE REPORT ■

Focal Hematopoietic Hyperplasia of Rib: A Rare Pseudotumor and Review of Literature

Maneesh Vijay · Asit Ranjan Mridha · Ruma Ray · Prateek Kinra · Biplab Mishra[1] · H. S. Chandrashekhar[2]

Departments of Pathology, [1]Surgery, and [2]Radiodiagnosis, All India Institute of Medical Sciences, New Delhi, India

Primary tumors of the rib are uncommon, comprising 5%–10% of all bony tumors. Benign tumors constitute 63% of this group.[1] Common benign entities include osteochondroma, enchondroma, and fibrous dysplasia, while common malignant tumors of the ribs include plasmacytoma, chondrosarcoma, osteosarcoma, and Ewing's sarcoma.[1] Focal hematopoietic hyperplasia (FHH) is an unusual benign lesion characterized by an expansive osteolytic mass involving the rib in all reported cases.[2-4] Most cases were detected incidentally on routine chest radiography performed for unrelated reasons. The lesion is typically composed of hypercellular marrow containing all three lineages of hematopoietic cells with interspersed fatty marrow; no hematopoietic dyspoiesis or malignancy is seen. Though clinical signs and radiological features of the lesion often simulate a true neoplasm, in reality it is a pseudotumor. Follow-up investigation has failed to show any recurrence or neoplastic transformation after resection of the lesion.[2] To the best of our knowledge, to date only four cases have been reported in the English literature.[2-4] We report a case of FHH in the right second rib in a 26-year-old female who underwent surgery after radiological diagnosis of osteochondroma.

CASE REPORT

A 26-year-old female patient presented with upper backache and pain in the right side of the neck for 2 months in duration. There was no history of trauma, tuberculosis, hypertension or diabetes. Physical examination, and hematological and biochemical investigation did not reveal any abnormalities. Routine chest radiography showed a well-defined, expansile sclerotic mass in the right second rib (Fig. 1A). Subsequent computed tomography revealed a 5.0×4.5-cm mass in the body of the rib with internal linear calcification. There was cortical bulging and thinning of the inner surface without cortical destruction (Fig. 1B, C). The patient underwent surgery with a radiological diagnosis of osteochondroma. The mass was completely excised, fixed in 10% buffered formalin and processed for paraffin embedding after decalcification in 5% nitric acid. Microscopic examination revealed an inner shell with essentially normal trabeculae and a focal haphazard arrangement (Fig. 2A). Hypercellular marrow containing normal hematopoietic cells of all three lineages intermixed with fatty marrow in the inter-trabecular spaces was observed (Fig. 2B, C). No dyspoiesis or hematological malignancy was seen, nor was there any fibrosis. Postoperative follow-up of the patient was uneventful.

DISCUSSION

The term "focal hematopoietic hyperplasia of rib" or "hematopoietic pseudotumor" was first coined by Edelstein and Kyriakos in 1984.[2] They reported two cases of incidentally-detected lesions in a 66-year-old female and a 71-year-old male during routine radiologic investigation for other reasons. The typical radiologic manifestation of the pseudotumor is an expansive, solitary, osteolytic mass of the rib with internal ill-defined linear hyperdense areas and calcification. There is expansion and thinning of the bony cortex without destruction.[2-4] Histologically, the lesion is characterized by focal hyperplasia of normal

Corresponding Author
Asit Ranjan Mridha, M.D.
Department of Pathology, All India Institute of Medical Sciences, Ansari Nagar, New Delhi 110029, India
Tel: +91-11-26593227, Fax: +91-11-26588641, E-mail: asit_aiims@yahoo.co.in

Received: May 31, 2013 **Revised:** September 28, 2013
Accepted: October 2, 2013

pISSN 2383-7837
eISSN 2383-7845

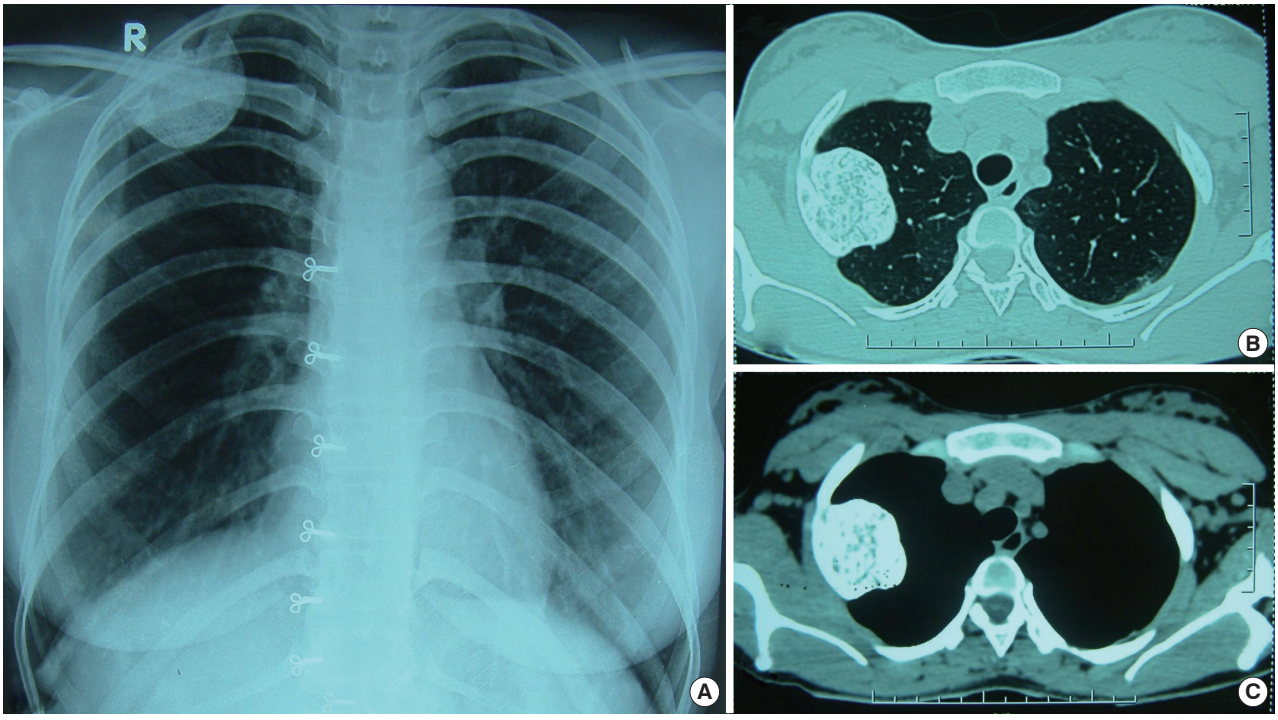

Fig. 1. Radiologic features of focal hematopoietic hyperplasia. (A) Chest radiograph showing a well-defined sclerotic bony lesion arising from the right second rib and projecting into the right upper zone. (B, C) Axial computed tomography images of the lung and mediastinal window demonstrating a well-defined sclerotic osseous lesion arising from the lateral aspect of the right second rib. The lesion has an intrathoracic, extrapleural component, which indents the upper lobe of right lung.

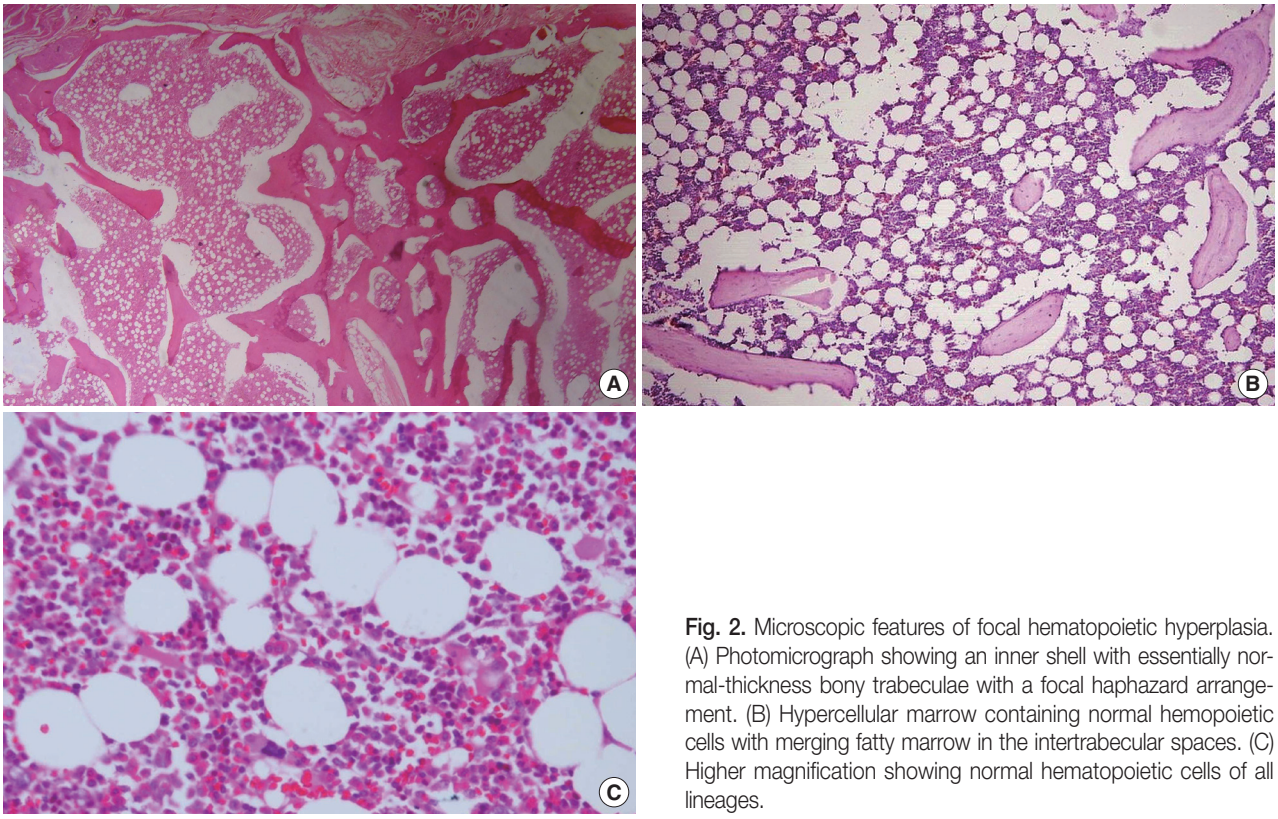

Fig. 2. Microscopic features of focal hematopoietic hyperplasia. (A) Photomicrograph showing an inner shell with essentially normal-thickness bony trabeculae with a focal haphazard arrangement. (B) Hypercellular marrow containing normal hemopoietic cells with merging fatty marrow in the intertrabecular spaces. (C) Higher magnification showing normal hematopoietic cells of all lineages.

http://dx.doi.org/10.4132/jptm.2013.10.02

hematopoietic elements including myeloid, erythroid and megakaryocytic cells. Hyperplastic marrow merging with fatty marrow is a characteristic finding, while no hematopoietic dyspoiesis or malignancy has been reported.[2,3] Diagnosis is often made after excision of the lesion. The clinical and radiological manifestations of this lesion are like that of a true neoplasm, and, consequently, the differential diagnoses on radiology commonly considered are aneurysmal bone cyst, osteochondroma, chondrosarcoma, fibrous dysplasia, plasmacytoma, and metastatic tumor.[2] Only four cases of FHH have been reported in the literature.[2-4] A diagnosis was made based on postoperative specimens in three cases; only one case was diagnosed based on radiology, with confirmation by fine needle aspiration cytology.[4] Similar to the other reported cases, the present case was also detected incidentally on routine chest radiography performed for the investigation of upper backache. A radiological diagnosis of osteochondroma was initially considered, and a definite diagnosis was made after microscopic examination.

Certain hematologic disorders such as chronic anemia, thalassemia, leukemia and myelofibrosis can demonstrate increased hematopoiesis with marrow hyperplasia, fatty marrow and thin bony trabeculae.[5] In chronic hemolysis like thalassemia, medullary expansion of multiple bones including the craniofacial bones, vertebrae, pelvic bones and ribs is common.[5] In this condition, the ribs usually show prominent cortical expansion in the posterior aspect and increased normoblastic erythropoiesis, and the patients typically present with anemia, hepatosplenomegaly and skeletal deformity.[6] In contrast, anemia and hepatosplenomegaly are not associated with FHH and no such clinical features were present in our case. In myelofibrosis, the trilineage proliferation of hematopoietic cells, including normoblasts, granulocyte precursors and megakaryocytes, is accompanied by a varying degree of marrow fibrosis.[7] Our case revealed trilineage proliferation of marrow cells without any fibrosis. The majority of the patients with myelofibrosis present clinically with anemia and hepatosplenomegaly; expanding bone mass is not a typical clinical manifestation of myelofibrosis.

Myelolipoma can also demonstrate similar morphology to that seen in our case.[8] The most common location of myelolipoma is the adrenal gland;[8] however, a number of extra-adrenal myelolipomas have been reported in soft tissue, mostly in presacral locations, as well as in the retroperitoneum, pelvis, stomach, musculofascial tissue and in the nose.[9] Only three cases of intraosseous myelolipoma have been described in the literature.[10] Sundaram *et al.*[10] reported two cases occurring in the roof of the acetabulum and the proximal femur in 35-year-old and 51-year-old patients, respectively. According to the available literature, a classical intraosseous myelolipoma radiologically appears as an osteolytic and or osteosclerotic intramedullary lesion without any cortical expansion. In contrast, the typical radiologic features of FHH are an expansive, osteolytic lesion with internal calcification, as seen in our case. Microscopically FHH exhibits hypercellularity of marrow elements for the age as compared to myelolipoma wherein the cellularity is normal.

Two possible mechanisms that have been proposed in the pathogenesis of FHH include 1) the reactive process after trauma and inflammation, and 2) developmental anomaly.[2] Our patient had no history of trauma or any preceding infection in this location. She had no other abnormality on physical examination to suggest a developmental anomaly.

Irrespective of these putative mechanisms, FHH of the rib is a rare non-neoplastic lesion with a characteristic radiologic appearance. The microscopic features are similar to hyperplastic marrow and myelolipoma, and a high index of clinical and radiological suspicion is required for the diagnosis of this pseudotumor. Radiologists should be aware of this incidentally-detected lesion of the rib. Histopathologists need to recognize this pseudotumor keeping in mind the differential diagnosis of intraosseous myelolipoma. Awareness of this entity will help to prevent unnecessary biopsy and surgical procedures.

Conflicts of Interest

No potential conflict of interest relevant to this article was reported.

REFERENCES

1. Aydogdu K, Findik G, Agackiran Y, Kaya S, Karaoglanoglu N, Tastepe I. Primary tumors of the ribs; experience with 78 patients. Interact Cardiovasc Thorac Surg 2009; 9: 251-4.
2. Edelstein G, Kyriakos M. Focal hematopoietic hyperplasia of the rib: a form of pseudotumor. Skeletal Radiol 1984; 11: 108-18.
3. Lee KB, Kim BS, Cho JH. Focal hematopoietic hyperplasia of the rib. Skeletal Radiol 2002; 31: 175-8.
4. Galindo LM, Soans S, Chiaramonte C, Garcia FU. Focal hematopoietic hyperplasia of the rib. Report of a case diagnosed by fine needle aspiration. Acta Cytol 1998; 42: 987-90.
5. Greer JP, Foerster J, Rodgers GM, *et al.* Wintrobe's clinical hematology. 12th ed. Philadelphia: Lippincott Williams & Wilkins, 2009.
6. Resnick D. Bone and joint imaging. 3rd ed. Philadelphia: W.B. Saunders, 2004.
7. McCarthy EF, Frassica FJ. Pathology of bone and joint disorders with

clinical and radiographic correlation. Philadelphia: W.B. Saunders, 1998.
8. Weiss SW, Goldblum JR. Enzinger and Weiss's soft tissue tumors. 6th ed. St. Louis: Mosby, 2014.
9. Pascual García X, Bujons Tur A, Rodríguez Faba O, Gómez Ruiz JJ, Palou Redorta J, Villavicencio Mavrich H. Extraadrenal perirenal myelolipoma: report of a case and review of the literature. Actas Urol Esp 2007; 31: 932-4.
10. Sundaram M, Bauer T, von Hochstetter A, Ilaslan H, Joyce M. Intraosseous myelolipoma. Skeletal Radiol 2007; 36: 1181-4.

 http://dx.doi.org/10.4132/jptm.2013.10.02

Journal of Pathology and Translational Medicine 2015; 49: 163-166
http://dx.doi.org/10.4132/jptm.2013.11.25

■ BRIEF CASE REPORT ■

Serous Cystadenoma and Fibrothecoma: A Rare Combination in Collision Tumor of Ovary with Pseudo–Meigs Syndrome

Shirish S. Chandanwale · Sukanya S. Pal · Harsh B. Kumar · Amit B. Sammi

Department of Pathology, Dr. D. Y. Patil Medical College, Pimpri, India

Collision tumors are best considered as separate primary neoplasms. These tumors have been reported in various organs, such as the esophagus, stomach, liver, thyroid gland, ovary, and lung, but they are extremely rare in the ovaries.[1] The majority of these tumors are a collision between carcinomas and sarcomas or lymphomas, and rarely between two types of carcinoma.[2] The most common histological combination of collision tumor in the ovary is the coexistence of teratoma with mucinous tumors (mucinous cystadenoma or carcinoma).[1] Here we report a very unusual combination of fibrothecoma and serous cystadenoma in the left ovary of an elderly woman who presented with an abdominal lump and ascites.

CASE REPORT

A 63-year-old, parous, menopausal woman was admitted with complaints of abdominal distention for 3 months and difficulty in passing urine for 1 month. Physical examination revealed an abdominal lump and ultrasonography revealed a large cystic mass. A computed tomography (CT) scan revealed a large cystic lesion (22.7×15×20 cm) occupying the pelvis and abdomen, with a well delineated solid area (9×5 cm) within it. Minimal ascites were noted (Fig. 1A, B). No other significant findings, including pleural or pericardial effusion, were noted. Malignant neoplasm of the ovary was suspected.

Corresponding Author
Shirish S. Chandanwale, M.D.
75/1+2/1, Krishna Appt, Behind Indraprastha BLD, New Sangvi, Pune, Maharashtra 411027, India
Tel: +98-90144517, Fax: +98-020-27805217,
E-mail: shirishchandanwale@gmail.com

Received: September 26, 2013 **Revised:** November 17, 2013
Accepted: November 25, 2013

Cytology of ascitic fluid showed a few reactive mesothelial cells. Malignant cells were not seen. Carcinoma antigen 125 (CA-125) levels were mildly elevated (0.42 IU/mL). A specimen from radical hysterectomy, including a left ovarian cystic mass, was received for histopathological examination.

On cutting, the left ovarian cyst leaked blood-tinged, serous fluid. The cut surface showed a large, uniloculated, thin walled cyst (20×18 cm) with a smooth surface and congested vessels. At one end of the cyst, we observed a well-demarcated, solid, homogeneous, yellow-white mass (8×6 cm) (Fig. 1C, arrows). A few areas of cystic changes were seen. Compressed ovarian tissue at the periphery and fallopian tube could be identified.

Histopathological examination of the solid area in the left ovarian mass showed a tumor composed of fascicles of loosely arranged spindle cells with variable cellularity and a variable amount of intervening collagen. The cells had oval to elongate nuclei with a moderate amount of pale to vacuolated cytoplasm (Fig. 2A, B). Nuclear atypia, mitotic activity, and edema were not seen in the tumor tissue. In places, closely packed spindle stromal cells were arranged in fascicles and a storiform pattern with hyaline collagen bands (Fig. 2C, D). No glandular structures were seen. A diagnosis of fibrothecoma was made.

Histopathological examination of the cyst showed a fibrocollagenous wall lined in places by cuboidal epithelium with cilia (Fig. 3A). Papillae were not seen. A diagnosis of serous cystadenoma was made. Sections from the junction of the two tumors showed normal ovarian stromal tissue with congested blood vessels (Fig. 3B). A final histological diagnosis of an ovarian collision tumor consisting of fibrothecoma and serous cystadenoma was made.

pISSN 2383-7837
eISSN 2383-7845

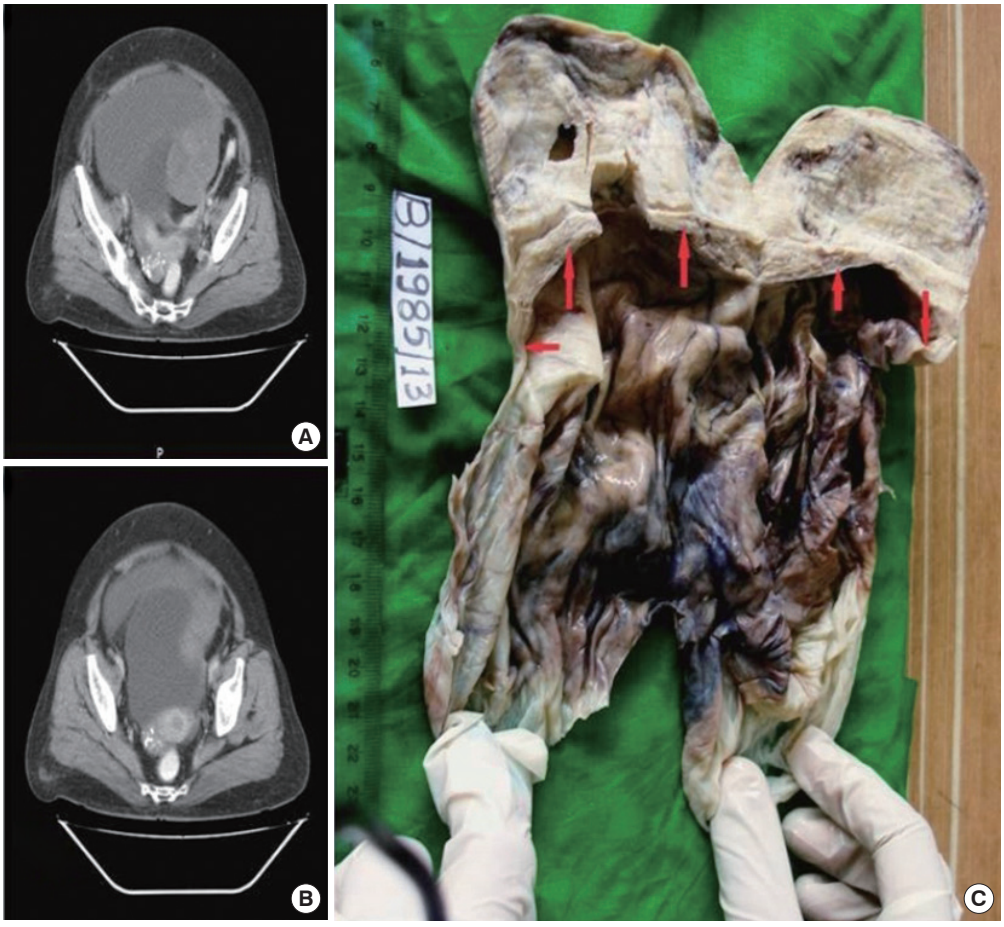

Fig. 1. (A, B) Computed tomography scan showing a large cystic lesion occupying the pelvis and abdomen (solid area), and minimal ascites. (C) Specimen of left ovarian cyst with well-demarcated solid yellow tumor mass (arrows).

DISCUSSION

Collision tumors are defined as two adjacent but histologically distinct tumors, without admixture, in the same tissue or organ.[1] These tumors are rare clinical entities.

The majority of these tumors are a collision between carcinomas and sarcomas or lymphomas and have been reported in various organs. Collision tumors involving ovaries are extremely rare. Many hypotheses have been put forward to explain the rare phenomenon of collision tumors: coincidental occurrence; carcinogenic agents of a primary tumor; oncogenic growth factors produced by a metastatic tumor; and alterations in the microenvironment.[1] In this case, the finding was coincidental. Very few reports of collision tumors involving ovaries have been reported in the literature.[1,3,4]

The pathology of collision tumors reveal two different types of coexisting neoplastic tissues, with a sharp demarcation between the two and without a substantial admixture of histology at the interface. The most common combination of collision tumor in the ovary involves teratoma with mucinous tumors (cystadenoma and carcinoma).[1]

Thecoma and fibroma often merge, therefore the term fibrothecoma is appropriate. Pure thecomas are typically associated with estrogenic manifestations, which were not seen in our case. Ovarian fibrothecomas often clinically present as a solid adnexal mass and can mimic malignant ovarian tumors.

Ultrasonography features of fibrothecoma are usually nonspecific, and magnetic resonance imaging (MRI) is often needed for further differentiation from other solid ovarian masses.[5] MRI was not done in our case. Ovarian fibromas and fibrothecomas can be associated with ascites, sometimes in combination with pleural effusion, which may lead to a mistaken impression of inoperable ovarian neoplasm.[5]

In 1937, Meigs described seven cases of combined pleural effusion, ascites, and ovarian fibroma and named it Meigs syndrome.[6] In 1954, he limited the syndrome to cases where tu-

 http://dx.doi.org/10.4132/jptm.2013.11.25

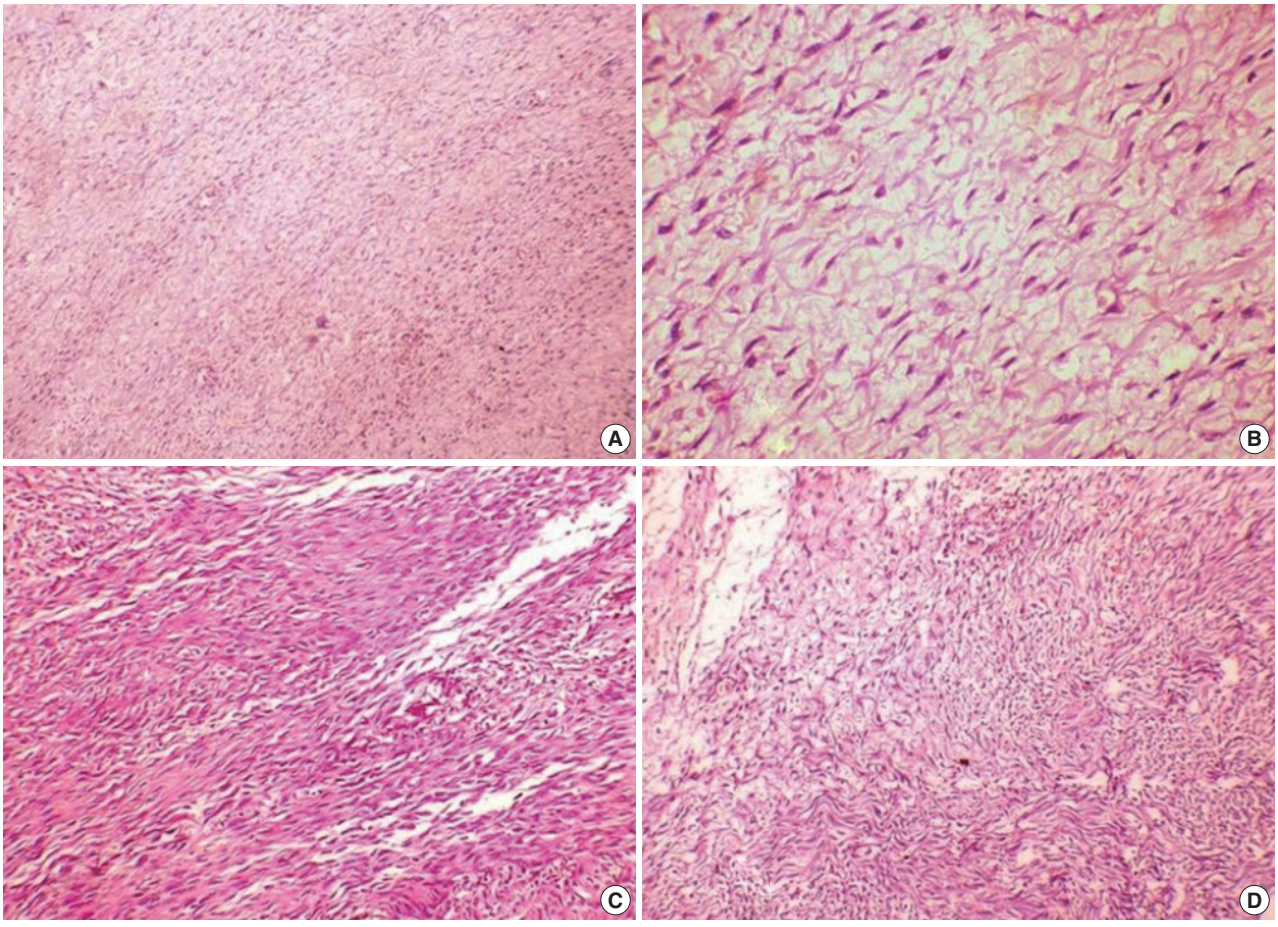

Fig. 2. Microscopy of solid tumor showing areas of thecoma (A, B), fibroma (C), and mixture of fibroma and thecoma (D).

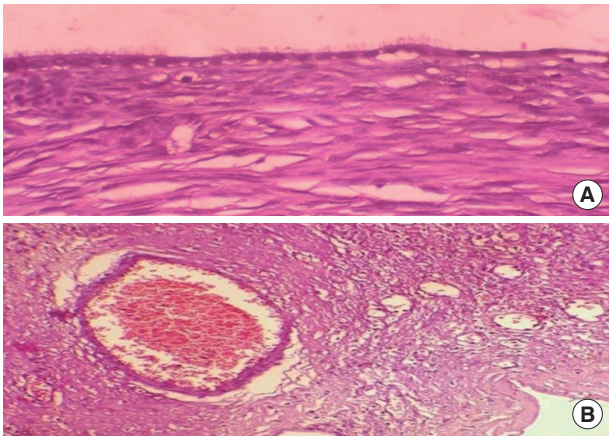

Fig. 3. (A) Microscopy of cyst wall showing lining of cuboidal epithelium with cilia. (B) Microscopy from the junction of solid and cystic tumors showing congested ovarian stroma.

mor removal cures the disease.[6] Pseudo-Meigs is a variant, not possessing the original tumor cell types described by Meigs.[7]

Proposed mechanisms for the ascites in Meigs syndrome are production of ascitic fluid by the tumor; lymphatic obstruction; hormonal stimulation; release of inflammatory mediators; and tumor torsion. Pleural effusion is thought to be caused by the migration of fluid and protein—perhaps by lymphatic channels— across the diaphragm.[6] In the present case, pleural effusion was not present, which was possibly due to the minimal amount of ascitic fluid. Elevated serum CA-125 levels, which are seen in Meigs or atypical Meigs syndrome, were seen in this case.[8]

To the best of our knowledge, we are presenting the first case in the English literature of collision of fibrothecoma and serous cystadenoma in an ovary with Pseudo-Meigs syndrome. For correct diagnosis, these tumors need to be differentiated from fibrothecoma with massive cystic changes and serous cystadenofibroma. The presence of cuboidal lining epithelium with cilia in the cyst wall ruled out massive cystic changes in fibrothecoma and a follicular cyst. The absence of glandular structures in fibrothecoma ruled out serous cystadenofibroma. Follow up examination of the patient postoperatively showed the disappear-

ance of ascitic fluid on a CT scan.

We conclude that a diagnosis of collision tumor involving an ovary is challenging and often made postoperatively. The collision of fibrothecoma and serous cystadenoma is a rare combination and can cause Meigs or Pseudo-Meigs syndrome. Elevated serum CA-125 levels alone cannot differentiate between benign and malignant ovarian masses.

Conflicts of Interest

No potential conflict of interest relevant to this article was reported.

REFERENCES

1. Bige O, Demir A, Koyuncuoglu M, Secil M, Ulukus C, Saygili U. Collision tumor: serous cystadenocarcinoma and dermoid cyst in the same ovary. Arch Gynecol Obstet 2009; 279: 767-70.
2. Murthaiah P, Truskinovsky AM, Shah S, Dudek AZ. Collision tumor versus multiphenotypic differentiation: a case of carcinoma with features of colonic and lung primary tumors. Anticancer Res 2009; 29: 1495-7.
3. Papaziogas B, Souparis A, Grigoriou M, *et al.* A rare triple coexistence of a collision tumor, a benign mature cystic teratoma and a hemorrhagic follicular cyst of the ovaries. Internet J Surg 2008; 14: 19-24.
4. Moid FY, Jones RV. Granulosa cell tumor and mucinous cystadenoma arising in a mature cystic teratoma of the ovary: a unique case report and review of literature. Ann Diagn Pathol 2004; 8: 96-101.
5. Kitajima K, Kaji Y, Sugimura K. Usual and unusual MRI findings of ovarian fibroma: correlation with pathologic findings. Magn Reson Med Sci 2008; 7: 43-8.
6. Thaker DA, Stride PJ, Dettrick A. A pseudo case of atypical pseudo-Meigs syndrome. Indian J Cancer 2011; 48: 364-6.
7. Kazanov L, Ander DS, Enriquez E, Jaggi FM. Pseudo-Meigs' syndrome. Am J Emerg Med 1998; 16: 404-5.
8. Renaud MC, Plante M, Roy M. Ovarian thecoma associated with a large quantity of ascites and elevated serum CA 125 and CA 15-3. J Obstet Gynaecol Can 2002; 24: 963-5.

http://dx.doi.org/10.4132/jptm.2013.11.25

Journal of Pathology and Translational Medicine 2015; 49: 167-170
http://dx.doi.org/10.4132/jptm.2014.04.02

■ BRIEF CASE REPORT ■

Unicystic Granulosa Cell Tumor

Nalli R. Sumitra Devi · Sathya Lakshmi Ramu · Arun Prabhakaran · Deepa Devi Govindaswamy

Department of Pathology, Stanley Medical College, Chennai, Tamil Nadu, India

Granulosa cell tumors are the most frequent sex cord stromal tumor and account for approximately 5% of all primary ovarian tumors. About 5% occur before puberty and 40% occur in the menopausal age group; however, these tumors have an indolent biological behavior.[1] The clinical presentation in most cases is due to estradiol secretion but some may be nonfunctional or may present with virilizing symptoms. Unilocular and multilocular cystic granulosa cell tumors have been reported in the literature but are rare disease processes.[2,3]

CASE REPORT

A 57-year-old woman presented with lower abdominal pain and abdominal distention for 3 months duration. The patient reached menopause 10 years prior. She had no symptoms or signs of hyperestrinisim or virilization. Abdominal examination revealed a mass consistent with 20 weeks of pregnancy extending to the umbilicus. On palpation, the mass was mobile and cystic. Ultrasound examination showed a mixed echogenic mass measuring 13×8.8 cm, which arised from the left side of the pelvis (Fig. 1A). A computed tomography (CT) scan revealed a large cystic space occupying lesion with thick septa measuring 18.5×11.9×14.4 cm arising from the pelvis (Fig. 1B). A possible diagnosis of a mucinous cyst adenoma/carcinoma was made. Lab investigations were within normal limits with cancer antigen 125 levels being 5–12 U/mL (normal value, 0 to 35 U/mL). The patient underwent a total abdominal hysterectomy with bilateral salphingo-oopherectomy. Grossly, the left ovarian cyst measured 20×14×10 cm. The external surface of the cyst was smooth with prominent vasculature and the cut surface revealed a unilocular and thin-walled cyst filled with 500 mL of hemorrhagic fluid. The inner surface was smooth with tiny focal papillary projections (Fig. 2). Histomorphology revealed a unicystic lesion lined by multi-layered granulosa cells with interspersed Call-Exner bodies (Fig. 3A, B). The neoplastic cells were round to polygonal with moderate to scant cytoplasm and round to oval nuclei with some showing prominent grooving (Fig. 3C). The immunohistochemical markers, inhibin and vimentin, were positive (Fig. 3D, E). A final diagnosis of unicystic granulosa cell tumor was made.

DISCUSSION

Sex cord stromal tumors comprise approximately 8% of primary ovarian neoplasms, and among these tumors, the granulosa cell tumor is the most common and accounts for approximately 1.5% of primary ovarian tumors. Granulosa cell tumors were first described by Rokitansky in the year 1859.[4] Histogenesis of sex cord stromal tumors is uncertain; however, at present, the origin is considered to be coelomic epithelium or gonadal sex cord.[2] There are two well-defined patterns of granulosa cell tumor, the common adult granulosa cell tumor and the less frequent juvenile type, which are based on clinical and histopathological features. The adult granulosa cell tumor accounts for 95% of all ovarian tumors, and most commonly presents in the peri or postmenopausal period with a peak incidence between 50–54 years.[5]

The usual presentation of these tumors are symptoms associated with hyperestrinism leading to isosexual pseudoprecocity in children and metrorrhagia in adults. A large number of androgenic granulosa cell tumors present as unilocular or multilocular cysts.[6] The association with androgen production and

Corresponding Author
Nalli R. Sumitra Devi, M.D.
Stanley Medical College, 5E, Old Tower Block, Nandanam Extension, Chennai 600035, Tamil Nadu, India
Tel: +91-9445001778, E-mail: drnallisumitra@yahoo.co.in

Received: January 24, 2014 **Revised:** March 22, 2014
Accepted: April 2, 2014

pISSN 2383-7837
eISSN 2383-7845

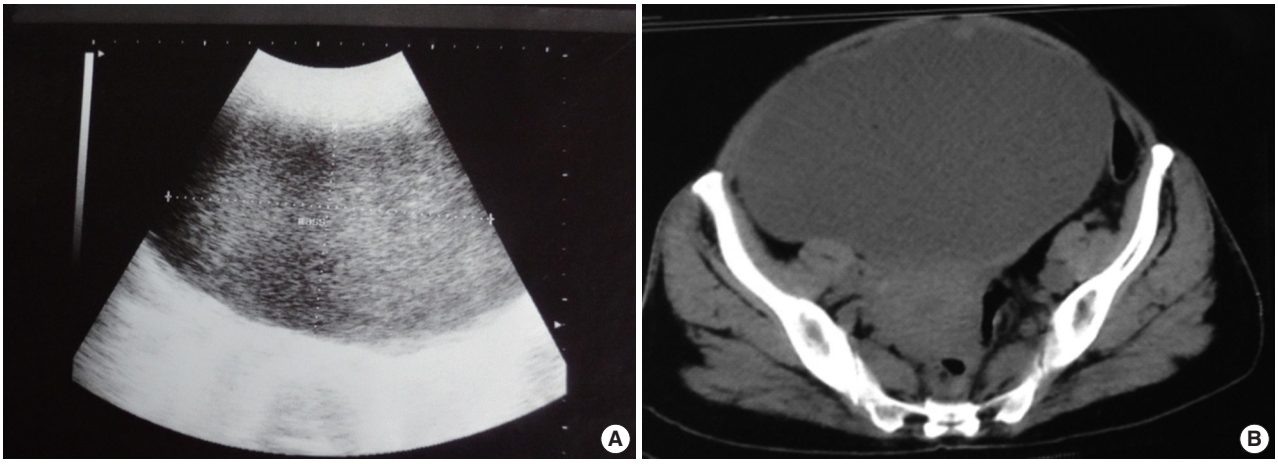

Fig. 1. (A) Mixed echogenic mass measuring 13×8.8 cm arising from the left side of the pelvis. (B) Large cystic space-occupying lesion with thick septa measuring 18.5×11.9×14.4 cm arising from the pelvis.

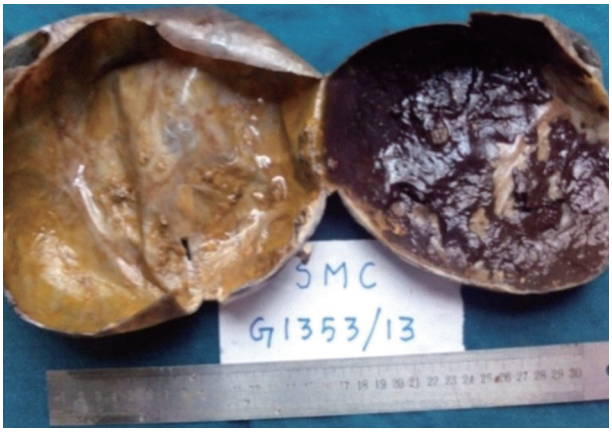

Fig. 2. Cut surface showing a thin walled unilocular cyst with a smooth inner surface and multiple tiny papillary excrescences and hemorrhagic areas.

the formation of unilocular cystic type of granulosa cell tumor remains an enigma.[7] Sonographically and based on CT images, five morphological patterns were categorized including multilocular cystic, thick-walled unilocular cystic, thin-walled unilocular cystic, homogenously solid, and heterogeneously solid masses.

Grossly, granulosa cell tumors are usually unilateral and encapsulated with a smooth lobulated outline and predominantly solid or solid and cystic with a yellow to white cut surface. Cystic degeneration and hemorrhage are common. Occasionally, the tumors may resemble a thin-walled unilocular or multilocular cystadenoma.[2]

The histomorphology of adult granulosa cell tumors includes well-differentiated and less well-differentiated types. The well-differentiated group is composed of microfollicular, macrofollicular, trabecular, and insular patterns with the microfollicular pattern being the most common of all subtypes and contains Call-Exner bodies. Diffuse and watered silk or gyriform patterns fall under the less well differentiated group. Sclerotic stroma is a secondary degenerative change commonly seen in granulosa cell tumors, which most likely arises due to ischemia.[7,8] Differential diagnosis for granulosa cell tumors include low-grade stromal sarcomas, small cell carcinomas, and carcinoid tumors on low power magnification. These tumors lack nuclear grooving, are more hyperchromatic, and often contain more mitotic figures than typical granulosa cell tumors. The nuclear appearance, mitotic rate, and presence of Call-Exner bodies have a diagnostic value in differentiating granulosa cell tumors from other malignant tumors.

Elevated levels of alpha inhibin and/or Müllerian-inhibiting substance (MIS) or anti-Müllerian hormone are useful and specific markers for early diagnosis and follow-up of granulosa cell tumors. This case was positive for alpha inhibin and vimentin. Therefore, the diagnosis of unilocular cystic granulosa cell tumors is based on the histological examination with a monotonous population of round to oval cells with Call-Exner bodies, nuclear grooves, low mitotic activity, infrequent diagnostic serum markers, and immunohistochemical profile. The spectrum of differentiation correlates poorly with the clinical outcomes and all granulosa cell tumors are considered low grade malignancies. Granulosa cell tumors are slow growing tumors, and late recurrence is a common feature. Clinicopathologic prognostic markers include the tumor stage as well as tumor size and rupture, of which staging is the most important prognostic fac-

 http://dx.doi.org/10.4132/jptm.2014.04.02

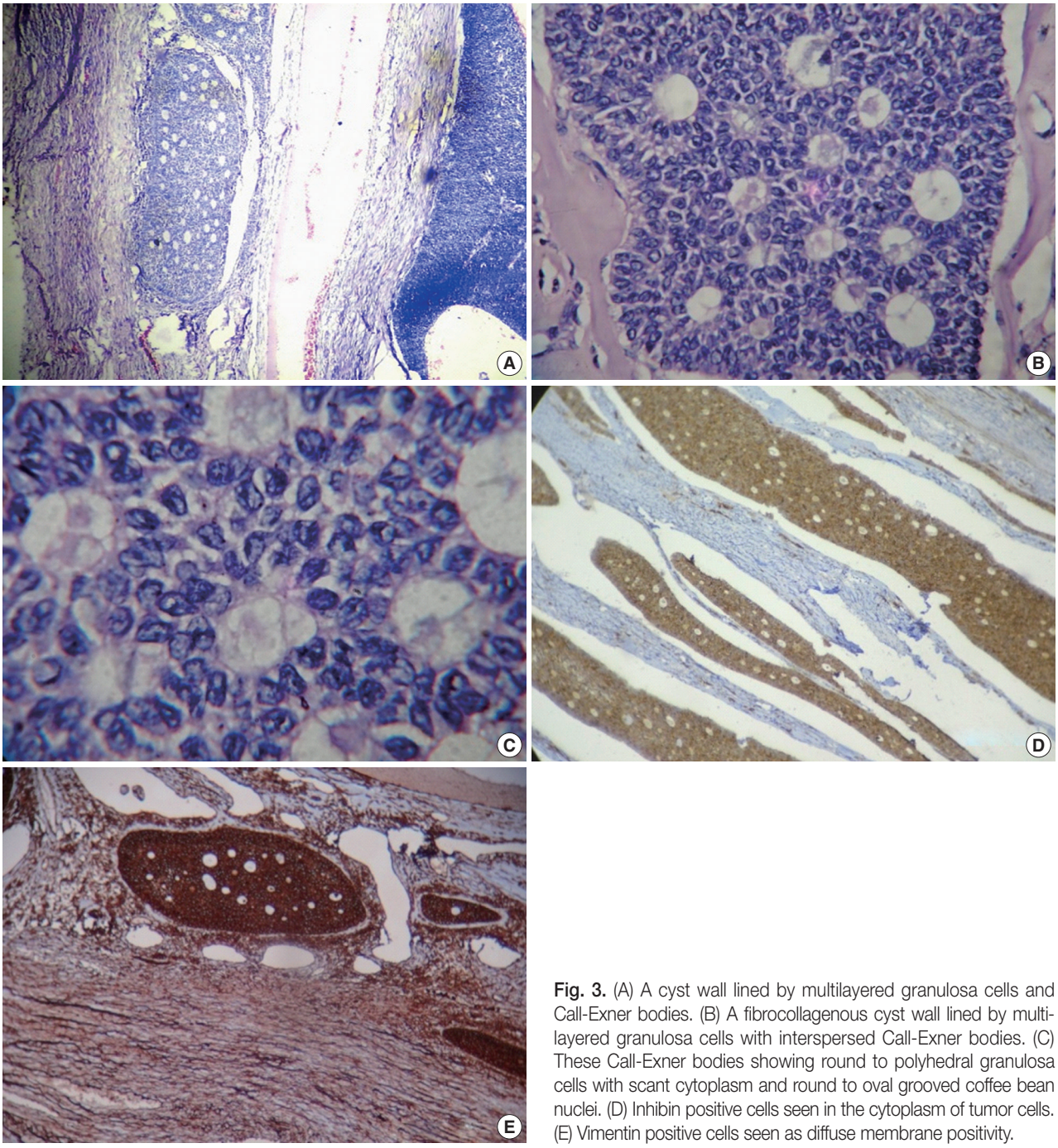

Fig. 3. (A) A cyst wall lined by multilayered granulosa cells and Call-Exner bodies. (B) A fibrocollagenous cyst wall lined by multilayered granulosa cells with interspersed Call-Exner bodies. (C) These Call-Exner bodies showing round to polyhedral granulosa cells with scant cytoplasm and round to oval grooved coffee bean nuclei. (D) Inhibin positive cells seen in the cytoplasm of tumor cells. (E) Vimentin positive cells seen as diffuse membrane positivity.

tor.[9] The 5-year survival rate for stage 1 disease ranges from 75% –95%. Presence of tumors greater than 10–15 cm in diameter carries a poor prognosis independent of stage. A mitotic index of more than or equal to 10 mitotic figures per high power field (×10) has a poor prognosis. Other histopathological variables used to determine prognosis include p53 status, histological pattern, disease stage, mitotic index, and lymphovascular invasion. Of these factors, mitotic index and lymphovascular invasion were the most important and are independent factors that determine prognosis.[10] Life-long follow-up with clinical examinations and measurement of tumor markers such as inhibin B are recommended.

Conflicts of Interest

No potential conflict of interest relevant to this article was reported.

REFERENCES

1. Roth LM. Sex cord stromal tumors of the ovary. In: Fox H, Wells M, eds. Haines and Taylor obstetrical and gynaecological pathology. New York: Churchill Livingstone, 1995; 824-30.
2. Scully RE. Tumors of the ovary and maldeveloped gonads. In: Hartmann WH, Cowan WR, eds. Atlas of tumor pathology, series 2, fascicles 16. Washington, DC: Armed Forces Institute of Pathology, 1979; 239-312.
3. Zaloudek C. The ovary. In: Gompel C, Silverberg SG, eds. Pathology in gynecology and obstetrics. 4th ed. Philadelphia: Lippincott, 1994; 313-413.
4. Rokitansky CV. Uber abnormalitaten des corpus luteum. Wien Med Ztc 1859; 4: 253-4.
5. Scully RE. Juvenile granulosa cell tumor. Pediatr Pathol 1988; 8: 423-7.
6. Nakashima N, Young RH, Scully RE. Androgenic granulosa cell tumors of the ovary: a clinicopathologic analysis of 17 cases and review of the literature. Arch Pathol Lab Med 1984; 108: 786-91.
7. Kurman RJ. Blaustein's pathology of the female genital tract. 5th ed. New York: Springer-Verlag, 2002; 907.
8. Al-Nafussi AI. Tumor diagnosis: practical approach and pattern analysis. 2nd ed. New York: Oxford University Press, 2005; 491-2.
9. Fox H, Agrawal K, Langley FA. A clinicopathologic study of 92 cases of granulosa cell tumor of the ovary with special reference to the factors influencing prognosis. Cancer 1975; 35: 231-41.
10. Fujimoto T, Sakuragi N, Okuyama K, *et al.* Histopathological prognostic factors of adult granulosa cell tumors of the ovary. Acta Obstet Gynecol Scand 2001; 80: 1069-74.

http://dx.doi.org/10.4132/jptm.2014.04.02

Journal of Pathology and Translational Medicine 2015; 49: 171-173
http://dx.doi.org/10.4132/jptm.2013.10.14

■ BRIEF CASE REPORT ■

Retiform Hemangioendothelioma of the Neck

Chin-Lung Kuo[1,2,3,4] · Paul Chih-Hsueh Chen[5,6] · Wing-Yin Li[5,6] · Pen-Yuan Chu[1,3]

[1]Department of Otorhinolaryngology-Head and Neck Surgery, Taipei Veterans General Hospital, Taipei; [2]Department of Otorhinolaryngology, Taoyuan Armed Forces General Hospital, Taoyuan; [3]Department of Otorhinolaryngology, [4]Institute of Brain Science, National Yang-Ming University, Taipei; [5]Department of Pathology and Laboratory Medicine, Taipei Veterans General Hospital, Taipei; [6]Department of Pathology, National Yang-Ming University School of Medicine, Taipei, Taiwan

Vascular tumors are categorized into benign hemangiomas, frankly malignant angiosarcomas, and tumors of intermediate malignancy. Hemangioendotheliomas are of intermediate malignancy and encompass a broad range of histologic entities, including retiform, epithelioid, kaposiform, polymorphous, and composite sub-types.[1] Retiform hemangioendothelioma (RH) is an extremely rare disease entity of unknown etiology that was first described by Calonje *et al.*[2] in 1994 as a vascular neoplasm of intermediate malignancy. It is characterized by a high rate of local recurrence and a low frequency of metastasis, and its biologic potential is between that of hemangiomas and angiosarcomas. RH reportedly presents primarily as an exophytic dermal tumor of the extremities.[3] We present the first report of RH arising in the neck without dermal involvement.

CASE REPORT

A previously healthy 27-year-old woman presented to the out-patient department of our institution in February 2012 with a painless mass on the left side of the neck, which had increased in size over the course of one year. She had no constitutional symptoms such as weight loss, fever, or decreased appetite, and the rest of her medical history was also unremarkable. Physical examination revealed a 4×3-cm mass occupying the left side of the neck at the level III lymph node region. On palpation, the lesion was non-tender, hard, movable, and showed well-defined and smooth borders. The overlying skin was normal. Cervical lymph node enlargement was not observed, and the remainder of the otolaryngopharyngeal examination was unremarkable. Ultrasound-guided fine-needle aspiration was performed, and the cytology results were negative for malignancy. Computed tomography of the neck showed a well-defined heterogeneous mass with prominent ring enhancement occupying the left side of the neck at the level III lymph node region (Fig. 1). Surgical excision revealed a well-encapsulated and hypervascular tumor within the left anterior neck triangle.

Histologic examination revealed a 3.8×2×2-cm solid tumor with clear surgical margins. The tumor was composed of vascular structures containing elongated and narrow arborizing vascular channels simulating the structure of a rete testis (Fig. 2). The vascular channels were lined with hobnail endothelial cells (Fig. 3), which demonstrated rare mitosis. The tumor cells were immune-reactive for CD31 and friend leukemia virus integration 1 (Fli-1), but not for smooth muscle actin. Based on these histopathologic and immunohistochemical features, a diagnosis of RH was reached.

After discussion with the head and neck oncology multidisciplinary team, a regular follow-up program was scheduled for the patient without postoperative radiation or chemotherapy, because of the clear surgical margins and rare mitosis observed, and to avoid the potential life-long complications associated with radiation therapy. No recurrence was evident at 1-year follow-up.

DISCUSSION

To date, only 32 cases of RH have been reported in the English literature.[4] The etiology of this disease remains unclear; although cases related to previous epidermal malignant neoplasms, radiotherapy, human herpes virus type 8 and lymphedema have

Corresponding Author
Pen-Yuan Chu, M.D.
Department of Otorhinolaryngology-Head and Neck Surgery, Taipei Veterans General Hospital, 201, Sec 2, Shih-Pai Road, Taipei 112, Taiwan
Tel: +886-2-2875-7337, Fax: +886-2-2875-7338, E-mail: pychu@vghtpe.gov.tw

Received: June 11, 2013 **Revised:** October 6, 2013
Accepted: October 14, 2013

pISSN 2383-7837
eISSN 2383-7845

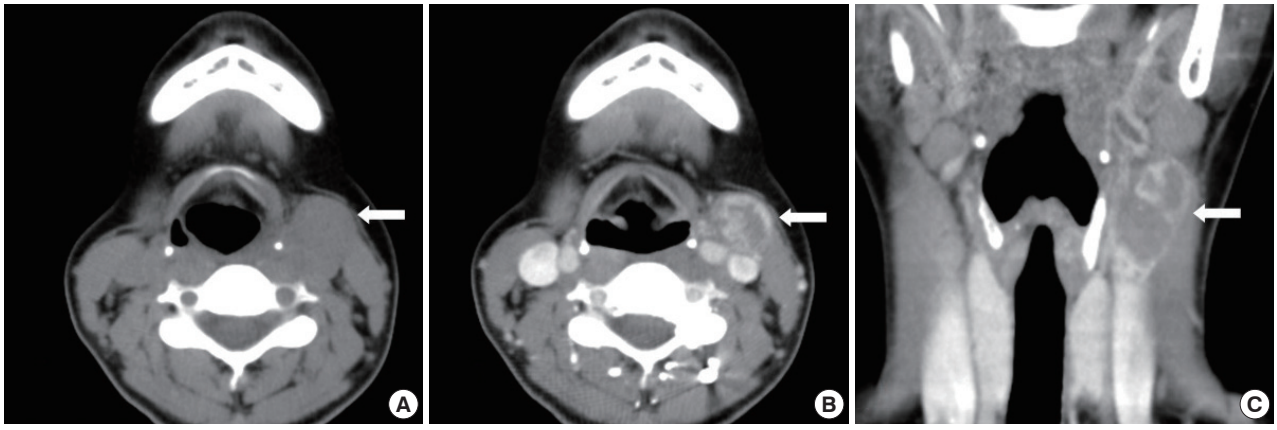

Fig. 1. Computed tomography without contrast shows a mass occupying the left side of the neck at the level III lymph node region (A, arrow); with contrast, the well-defined mass reveals heterogeneous enhancement, with prominent ring enhancement (arrows) (B, C).

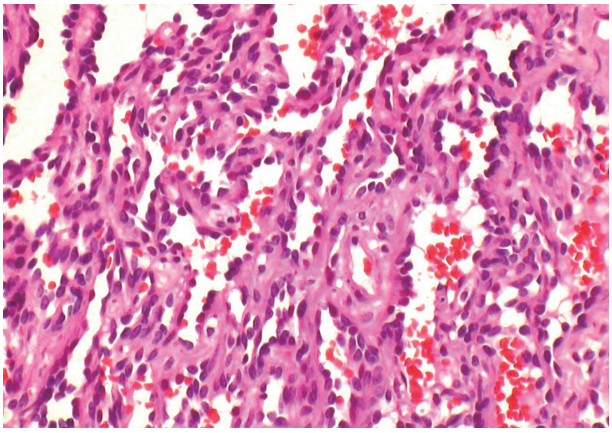

Fig. 2. Tumor histopathology shows complex branching vessels, resembling a rete testis.

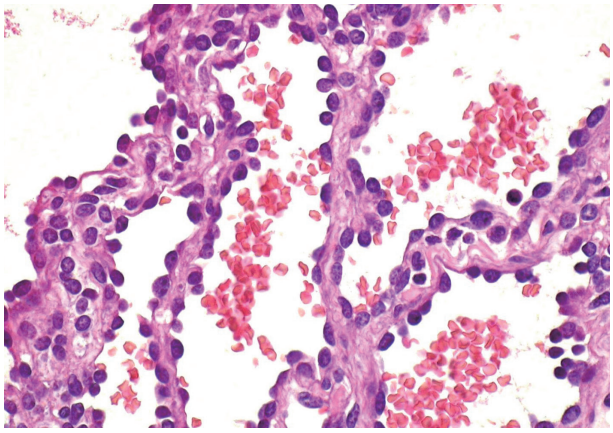

Fig. 3. The vessels are lined by monomorphic hobnail-like endothelial cells, without significant morphologic atypia.

been reported, the exact associations have not been clearly established.[2,4,5] Disease duration from the time of diagnosis ranges from 2 months to several years.[2,3,6] Most patients present between the second to fourth decades of life (mean age, 36 years).[2] There is a female predominance, with a female-to-male ratio of 2:1.[2,3,6] RH can develop as either exophytic or plaque-like lesions with size ranging from 1 to 30 cm.[3,6] Most cases appear in the extremities, with a higher incidence in the lower limbs. Occasionally, this disease occurs in the trunk, scalp, pinna, and penis.[2-5] An RH presenting as a neck mass, as seen in this case, is unusual and has not been previously reported. The differential diagnoses generally include angiosarcoma, papillary intralymphatic angioendothelioma (PILA), hobnail hemangioma and Dabska-RH.[3-5,7,8]

The most important differential diagnosis of RH is angiosarcoma because of the therapeutic and prognostic considerations. Angiosarcoma is an aggressive neoplasm with a high mortality rate and a very high incidence of local recurrence and metastasis.[6] RH also exhibits frequent local recurrence, but rarely metastasizes,[2,3] and no tumor-related deaths have been reported.[6] The vessels of angiosarcoma usually do not have a retiform appearance. Angiosarcoma is characterized by more nuclear atypia, conspicuous mitotic activity, tumor infiltration between individual collagen bundles, and multi-layering of endothelial cells without hobnail morphology.[3,6] PILA is another important differential diagnosis of RH. Although the histologic features of RH overlap with those of PILA, PILA lacks a retiform growth pattern, and is characterized by cavernous lymphangioma-like vascular spaces. Unlike RH, which typically occurs in the extremities, PILA shows no preference for a specific anatomic site.[7] Hobnail hemangioma can be confused with RH due to its similar hobnail endothelial cells. Hobnail hemangioma, however, lacks the complex retiform vessels and is a circumscribed tumor. Furthermore, the hobnail endothelial cells of hobnail hemangi-

http://dx.doi.org/10.4132/jptm.2013.10.14

oma are seen in only the most superficial vessels. Collagen dissection is usually present, and an inflammatory infiltrate is not usually prominent.[3] Dabska-retiform hemangioendothelioma and RH are closely related tumors characterized by the presence of "hobnail"-type endothelial cells. Although RH typically appears in young to middle-age adults in the lower limbs and trunk, Dabska tumors have no particular pattern in terms of age or anatomical site. In addition, RH is considered to be a vascular tumor, while Dabska-RHs have a lymphatic endothelial phenotype.[8]

Cytologic or pathological examination reports may provide surgeons with appropriate guidelines for the treatment of patients, and the most compelling evidence in the differential diagnosis of RH is provided by immunohistochemistry, in which tumor cells react with endothelial markers (e.g., CD31, Fli-1, and factor VIII-related antigen).[2,5,9,10] CD31 is generally regarded as the single best marker of endothelial cell differentiation because it is expressed in 90% of endothelial cell tumors, but very rarely in carcinomas, lymphomas, and mesotheliomas.[9] Factor VIII-related antigen has low sensitivity, and frequent presence of significant "background" due to staining of circulating antigen greatly limits the use of this marker.[10] Hence, the expression of this marker was not determined in this patient.

There are differences between the present case and those in previous reports of RH in terms of disease location (neck vs mainly extremities), morphology (encapsulated mass vs mainly exophytic lesion), and histology (deep soft tissue vs mainly dermal involvement). These differences may expand the understanding of RH. In summary, there can be diagnostic pitfalls in general practice when managing neck masses, particularly an uncommon tumor in an unusual site. Awareness of this unique RH with uncertain malignant behavior is essential. In addition, as the prognosis and adjuvant therapy for RH and angiosarcoma are very different, it is important to distinguish them histopathologically.

Conflicts of Interest

No potential conflict of interest relevant to this article was reported.

Acknowledgments

We thank the Department of Pathology and Laboratory Medicine, Taipei Veterans General Hospital, Taipei, Taiwan, R.O.C. for assistance in the manuscript preparation.

REFERENCES

1. Chu YC, Choi SJ, Park IS, Kim L, Han JY, Kim JM. Composite hemangioendothelioma: a case report. Korean J Pathol 2006; 40: 142-7.
2. Calonje E, Fletcher CD, Wilson-Jones E, Rosai J. Retiform hemangioendothelioma: a distinctive form of low-grade angiosarcoma delineated in a series of 15 cases. Am J Surg Pathol 1994; 18: 115-25.
3. Tan D, Kraybill W, Cheney RT, Khoury T. Retiform hemangioendothelioma: a case report and review of the literature. J Cutan Pathol 2005; 32: 634-7.
4. O'Duffy F, Timon C, Toner M. A rare angiosarcoma: retiform haemangioendothelioma. J Laryngol Otol 2012; 126: 200-2.
5. Ioannidou D, Panayiotides J, Krasagakis K, Stefanidou M, Manios A, Tosca A. Retiform hemangioendothelioma presenting as bruise-like plaque in an adult woman. Int J Dermatol 2006; 45: 53-5.
6. Hirsh AZ, Yan W, Wei L, Wernicke AG, Parashar B. Unresectable retiform hemangioendothelioma treated with external beam radiation therapy and chemotherapy: a case report and review of the literature. Sarcoma 2010; 2010: 756246.
7. Fanburg-Smith JC, Michal M, Partanen TA, Alitalo K, Miettinen M. Papillary intralymphatic angioendothelioma (PILA): a report of twelve cases of a distinctive vascular tumor with phenotypic features of lymphatic vessels. Am J Surg Pathol 1999; 23: 1004-10.
8. Yarmel D, Dormans JP, Pawel BR, Chang B. Recurrent pedal hobnail (Dabska-retiform) hemangioendothelioma with forefoot reconstructive surgery using a digital fillet flap. J Foot Ankle Surg 2008; 47: 487-93.
9. Pusztaszeri MP, Seelentag W, Bosman FT. Immunohistochemical expression of endothelial markers CD31, CD34, von Willebrand factor, and Fli-1 in normal human tissues. J Histochem Cytochem 2006; 54: 385-95.
10. Billings SD, Folpe AL, Weiss SW. Epithelioid sarcoma-like hemangioendothelioma. Am J Surg Pathol 2003; 27: 48-57.

Journal of Pathology and Translational Medicine 2015; 49: 174-176
http://dx.doi.org/10.4132/jptm.2015.02.10

■ BRIEF CASE REPORT ■

Metastatic Endobronchial Adenocarcinoma from the Uterine Cervix Verified by Human Papillomavirus Genotyping

Jisup Kim · Sungsoo Lee[1] · Heae Surng Park

Departments of Pathology and [1]Thoracic and Cardiovascular Surgery, Gangnam Severance Hospital, Yonsei University College of Medicine, Seoul, Korea

Endobronchial metastasis is defined by bronchoscopically visible extrapulmonary tumors with lesions histologically identical to the primary tumors. Carcinomas of the breast, kidney, and colorectum are the most commonly encountered solid tumors causing endobronchial metastases,[1] whereas such metastases arising from the tumors of uterine cervix are relatively rare. While there have been many case reports on endobronchial metastasis of uterine cervical squamous cell carcinoma, there is only one reported case of metastatic endobronchial adenocarcinoma from the uterine cervix[2] and this report focused only on endoscopic treatment. Herein, we report a case of metastatic endobronchial adenocarcinoma from the uterine cervix with discuss on the differential diagnosis.

CASE REPORT

A 59-year-old woman presented with cough, sputum, and dyspnea on exertion. Four years previously, she was diagnosed with uterine cervical cancer and had undergone radical hysterectomy and bilateral salpingo-oophorectomy with adjuvant radiotherapy in an overseas hospital. Chest computed tomography revealed an endobronchial mass in the distal right main bronchus. Whole body positron emission tomography (PET) showed intense 18F-fluorodeoxyglucose uptake in the endobronchial mass with no other abnormally hypermetabolic lesions. Bronchoscopic examination with biopsy was performed, and the pathologic finding was poorly differentiated carcinoma with necrosis and focal mucin formation (Fig. 1A). The tumor had been considered as poorly differentiated pulmonary adenocarcinoma, but it was negative for thyroid transcription factor-1 (TTF-1) and napsin A immunostaining. The patient underwent right pneumonectomy with mediastinal lymph node dissection.

Macroscopically, a 6.5-cm-sized endobronchial mass was noted originating from the right lower lobar bronchus. Microscopically, the tumor showed large, confluent cribriform glands with focal papillary growth and intraluminal necrotic debris (Fig. 1B). The tumor cells were tall and columnar, showing elongated, vesicular nuclei and amphophilic cytoplasm. Metastases to the peribronchial and subcarinal lymph nodes were observed. Since the microscopic findings were unusual for primary lung adenocarcinoma and the patient had a history of uterine cancer, extensive immunohistochemical staining was performed. The tumor was positive for cytokeratin (CK) 7, carcinoembryonic antigen, and p16, and negative for TTF-1, napsin A, estrogen receptor, progesterone receptor, vimentin, CK20, and caudal-related homeobox gene 2 (Fig. 1C, D). Human papillomavirus (HPV) genotyping (GeneFinder HPV Liquid Bead Microarray Kit, Infopia, Anyang, Korea) revealed the presence of HPV type 18 genome in the tumor. The final pathological diagnosis was metastatic adenocarcinoma from the uterine endocervix.

DISCUSSION

Diffuse positive immunostaining for p16 is a good surrogate marker of high-risk HPV infection in uterine cervical and oropharyngeal cancer.[3] Primary lung cancers can also overexpress p16, but mainly in a focal distribution in approximately 32% of cases.[4] However, high-risk HPV genomes are nearly nonexis-

Corresponding Author
Heae Surng Park, M.D.
Department of Pathology, Gangnam Severance Hospital, Yonsei University College of Medicine, 211 Eonju-ro, Gangnam-gu, Seoul 135-720, Korea
Tel: +82-2-2019-3545, Fax: +82-2-3463-2103, E-mail: turtle98p@yuhs.ac

Received: January 23, 2015 **Accepted:** February 10, 2015

pISSN 2383-7837
eISSN 2383-7845

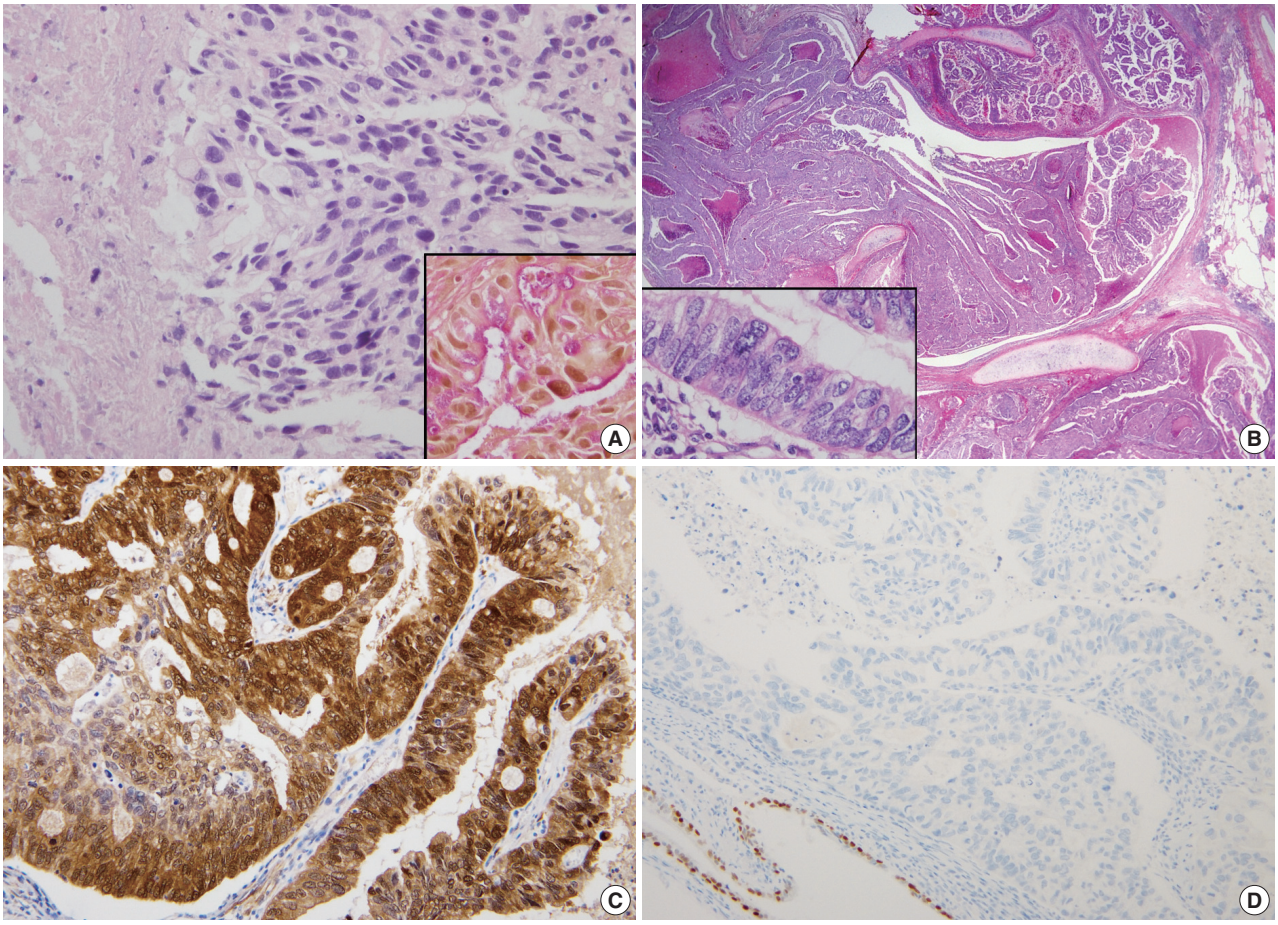

Fig. 1. (A) Histology of bronchoscopic biopsy shows poorly differentiated carcinoma with necrosis and focal mucin production (inset, mucicarmine stain). (B) Histology of the pneumonectomy specimen shows confluent cribriform glands with focal papillary growth and intraluminal necrotic debris. Tall columnar tumor cells have elongated, vesicular nuclei and amphophilic cytoplasm (inset). (C) Immunohistochemical staining for p16 shows diffuse strong nuclear and cytoplasmic positivity in tumor cells. (D) Immunohistochemical staining for thyroid transcription factor-1 shows non-reactivity of tumor cells.

tent in lung cancer.[4,5] Accordingly, confirmation of HPV infection is important to determine whether lung tumor has metastasized from an HPV-associated primary cancer elsewhere in the body, such as the uterine cervix. In this case, HPV type 18 was detected in the tumor and a diagnosis of metastatic endocervical adenocarcinoma was made although the primary cancer tissue was no longer available.

At the time of bronchoscopic biopsy, the patient's history of uterine cancer was not known and whole body PET showed no other abnormal lesions except the endobronchial mass. Retrospective pathologic review of the biopsy showed no specific histologic findings to suggest uterine endocervical adenocarcinoma. While positive immunostaining for both TTF-1 and napsin A is highly specific and relatively sensitive for primary lung adenocarcinoma, negative immunostaining for both TTF-1 and napsin A has been reported in a small fraction of primary lung adenocarcinoma.[6] Therefore, primary lung adenocarcinoma could not be excluded from the biopsy specimen alone. Since the tumor was an endobronchial lesion, mucoepidermoid carcinoma was considered in the differential diagnosis. We retrospectively performed immunohistochemical staining for p16 as well as paired box 8 (PAX8), which is expressed in carcinomas arising in the endometrium, endocervix, ovary, thyroid, kidney, and urothelium. The tumor from the bronchoscopic biopsy showed positive immunoreactivity for p16, but negative immunoreactivity for PAX8.

Diagnosis of an extrapulmonary malignancy in a small biopsy is challenging in the absence of information on the patient's history of cancer. A combination of TTF-1 and napsin A immunostaining is useful to differentiate between pulmonary and extrapulmonary carcinoma in a proper clinical setting. When a non-squamous carcinoma from the bronchus is negative for both

TTF-1 and napsin A, the possibility of an extrapulmonary lesion may be considered and ancillary testing with clinical correlation should be pursued.

Conflicts of Interest

No potential conflict of interest relevant to this article was reported.

REFERENCES

1. Marchioni A, Lasagni A, Busca A, *et al.* Endobronchial metastasis: an epidemiologic and clinicopathologic study of 174 consecutive cases. Lung Cancer 2014; 84: 222-8.
2. Luciani S, Bertoletti L, Vergnon JM. Endoscopic treatment of endobronchial metastases from adenocarcinoma of the uterine cervix. Rev Mal Respir 2010; 27: 759-63.
3. Doxtader EE, Katzenstein AL. The relationship between p16 expression and high-risk human papillomavirus infection in squamous cell carcinomas from sites other than uterine cervix: a study of 137 cases. Hum Pathol 2012; 43: 327-32.
4. Yanagawa N, Wang A, Kohler D, *et al.* Human papilloma virus genome is rare in North American non-small cell lung carcinoma patients. Lung Cancer 2013; 79: 215-20.
5. van Boerdonk RA, Daniels JM, Bloemena E, *et al.* High-risk human papillomavirus-positive lung cancer: molecular evidence for a pattern of pulmonary metastasis. J Thorac Oncol 2013; 8: 711-8.
6. Ye J, Findeis-Hosey JJ, Yang Q, *et al.* Combination of napsin A and TTF-1 immunohistochemistry helps in differentiating primary lung adenocarcinoma from metastatic carcinoma in the lung. Appl Immunohistochem Mol Morphol 2011; 19: 313-7.

http://dx.doi.org/10.4132/jptm.2015.02.10

Journal of Pathology and Translational Medicine 2015; 49: 177-179
http://dx.doi.org/10.4132/jptm.2015.02.04

■ BRIEF CASE REPORT ■

Malakoplakia Affecting the Umbilical Cord

Song-Hee Han · Mee Joo · Sunhee Chang · Han-Seong Kim

Department of Pathology, Inje University Ilsan Paik Hospital, Inje University College of Medicine, Goyang, Korea

Malakoplakia, meaning soft (malako) plaque (plakia), is a rare benign inflammatory lesion. The disease was initially described in the bladder by Michaelis and Gutmann[1] in 1902 and named by von Hansemann[2] in 1903. Since its initial description, many cases have been described in numerous anatomic locations including the genitourinary tract, gastrointestinal tract, pancreas, liver, oropharynx, retroperitoneum, thyroid gland, lymph nodes, lung, bone/joint, brain, skin, and other tissues.[3-5] To our knowledge, this is the first case of malacoplakia affecting the umbilical cord.

CASE REPORT

A 33-year-old primigravida and nullipara woman in preterm labor at 32 weeks of gestation was referred to our hospital. Upon presentation, she had a temperature of 37.3°C, a pulse rate of 108 beats per minute, and leukocytosis (white blood cells count >22,000 mm^2). Vaginal examination revealed no pooling of fluid. She gave birth to a 2,000 g female infant by vaginal delivery, with Apgar scores of 7 and 9 at 1 and 5 minutes, respectively.

Grossly, the placenta was 18×14×2.5 cm and 510 g. The attached cord measured 30 cm in length and 2 cm and 1.3 cm in maximal and minimal diameters, respectively. The middle portion of the umbilical cord was focally enlarged, measuring 2 cm in length and 2 cm in diameter. The cut surface showed an ill-defined white to brown horseshoe-shaped area surrounding the umbilical vessels, measuring 2 cm in length and 0.2 cm in thickness (Fig. 1A). The chorionic plate had a patchy appearance and was covered by a purulent exudate.

Microscopically, there was a horseshoe-shaped calcified area located within the Wharton's jelly. The calcified area consisted of multiple, small, round to oval, and calcified bodies (calcospherites), which were both intra- and extracellular. Many of the inclusions were confirmed to be within macrophages on CD68 immunohistochemical stain. The majority of the lesion was necrotic and contained an inflammatory infiltrate composed mainly of neutrophils and macrophages. The macrophages had abundant eosinophilic cytoplasm with eccentric, hyperchromatic, and round nuclei (Fig. 1B). Concentrically laminated, round-ovoid, and basophilic calcified bodies, which are referred to as Michaelis-Gutmann bodies, were also seen (Fig. 1C, D). These bodies stained positive for von-Kossa and periodic acid–Schiff. Acute inflammation of the choriodecidua, amnion, and chorionic plate was noted. Based on the above findings, the diagnosis of malakoplakia of the umbilical cord, acute chorioamnionitis, and funisitis was made. Unfortunately, intracellular and extracellular bacterial organisms were not revealed on special stains.

DISCUSSION

The pathogenesis of malakoplakia is thought to be related to infections and/or immunosuppressed states, such as human immunodeficiency virus infection, cancer chemotherapy, post organ or bone marrow transplant states, and congenital immunodeficiency associated with an acquired bactericidal defect of macrophages.[6] The presence of a bacterial infection is clear in almost all reported cases, regardless of the site of organ involvement. *Klebsiella pneumoniae* and *Escherichia coli* are the most common cultured microorganisms in lesions of malakoplakia, although other gram-negative, gram-positive, and acid-fast bacilli have been implicated.[5] In addition, the patients of several prior re-

Corresponding Author
Hanseong Kim, M.D.
Department of Pathology, Inje University Ilsan Paik Hospital, Inje University College of Medicine, 170 Juhwa-ro, Ilsanseo-gu, Goyang 411-706, Korea
Tel: +82-31-910-7142, Fax: +82-31-910-7139, E-mail: hskim@paik.ac.kr

Received: December 11, 2014 **Revised:** February 4, 2015
Accepted: February 4, 2015

pISSN 2383-7837
eISSN 2383-7845

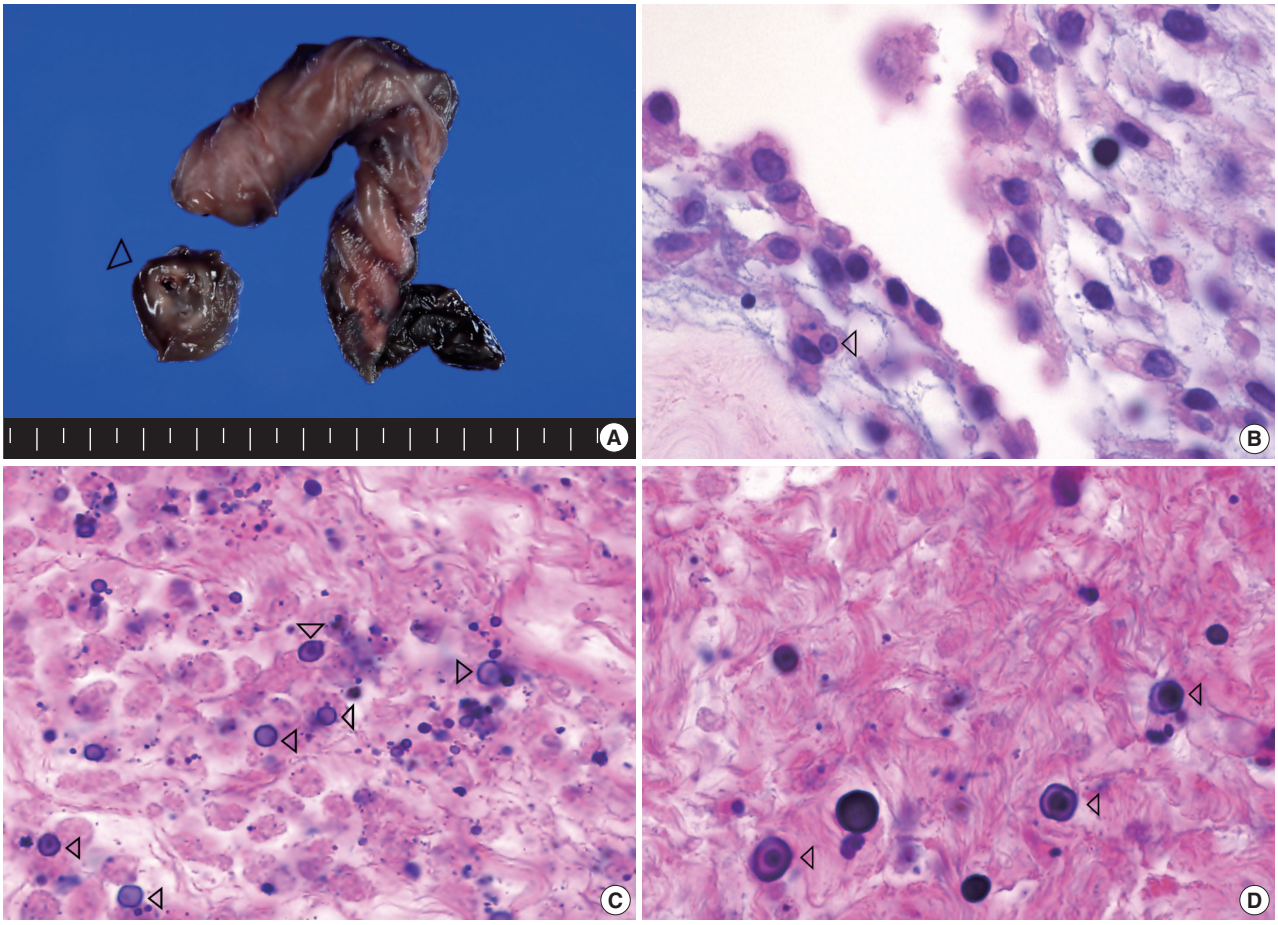

Fig. 1. Representative macroscopic and microscopic images of the lesion. (A) The middle portion of umbilical cord is focally enlarged, inside which an ill-defined white to brown horseshoe-shaped area (arrowhead) surrounding the umbilical vessels is noted. (B) The concentrically laminated, round-ovoid, basophilic calcified bodies, referred to as Michaelis-Gutmann bodies, are seen within macrophages (arrowhead). (C) This lesion is composed of multiple, small, round to oval, calcified bodies (calcospherites), Michaelis-Gutmann bodies (arrowheads), and an inflammatory infiltrate containing mainly necrotic macrophages. (D) The Michaelis-Gutmann bodies (arrowheads) are also observed in the noncalcified area.

ports have been immunosuppressed or had an autoimmune disease, neoplasm, or organ transplant. Thorning and Vracko[6] suggested that malakoplakia may be caused by impaired phagocytosis and a specific defect in the acidification of lysosomal vacuoles containing partially digested bacterial particulates, and therefore, as mentioned above, macrophages are able to ingest but not kill specific organisms.

While pregnancy is not an immunosuppressed state, immunologic changes during pregnancy may increase the susceptibility to certain pathogens, including viruses, bacteria, and parasites. Therefore, pregnancy is associated with an increased risk of infection. Given that our patient presented with a mild fever, leukocytosis, and tachycardia, it was highly suspected to be an infection. Clinical and histological chorioamnionitis was confirmed. The pathogenesis of chorioamnionitis is marked by the passage of infectious organisms to the chorioamnion and/or the umbilical cord of the placenta.[7] This passage occurs most commonly by an ascending infection from the lower genital tract.[7] In pregnancy, two cases of malakoplakia have been reported. One case involved the pelvic peritoneum and the other involved the cerebrum.[8,9] A urinary tract infection was the cause of infection in both cases.[8,9] Unfortunately, the offending organism in the present case was not isolated making the cause unclear.

During normal pregnancy, there is an increase in innate immune cells, such as macrophages and natural killer cells. These macrophages may be important for local immune function as well as the placental development by promoting trophoblast recruitment, spiral artery remodeling, and angiogenesis.[10] However, it is currently unknown why some patients develop the dysfunctional changes of macrophages that can predispose pa-

 http://dx.doi.org/10.4132/jptm.2015.02.04

tients to malakoplakia.

This is the first case of malakoplakia affecting the umbilical cord. Our findings illustrate that in cases with clinical features associated with clinical chorioamnionitis including maternal fever and tachycardia (>100/min), fetal tachycardia (>160/min) and purulent or foul-smelling amniotic fluid, malakoplakia should be suspected.

Conflicts of Interest

No potential conflict of interest relevant to this article was reported.

REFERENCES

1. Michaelis L, Gutmann C. Uber einschlusse in blasentumoren. Z Klin Med 1902; 47: 208-15.
2. Von Hansemann D. Uber malakoplakie der harnblase. Virchows Arch Pathol Anat Physiol Klin Med 1903; 173: 302-8.
3. Afonso JP, Ando PN, Padilha MH, Michalany NS, Porro AM. Cutaneous malakoplakia: case report and review. An Bras Dermatol 2013; 88: 432-7.
4. Hamvas A, Detre Z, Szinnay G. Malakoplakia of kidney and urinary tract: report of a case of fatal outcome. Int Urol Nephrol 1981; 13: 55-63.
5. Wagner D, Joseph J, Huang J, Xu H. Malakoplakia of the prostate on needle core biopsy: a case report and review of the literature. Int J Surg Pathol 2007; 15: 86-9.
6. Thorning D, Vracko R. Malakoplakia: defect in digestion of phagocytized material due to impaired vacuolar acidification? Arch Pathol 1975; 99: 456-60.
7. Czikk MJ, McCarthy FP, Murphy KE. Chorioamnionitis: from pathogenesis to treatment. Clin Microbiol Infect 2011; 17: 1304-11.
8. Rose G, Morrison EA, Kirkham N, Machling R. Malakoplakia of the pelvic peritoneum in pregnancy: case report. Br J Obstet Gynaecol 1985; 92: 170-2.
9. Blumbergs PC, Hallpike JF, McClure J. Cerebral malakoplakia. J Clin Pathol 1981; 34: 875-8.
10. Svensson-Arvelund J, Ernerudh J, Buse E, *et al*. The placenta in toxicology. Part II: systemic and local immune adaptations in pregnancy. Toxicol Pathol 2014; 42: 327-38.

J Pathol Transl Med
pISSN: 2383-7837
eISSN: 2383-7845

Executive Members

The Korean Society of Pathologists

President	Chang Suk Kang (*Catholic Univ.*)
Vice President	Kyu Sang Song (*Chungnam National Univ.*)
	In Ae Park (*Seoul National Univ.*)
Auditor	Woo Ick Yang (*Yonsei Univ.*)
	Chan Choi (*Chonnam National Univ.*)
Director General	Eunsil Yu (*Univ. Ulsan*)
Secretary General	Ae Ree Kim (*Korea Univ.*)
Director, the Communications	Seung Mo Hong (*Univ. Ulsan*)
Treasurer	Yun Kyung Kang (*Inje Univ.*)
Director, the Training Board	Young Ha Oh (*Hanyang Univ.*)
Director, the Strategy and Planning	Yoon La Choi (*Sungkyunkwan Univ.*)
Director, the Insurance and Policy	Youn Soo Lee (*Catholic Univ.*)
Director, the Legal Affairs	Chang Hun Lee (*Busan Univ.*)
Director, the Information	Dae Cheol Kim (*Dong-A Univ.*)
Director, the Scientific Programs	Yong Mee Cho (*Univ. Ulsan*)
Director, the Education	Jung Sun Kim (*Sungkyunkwan Univ.*)
Director, the Compilation	Soon Won Hong (*Yonsei Univ.*)
Director, the Cytopathology	Wan Seop Kim (*Konkuk Univ.*)
Director, the Quality Improvement	Dong Wook Kang (*Eulji Univ.*)
Director	Jean A Kim (*Catholic Univ.*)
	Ho Jung Kim (*T&C Diagnostic Pathology Clinic*)
	In Suh Park (*Inha Univ.*)
	Jae Hee Suh (*Univ. Ulsan*)
	Ghil Suk Yoon (*Kyungpook National Univ.*)
	Soong Deok Lee (*Seoul National Univ.*)
	Sung Chul Lim (*Chosun Univ.*)
	Kyu Yun Jang (*Chonbuk National Univ.*)
	Jong Jae Jung (*ForYou Pathology Lab.*)
	Hyeon Joo Jeong (*Yonsei Univ.*)
	Mee Joo (*Inje Univ.*)
	Kyung Chan Choi (*Hallym Univ.*)
	Hye Seung Han (*Konkuk Univ.*)

The Korean Society for Cytopathology

President	So Young Jin (*Soon Chun Hyang Univ.*)
Vice President	Hye Kyoung Yoon (*Inje Univ.*)
Chairperson, the Cytotechnologists Guidance Council	Han Kyeom Kim (*Korea Univ.*)
Secretary General	Yoon Jung Choi (*Ilsan Hospital*)
Director, the Scientific Programs	Hyun Lee Yim (*Ajou University Hospital*)
Director, the Education	Eun Kyung Kim (*Eulji Univ.*)
Director, the Legal Affairs	Chang Hun Lee (*Pusan National Univ.*)
Director, the Quality Improvement	Dong Hoon Kim (*Sungkyunkwan Univ.*)
Director, Strategy and Planning	Chong Woo Yoo (*National Medical Center*)
Chairperson, the International Cooperation Committee	Seung Yeon Ha (*Gachon Univ.*)
Director, the Cytotechnologists Cooperation	Hwa Jeong Ha (*Korea Cancer Center Hospital*)
Auditor	In Ae Park (*Seoul National Univ.*)
	Sung Ran Hong (*Catholic Kwandong Univ.*)
Chairperson, the Ethics Committee	Kyo Young Lee (*Catholic Univ.*)
Treasurer	Jee Young Han (*Inha Univ.*)
Director, the Compilation	Soon Won Hong (*Yonsei Univ.*)
Director, the Communications	Wan Seop Kim (*Konkuk Univ.*)
Director, the Informatics	Sang Yeop Yi (*Catholic Kwandong Univ.*)
Director, the Insurance & Poli	Se Hoon Kim (*Yonsei Univ.*)
Chairperson, the Certification Committee	Gyung Yub Gong (*Univ. Ulsan*)
Chairperson, the Early Cancer Screening Program Committee	Sung Chul Lim (*Chosun Univ.*)

BD SurePath™ liquid-based cytology

One solution for all your Non-Gyn cytology needs

BD

Helping all people live healthy lives

BD CytoRich™ non-gyn process combines the fixative properties of BD CytoRich™ Red and the discrete batch processing capabilities of BD PrepStain™ slide processor to provide you with one solution for all your non-gynecological cytology needs.

BD CytoRich™
Red Preservative

+

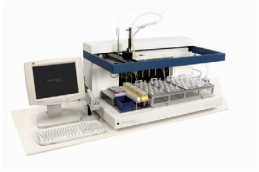

BD PrepStain™
Slide Processor

=

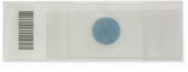

Unobscured slides that are easy to screen and intepret

BD Diagnostics - Diagnostic Systems
서울시 강남구 역삼동 788-2 임성빌딩 5층 (135-080)
Tel. (02) 3404-3700 Fax. (02) 557-4048
www.bd.com